

การตอบสนองของเนื้อเยื่อและการย่อยสลายทางชีวภาพของ
โครงเลี้ยงเซลล์ไฟโบรอินไหมไทย/เจลาติน/ไฮดรอกซีอะพาไทต์

นางสาว หทัยรัตน์ ตั้งทัศนาศนา

วิทยานิพนธ์นี้เป็นส่วนหนึ่งของการศึกษาตามหลักสูตรปริญญาวิทยาศาสตรมหาบัณฑิต

สาขาวิชาวิศวกรรมชีวเวช (สหสาขาวิชา)

บัณฑิตวิทยาลัย จุฬาลงกรณ์มหาวิทยาลัย

ปีการศึกษา 2552

ลิขสิทธิ์ของจุฬาลงกรณ์มหาวิทยาลัย

TISSUE RESPONSE AND BIODEGRADATION OF HYDROXYAPATITE/GELATIN/
THAI SILK FIBROIN SCAFFOLDS

Miss Hathairat Tungtasana

A Thesis Submitted in Partial Fulfillment of the Requirements
for the Degree of Master of Science Program in Biomedical Engineering
(Interdisciplinary Program)
Graduate School
Chulalongkorn University
Academic Year 2009
Copyright of Chulalongkorn University

หัตถ์วิจัยนี้ ตั้งที่ศึกษา : การตอบสนองของเนื้อเยื่อและการย่อยสลายทางชีวภาพของ
 โครงเลี้ยงเซลล์ไฟโบรอินไหมไทย/เจลาติน/ไฮดรอกซีอะพาไทต์. (TISSUE RESPONSE
 AND BIODEGRADATION OF HYDROXYAPATITE/GELATIN/THAI SILK FIBROIN
 SCAFFOLDS) อ.ที่ปรึกษาวิทยานิพนธ์หลัก : รศ.ดร.ศิริพร ดำรงค์ศักดิ์กุล, อ. ที่ปรึกษา
 วิทยานิพนธ์ร่วม : ผศ.นพ.ถนอม บรรณประเสริฐ, 129 หน้า.

งานวิจัยนี้ได้ทำการศึกษาค้นคว้าการตอบสนองต่อเนื้อเยื่อ การย่อยสลายทางชีวภาพทั้งในห้องปฏิบัติการ
 และในสัตว์ทดลองของโครงเลี้ยงเซลล์ที่ผลิตจากไฟโบรอินไหมไทยเป็นหลักจำนวน 4 ชนิด ได้แก่ โครงเลี้ยง
 เซลล์ไฟโบรอินไหมไทย, โครงเลี้ยงเซลล์คอนจูเกตเจลาติน/ไฟโบรอินไหมไทย, โครงเลี้ยงเซลล์ไฮดรอกซีอะพา
 ไทต์/ไฟโบรอินไหมไทย และ โครงเลี้ยงเซลล์ไฮดรอกซีอะพาไทต์/คอนจูเกตเจลาติน/ไฟโบรอินไหมไทย ซึ่งถูก
 เตรียมด้วยวิธีการกำจัดเกลือออก, การเชื่อมขวางด้วยสารละลายอีดีซี/เอ็นเอชเอส (EDC/NHS) และการแช่สลับ
 ผลของการย่อยสลายทางชีวภาพในห้องปฏิบัติการพบว่า น้ำหนักที่คงเหลืออยู่ภายหลังแช่ในสารละลายคอลลา
 เจนเนสเป็นเวลา 28 วัน เรียงลำดับ ได้ดังนี้ โครงเลี้ยงเซลล์คอนจูเกตเจลาติน/ไฟโบรอินไหมไทย>โครงเลี้ยงเซลล์
 ไฟโบรอินไหมไทย>โครงเลี้ยงเซลล์ไฮดรอกซีอะพาไทต์/ไฟโบรอินไหมไทย~โครงเลี้ยงเซลล์ไฮดรอกซีอะพาไทต์/
 คอนจูเกตเจลาติน/ไฟโบรอินไหมไทย โครงเลี้ยงเซลล์คอนจูเกตเจลาติน/ไฟโบรอินไหมไทยมีการย่อยสลายทาง
 ชีวภาพช้าที่สุด เนื่องมาจากการเชื่อมขวางโดยใช้ความร้อนร่วมกับการใช้สารละลาย EDC/NHS จากผลการ
 ทดลองการย่อยสลายทางชีวภาพในสัตว์ทดลอง พบว่าโครงเลี้ยงเซลล์ทั้ง 4 ชนิด ยังคงเหลืออยู่ภายหลังจากฝัง
 ขึ้นงานในชั้นใต้ผิวหนังของหนูวิสตาเป็นระยะเวลา 12 สัปดาห์ จากการเปรียบเทียบการย่อยสลายทางชีวภาพ
 ในห้องปฏิบัติการและในสัตว์ทดลอง พบว่า โครงเลี้ยงเซลล์คอนจูเกตเจลาติน/ไฟโบรอินไหมไทยมีการย่อย
 สลายช้าที่สุดในห้องปฏิบัติการ แต่โครงเลี้ยงเซลล์ไฮดรอกซีอะพาไทต์/คอนจูเกตเจลาติน/ไฟโบรอินไหมไทยมี
 การย่อยสลายช้าที่สุดในสัตว์ทดลอง การประเมินการตอบสนองต่อเนื้อเยื่อโดยการฝังตัวอย่างในชั้นใต้ผิวหนัง
 ของหนูตามมาตรฐาน ISO10993-6: การประเมินทางชีวภาพของวัสดุทางการแพทย์ พบว่าหลังจากการฝังเป็น
 เวลา 2 และ 4 สัปดาห์ โครงเลี้ยงเซลล์ทั้ง 4 ชนิดจัดอยู่ในกลุ่ม “ไม่ระคายเคือง” ถึง “ระคายเคืองเล็กน้อย” เมื่อ
 เทียบกับ Gelfoam® (วัสดุควบคุม) จากผลการศึกษาชี้ให้เห็นว่าโครงเลี้ยงเซลล์ที่ผลิตจากไฟโบรอินไหมไทยเป็น
 หลักมีศักยภาพสูงในการประยุกต์ใช้งานด้านวิศวกรรมเนื้อเยื่อ

สาขาวิชาวิศวกรรมชีวเวช..... ลายมือชื่อนิติ.....

ปีการศึกษา 2552..... ลายมือชื่ออ.ที่ปรึกษาวิทยานิพนธ์หลัก.....

ลายมือชื่ออ.ที่ปรึกษาวิทยานิพนธ์ร่วม.....

5087224020 : MAJOR BIOMEDICAL ENGINEERING

KEYWORDS : TISSUE RESPONSE / BIODEGRADATION / THAI SILK FIBROIN / GELATIN / HYDROXYAPATITE

HATHAIRAT TUNGTASANA : TISSUE RESPONSE AND BIODEGRADATION OF HYDROXYAPATITE/GELATIN/THAI SILK FIBROIN SCAFFOLDS. THESIS ADVISOR : ASSOC.PROF.SIRIPORN DAMRONGSAKKUL, Ph.D., THESIS CO-ADVISOR : ASST.PROF.TANOM BUNAPRASERT, M.D., 129 pp.

This study aimed to investigate tissue response, *in vitro* and *in vivo* biodegradation of four types of Thai silk fibroin based-scaffolds. Four types of scaffolds including Thai silk fibroin (SF), conjugated gelatin/Thai silk fibroin (CGSF), hydroxyapatite/Thai silk fibroin (SF4) and hydroxyapatite/conjugated gelatin/Thai silk fibroin scaffold (CGSF4) were fabricated by salt-leaching, EDC/NHS crosslinking and alternate soaking techniques. The results on *in vitro* biodegradation tests showed that the remaining weight of scaffolds after 28 days of incubation in collagenase solution was in the order of CGSF>SF>SF4~CGSF4. The CGSF scaffold was found to have the slowest biodegradability due to the crosslinking by dehydrothermal and EDC/NHS treatment. From *in vivo* biodegradation tests, all scaffolds could still be observed after 12 weeks of implantation in subcutaneous tissue of Wistar rat. Comparing *in vitro* and *in vivo* biodegradation, the CGSF scaffold showed the slowest *in vitro* degradation while *in vivo* the slowest degradation was observed in the case of CGSF4 scaffold. The tissue response was evaluated using subcutaneous implantation model following ISO10993-6: Biological evaluations of medical devices. At 2 and 4 weeks of implantation, it was shown that four types of scaffolds were classified as “non-irritant” to “slight irritant”, compared to Gelfoam[®] (control sample). The results indicated the high potential of Thai silk fibroin-based scaffolds for tissue engineering applications.

Field of Study : Biomedical Engineering..... Student's Signature

Academic Year : 2009..... Advisor's Signature

Co-Advisor's Signature

ACKNOWLEDGEMENTS

The research is completed with the aid and support of many people. First of all, I would like to express my deepest gratitude to Associate Professor Dr. Siriporn Damrongsakkul, my advisor, for her continuous guidance, helpful suggestions and warm encouragement. I wish to give my gratitude to Assistant Professor Tanom Bunaprasert, M.D., the thesis co-advisor, for his kind guidance about the regulation in medical devices and the surgery method. In addition, I would like to acknowledge my committee members, Associate Professor Suthiluk Patumraj, Ph.D., Assistance Professor Sorada Kanokpanont, Ph.D., Professor Saranatra Waikakul, M.D., whose comments are constructively and especially helpful.

I am also grateful to Somruetai Shuangshoti M.D. (pathologist), for her kind assistance on the evaluation of tissue response. For financial support from The 90th anniversary of Chulalongkorn University Fund (Ratchadaphiseksomphot Endowment Fund) is highly acknowledged.

I also would like to thank the present and past members of Polymer Engineering Research Group and Center of Excellence on Catalysis and Catalytic Reaction Engineering at the Department of Chemical Engineering as well as all members of i-Tissue Laboratory at the Department of Medicine, Chulalongkorn University for their suggestions in experimental work. I wish to thank Miss. Juthamas Ratanavaraporn, Mr. Isarawut Prasertsung and Miss Winkanda Tunterak for their helps in animal experiment.

Lastly, I thank to my parents, Mr. Chunchai Tungtasana and Mrs. Phetcharat Tungtasana, and everyone in my family for believing in me.

CONTENTS

	PAGE
ABSTRACT (THAI)	iv
ABSTRACT (ENGLISH)	v
ACKNOWLEDGEMENTS	vi
CONTENTS	vii
LIST OF TABLES	x
LIST OF FIGURES	xii
CHAPTER	
I INTRODUCTION	1
1.1 Background.....	1
1.2 Objectives.....	2
1.3 Scopes of research.....	2
II RELEVANT THEORY AND LITERATURE REVIEWS	4
RELEVANT THEORY	4
2.1 The inflammatory reaction and cell types	4
2.1.1 Tissue response to biomaterials.....	4
2.1.2 Evaluation of the biomaterial-tissue interactions as following ISO10993-6.....	9
2.1.3 Characteristic and function of inflammatory cell types.....	11
2.2 Biomaterials	15
2.2.1 Silk	15
2.2.2 Gelatin.....	20
2.2.3 Hydroxyapatite.....	22
2.3 Biodegradation of biomaterials.....	24
LITERATURE REVIEWS	27
III EXPERIMENTAL WORKS	39
3.1 Raw materials and chemicals.....	38
3.2 Equipments	40
3.3 Experimental procedures.....	41

CHAPTER

3.3.1 Preparation of four types of Thai silk fibroin-based scaffolds.....	42
3.3.1.1 Preparation of Thai silk fibroin scaffolds (SF).....	42
3.3.1.2 Preparation of conjugated type A gelatin/ Thai silk fibroin scaffolds (CGSF).....	42
3.3.1.3 Preparation of hydroxyapatite/Thai silk fibroin scaffold (SF4)...	43
3.3.1.4 Preparation of hydroxyapatite/conjugated gelatin/Thai silk fibroin scaffolds (CGSF4).....	43
3.3.2 Quality control of four types of Thai silk fibroin-based scaffolds.....	43
3.3.3 <i>In vitro</i> biodegradation of Thai silk fibroin-based scaffolds.....	45
3.3.3.1 Remaining weight of Thai silk fibroin-based scaffolds.....	45
3.3.3.2 Morphological observation of Thai silk fibroin-based scaffolds	45
3.3.3.3 Conformational structure of Thai silk fibroin-based scaffolds	46
3.3.4 <i>In vivo</i> biodegradation of Thai silk fibroin-based scaffolds	46
3.3.4.1 Physical appearance	48
3.3.4.2 Morphological observation by scanning electron microscope ...	48
3.3.4.3 Evaluation of the relative size of the scaffolds.....	48
3.3.5 Evaluation of the tissue response (local effects) of Thai silk fibroin-based scaffolds following ISO10993-6.....	49
3.3.5.1 Macroscopic assessment	50
3.3.5.2 Microscopic assessment.....	50
3.3.6 Ethic issues.....	52
3.3.6 Statistical analysis	52
IV RESULTS AND DISCUSSION.....	53
4.1 <i>In vitro</i> biodegradation of Thai silk fibroin-based scaffolds.....	53
4.1.1 Physical appearance of Thai silk fibroin-based scaffolds.....	53
4.1.2 Remaining weight of Thai silk fibroin-based scaffolds.....	56
4.1.3 Morphology of Thai silk fibroin-based scaffolds.....	58
4.1.4 Conformational structure of Thai silk fibroin-based scaffolds	66

CHAPTER	
4.1.4.1 XRD patterns of Thai silk fibroin-based scaffolds before degradation.....	66
4.1.4.2 XRD patterns of Thai silk fibroin-based scaffolds after degradation.....	69
4.2 <i>In vivo</i> biodegradation of Thai silk fibroin-based scaffolds.....	73
4.2.1 Physical appearance of Thai silk fibroin-based scaffolds.....	73
4.2.2 Remaining area of Thai silk fibroin-based scaffolds.....	76
4.2.3 Morphology of Thai silk fibroin-based scaffolds.....	78
4.3 Evaluation of the tissue response of Thai silk fibroin-based scaffolds following ISO10993-6.....	83
4.3.1 Macroscopic assessment	83
4.3.2 Microscopic assessment	85
V CONCLUSIONS AND RECOMMENDATIONS.....	93
5.1 Conclusions.....	93
5.2 Recommendations	94
REFERENCES.....	95
APPENDICES	101
APPENDIX A: Evaluation of scaffold area.....	102
APPENDIX B: Gelfoam®	105
APPENDIX C: Quality control of Thai silk fibroin scaffold.....	111
APPENDIX D: Raw data of remaining weight.....	114
APPENDIX E: Histological image.....	118
APPENDIX F: Semi-quantitative evaluation system according to ISO10993-6.....	121
Biography.....	129

LIST OF TABLES

TABLE	PAGE
2.1 Cells and components of vascularized connective tissue.....	5
2.2 Importance chemical mediators of inflammation derived from plasma, cells and injured tissue	6
2.3 Principle for various implant sites	10
2.4 Approximate percentages of leukocytes in adult human blood	12
2.5 Structure of silk fiber.....	16
2.6 Silk fibroin degradation <i>in vivo</i>	26
3.1 Quality control of Thai silk fibroin scaffolds.....	44
3.2 Weight percentage of silk, gelatin and hydroxyapatite in four types of scaffolds	44
3.3 Scoring systems used for biological evaluation-Cell types.....	50
3.4 Scoring systems used for biological evaluation-Response.....	51
3.5 Semi-quantitative evaluation system.....	52
4.1 Level of irritation of scaffolds after 2 weeks of subcutaneous implantation	86
4.2 Level of irritation of scaffolds after 4 weeks of subcutaneous implantation	87
C-1 Density of Thai silk fibroin scaffold	111
D-1 Remaining weight at various degradation time of Thai silk fibroin scaffolds (SF)	114
D-2 Remaining weight at various degradation time of hydroxyapatite/Thai silk fibroin scaffolds (SF4)	115
D-3 Remaining weight at various degradation time of conjugated gelatin/ Thai silk fibroin scaffolds (CGSF)	116
D-4 Remaining weight at various degradation time of hydroxyapatite/conjugated gelatin/Thai silk fibroin scaffolds (CGSF4)	117
F-1 Semi-quantitative evaluation of SF and SF4 scaffolds after 2 weeks of implantation (1 st evaluation).....	121
F-2 Semi-quantitative evaluation of CGSF and CGSF4 scaffolds after 2 weeks of implantation (1 st evaluation).....	122

F-3	Semi-quantitative evaluation of SF and SF4 scaffolds after 2 weeks of implantation (2 nd evaluation).....	123
F-4	Semi-quantitative evaluation of CGSF and CGSF4 scaffolds after 2 weeks of implantation (2 nd evaluation).....	124
F-5	Semi-quantitative evaluation of SF and SF4 scaffolds after 4 weeks of implantation (1 st evaluation)	125
F-6	Semi-quantitative evaluation of CGSF and CGSF4 scaffolds after 4 weeks of implantation (1 st evaluation).....	126
F-7	Semi-quantitative evaluation of SF and SF4 scaffolds after 4 weeks of implantation (2 nd evaluation).....	127
F-8	Semi-quantitative evaluation of CGSF and CGSF4 scaffolds after 4 weeks of implantation (2 nd evaluation).....	128

LIST OF FIGURES

FIGURE	PAGE
2.1 Sequence of events involved inflammatory and wound healing responses.....	4
2.2 Sequence of events following implantation of biomaterial	7
2.3 <i>In vivo</i> transition from blood-borne monocyte to biomaterial adherent monocyte /macrophage to foreign body giant cell at tissue/biomaterial interface	9
2.4 Neutrophil.....	12
2.5 Eosinophil.....	13
2.6 Basophil.....	13
2.7 Lymphocyte.....	14
2.8 Monocyte.....	14
2.9 Structure of raw silk fiber.....	16
2.10 Organization of hydrophilic and hydrophobic domains in fibroin.....	17
2.11 Structure of antiparalle β -sheet.....	17
2.12 Processing silk fibroin into 3D porous scaffolds	20
2.13 Structural silk fibroin transition from random coil to β -sheet structures.....	19
2.14 Preparation processes for acidic and basic gelatins from collagen.....	21
2.15 Structure of gelatin.....	21
2.16 Reaction of chemically crosslinked gelatin network.....	22
2.17 Structure of hydroxyapatite.....	23
2.18 Alternate soaking process.....	24
3.1 Flowchart of experimental procedures.....	41
3.2 Method of subcutaneous implantation	47
3.3 The group and the number of Wistar rats used to evaluate <i>in vivo</i> biodegradation.....	47
3.4 Implanted sites of Wistar rat	49
3.5 The group and the number of Wistar rats used to evaluate <i>in vivo</i> tissue response.....	49

4.1	Physical appearance of SF, SF4, CGSF, CGSF4 scaffolds after incubation in 1 U/ml collagenase for 1, 7, 14, 21 and 28 days.....	55
4.2	Remaining weight (%) of the scaffolds at each period of degradation time in collagenase.....	57
4.3	SEM micrographs of SF, SF4, CGSF and CGSF4 scaffolds before incubation in collagenase.....	60
4.4	SEM micrographs of SF scaffolds after incubation in collagenase for 1, 7, 14, 21 and 28 days.....	61
4.5	SEM micrographs of SF4 scaffolds after incubation in collagenase for 1, 7, 14, 21 and 28 days.....	62
4.6	SEM micrographs of CGSF scaffolds after incubation in collagenase for 1, 7, 14, 21 and 28 days.....	63
4.7	SEM micrographs of CGSF4 scaffolds after incubation in collagenase for 1, 7, 14, 21 and 28 days.....	64
4.8	SEM micrographs of SF, SF4, CGSF and CGSF4 scaffolds before and after incubation in collagenase for 21 days.....	65
4.9	X-ray diffraction patterns of SF, SF4, CGSF and CGSF4 scaffolds before incubation in collagenase solution.....	68
4.10	X-ray diffraction patterns of hydroxyapatite (Fluka, Germany) and Type A gelatin (Nitta, Japan).....	68
4.11	X-ray diffraction patterns of SF scaffold before and after incubation in collagenase solution for 0,1,7,14,21 and 28 days.....	71
4.12	X-ray diffraction patterns of SF4 scaffold before and after incubation in collagenase solution for 0,1,7,14,21 and 28 days.	71
4.13	X-ray diffraction patterns of CGSF scaffold before and after incubation in collagenase solution for 0,1,7,14,21 and 28 days.....	72
4.14	X-ray diffraction patterns of CGSF4 scaffold before and after incubation in collagenase solution for 0,1,7,14,21 and 28 days.....	72
4.15	Physical appearances of SF, SF4, CGSF and CGSF4 scaffolds after 2 and 4 weeks of implantation.....	74
4.16	Physical appearances of SF, SF4, CGSF and CGSF4 scaffolds after 12 weeks of implantation.....	75

4.17 Remaining area of cross-sectioned SF, SF4, CGSF and CGSF4 scaffolds after 2, 4 and 12 weeks.....	77
4.18 SEM micrographs of SF, SF4, CGSF and CGSF4 scaffolds after 2 weeks of implantation.....	80
4.19 SEM micrographs of SF, SF4, CGSF and CGSF4 scaffolds after 4 weeks of implantation.....	81
4.20 SEM micrographs of SF, SF4, CGSF and CGSF4 scaffolds after 12 weeks of implantation.....	82
4.21 Appearance of Wistar rat after implantation.....	84
4.22 Gross appearance of cross-section of retrieved material after 2 weeks of implantation.....	84
4.23 Gross appearance of cross-section of retrieved material after 4 weeks of implantation.....	84
4.24 Histological section of subcutaneously implanted SF scaffold in Wistar rat after 2 weeks of implantation.....	87
4.25 Histological section of subcutaneously implanted SF4 scaffold in Wistar rat after 2 weeks of implantation.....	88
4.26 Histological section of subcutaneously implanted CGSF scaffold in Wistar rat after 2 weeks of implantation.....	88
4.27 Histological section of subcutaneously implanted CGSF4 scaffold in Wistar rat after 2 weeks of implantation.....	89
4.28 Histological section of subcutaneously implanted Gelfoam [®] in Wistar rat after 2 weeks of implantation.....	89
4.29 Histological section of subcutaneously implanted SF scaffold in Wistar rat after 4 weeks of implantation.....	90
4.30 Histological section of subcutaneously implanted SF4 scaffold in Wistar rat after 4 weeks of implantation.....	90
4.31 Histological section of subcutaneously implanted CGSF scaffold in Wistar rat after 4 weeks of implantation.....	91
4.32 Histological section of subcutaneously implanted CGSF4 scaffold in Wistar rat after 4 weeks of implantation.....	91

4.33	Histological section of subcutaneously implanted Gelfoam [®] in Wistar rat after 4 weeks of implantation.....	92
A-1	Image J window	102
A-2	Opening the image file	102
A-3	Setting measurement scale	103
A-4	Measuring area of scaffold.....	104
C-1	SEM micrographs of Thai silk fibroin scaffold.....	113
E-1	Histological image of SF, SF4, CGSF and CGSF4 scaffolds after 2 weeks of subcutaneous implantation in Wistar rat.....	118
E-2	Histological image of SF, SF4, CGSF and CGSF4 scaffolds after 4 weeks of subcutaneous implantation in Wistar rat.....	119
E-3	Histological image of SF, SF4, CGSF and CGSF4 scaffolds after 12 weeks of subcutaneous implantation in Wistar rat.....	120

CHAPTER I

INTRODUCTION

1.1 Background

Bone tissue engineering is developed to heal bone loss due to trauma or disease without the limitations and drawbacks of current clinical autografting and allografting treatments [1]. One of the key components of bone tissue engineering paradigm is the scaffold, which functions as a structural support and delivery vehicle providing cells and bioactive molecules necessary for the formation of new bone tissue. The ideal scaffold should possess mechanical properties adequate to support bone tissue growing, degrade upon bone tissue growth, demonstrate good biocompatibility, and have high porosity to enable bone tissue ingrowth.

Polymeric scaffolds used for bone tissue engineering, such as poly(lactic-co-glycolic acid) or poly-lactic acid, can induce inflammation due to the acidity of their hydrolysis products [1]. Therefore, there is a need to identify alternate biomaterials to overcome these limitations and meet the challenging combination of biological, mechanical, and degradation features for bone tissue engineering. In the world of natural fibers, silk has long been recognized as the wonder fiber for its unique combination of high strength and rupture elongation [3]. Moreover, core silk fibroin fibers exhibit comparable biocompatibility with other used biomaterials such as polylactic acid and collagen [2]. Silk fibroin is recently explored as a biomaterial for orthopedic applications [4]. Kim *et al* revealed that osteoblast-like cells increased with culture time in human bone marrow stem cells-seeded silk fibroin scaffold [1]. Meinel *et al* reported that implantation of silk scaffold seeded with human mesenchymal stem cell into calvarial critical size defects in mice induced advanced bone formation within 5 weeks when compared to the implantation of silk scaffold alone [5].

From our previous work, Chamchongkaset [6] has developed three-dimensional salt-leached Thai silk fibroin scaffolds from cocoons of Nangnoi

Srisaket1. The surface of Thai silk fibroin scaffolds was modified by gelatin conjugation and hydroxyapatite deposition. The biological properties of salt-leached Thai silk fibroin scaffolds were investigated via *in vitro* tests using MTT assay. The results showed that gelatin conjugating was favorable to cell proliferation however hydroxyapatite growing did not affect the number of proliferated cells. In an attempt to apply Thai silk fibroin-based scaffolds in bone tissue engineering, tissue response and biodegradation of these scaffolds have to be explored.

It is therefore the aims of this work to investigate the tissue response *in vivo* and biodegradation of Thai silk fibroin-based scaffolds. The tissue response will be evaluated using the methods described in international organization for standardization 10993-Part 6: tests for local effects after implantation (ISO 10993-6) [7]. Biodegradation of these scaffolds will be investigated both *in vitro* and *in vivo*. For *in vitro*, the appearance, remaining weight, morphology and conformational structure of Thai silk fibroin-based scaffolds would be examined after incubating in collagenase solution. For *in vivo*, Thai silk fibroin-based scaffolds would be implanted in subcutaneous tissue of wistar rats and the remaining area and morphology of scaffolds would be estimated.

1.2 Objectives

- 1.2.1 To investigate *in vitro* and *in vivo* biodegradation of hydroxyapatite/gelatin /Thai silk fibroin scaffolds.
- 1.2.2 To evaluate the *in vivo* response of hydroxyapatite/gelatin/Thai silk fibroin scaffolds.

1.3 Scopes of Research

- 1.3.1 Preparation of four types of Thai silk fibroin-based scaffolds, as reported by Chamchongkaset [6]
 - Thai silk fibroin scaffolds (SF)
 - Conjugated gelatin/Thai silk fibroin scaffolds (CGSF)

- Hydroxyapatite/Thai silk fibroin scaffolds (SF4)
- Hydroxyapatite/conjugated gelatin/Thai silk fibroin scaffolds (CGSF4)

1.3.2 *In vitro* biodegradation of Thai silk fibroin-based scaffolds using 0.37 mg/ml collagenase at 37°C pH 7.4. The characteristics of degraded scaffolds were examined as follows. (Incubation periods : 1,7,14,21 and 28 days)

- Physical Appearance
- Remaining weight
- Morphology by Scanning electron microscopy (SEM)
- Conformational structure by X-ray diffraction (XRD)

1.3.3 *In vivo* biodegradation of Thai silk fibroin-based scaffolds in subcutaneous tissue of Wistar rats. (Implantation periods : 2, 4 and 12 weeks)

- Physical Appearance
- Evaluation of the relative areas of the scaffolds by H&E staining (using the image software)
- Morphology by scanning electron microscopy (SEM)

1.3.4 Evaluation of the tissue response of Thai silk fibroin-based scaffolds after implantation in subcutaneous tissue of Wistar rats following ISO10993-6: Tests for local effects after implantation (Implantation periods : 2 and 4 weeks)

Macroscopic assessment

- Gross examination of animals and implants at the time of sacrifices.

Microscopic assessment

- Semi-quantitative scoring systems (inflammatory cell types, neovascularisation, fibrosis and fatty infiltrate) from H&E staining results.

CHAPTER II

RELEVANT THEORY AND LITERATURE REVIEW

Relevant Theory

2.1 The inflammatory reaction and cell types

2.1.1 Tissue response to biomaterials [8, 9, 10]

The process of implantation of a biomaterial, prosthesis, or medical device results in injury to tissue or organ. Host reactions following implantation of biomaterials include injury, blood-material interactions, provisional matrix formation, acute inflammation, chronic inflammation, granulation tissue development, foreign body reaction and fibrosis/fibrous capsule development. The sequence of local events following implantation of medical devices was illustrated in Figure 2.1.

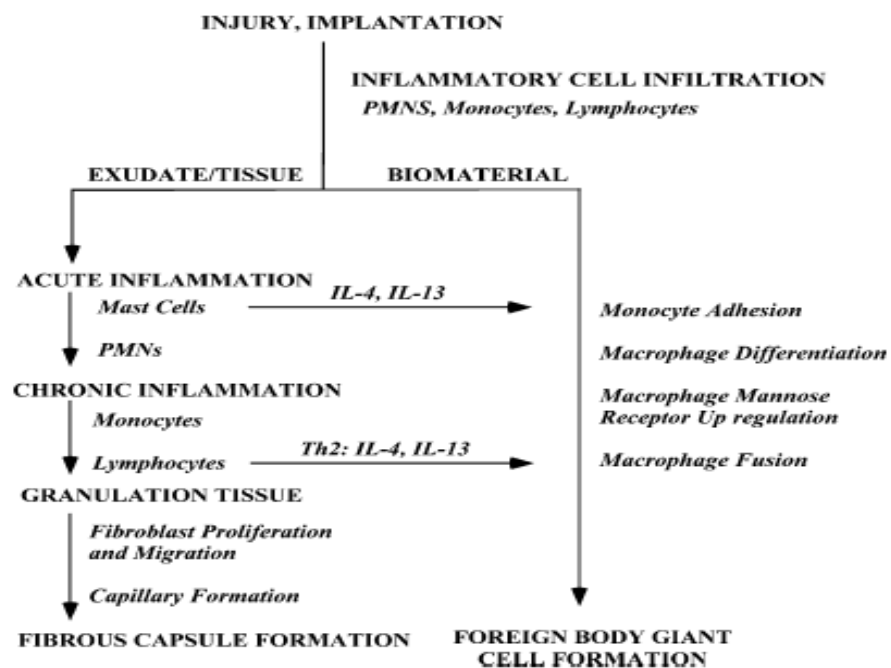


Figure 2.1 Sequence of events involved inflammatory and wound healing responses [9].

Blood- material interaction

The initial inflammatory response is activated by injury to vascularize connective tissue as shown in Table 2.1. Because blood and its components are involved in the initial inflammatory response, blood clot also form. Immediately following injury, changes occur in vascular flow, caliber and permeability. Fluid, proteins and blood cells escape from the vascular system into the injured tissue in a process called exudation. The effect of the injury and/or biomaterial in situ on plasma or cells can produce chemical factors. Important classes of chemical mediators of inflammation are present in Table 2.2. Chemical mediators are quickly inactivated or destroyed, suggesting that their action is predominantly at the implant site. Generally the lysosomal proteases and oxygen-derived free radicals produce the most significant damage or injury. These chemical mediators are also important in the degradation of biomaterials.

Table 2.1 Cells and components of vascularized connective tissue [11]

Intravascular (blood) cells	Connective tissue cells	Extracellular matrix components
Erythrocytes (RBC)	Mast cells	Collagens
Neutrophils	Fibroblasts	Elastin
Monocytes	Macrophages	Proteoglycans
Eosinophils	Lymphocytes	Fibronectin
Lymphocytes	-	Laminin
Basophils	-	-
Platelets	-	-

Table 2.2 Importance chemical mediators of inflammation derived from plasma, cells and injured tissue [11]

Mediators	Examples
Vasoactive agents	Histamines, serotonin, adenosine, endothelial-derived relaxing factor, prostacyclin, endothelin, thromboxane a ₂
Plasma proteases Kinin system Complement system Coagulation/fibrinolytic system	Bradykinin, kallikrein C3a, C5a, C3b, C5b-C9 Fibrin degradation products, activated Hageman factor (FXIIA), tissue plasminogen activator (tPA)
Leukotrienes	Leukotriene B ₄ (LTB ₄), hydroxyeicosatetraenoic acid (HETE)
Lysosomal proteases	Collagenase, elastase
Oxygen-derived free radicals	H ₂ O ₂ , Superoxide anion
Platelet activating factors	Cell membrane lipids
Cytokines	Interleukin (IL-1), Tumor necrosis factor (TNF)
Growth factors	Platelet derived growth factor (PDGF), fibroblast growth factor (FGF), transforming growth factor (TGF- α , TGF- β), epithelial growth factor (EGF)

Provisional matrix formation

Injury to vascularized tissue in the implantation procedure leads to immediate development of the provisional matrix at the implant site. This provisional matrix consists of fibrin, produced by activation of the coagulative and thrombosis systems, and inflammatory products, released by the complement system, activated platelets, inflammatory cells, and endothelial cells. Components within or released from the provisional matrix, i.e. fibrin network (thrombosis or clot), initiate the resolution, reorganization, and repair processes such as inflammatory cell and fibroblast recruitment. The provisional matrix appears to furnish both structural and biochemical components to the process of wound healing. The complex three-dimensional

structure of the fibrin network with attached adhesive proteins provides a substrate for cell adhesion and migration.

Temporal sequence of inflammation

Inflammation is generally defined as the reaction of vascularized living tissue to local injury. The sequence of events following implantation of a biomaterial is illustrated in Figure 2.2. The physical properties and chemical properties of the biomaterials may be responsible for variations in the intensity and time duration of the inflammatory and wound healing processes.

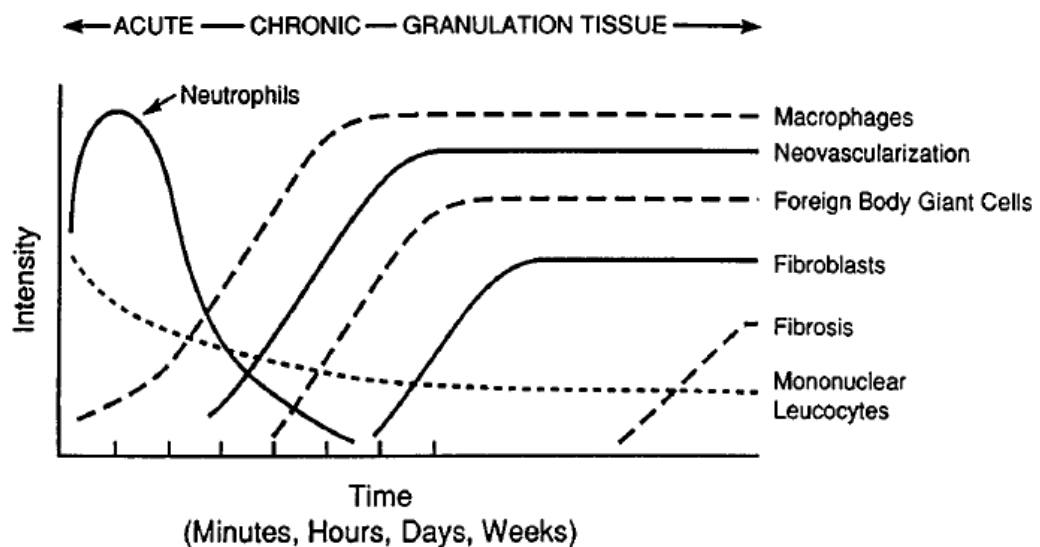


Figure 2.2 Sequence of events following implantation of biomaterial [8]

Acute inflammation is a short term process for minutes to hours to days, depending on the extent of injury. The process of acute inflammation is initiated by the blood vessels local to the injured tissue, which alter to allow the exudation of plasma proteins and leukocytes into the surrounding tissue. In general, neutrophils and other motile white cells move from the blood vessels to the perivascular tissues and the implant site. The major role of the neutrophil in acute inflammation is phagocytosis microorganisms and foreign materials.

Chronic inflammation which is a process for a prolonged period of time is characterized by the infiltration of mononuclear immune cells (i.e. monocytes, lymphocytes) at the implant site. The chronic inflammatory response is composed of

mononuclear cells usually lasting no longer than two weeks. Chronic inflammation occurs tissue destruction and attempts at healing which includes angiogenesis and fibrosis.

Granulation tissue derives its name from the pink, soft granular appearance on the surface of healing wounds and its characteristic histological features include the proliferation of new small blood vessels and fibroblasts. Fibroblasts are active in synthesizing collagen, especially type III. Depending on the extent of injury, granulation tissue may be seen as early as three to five days following implantation of a biomaterial. Within one day following implantation of a biomaterial, the healing response is initiated by the action of macrophages, followed by proliferation of fibroblasts and vascular endothelial cells at the implant site, leading to the formation of granulation tissue. Granulation tissue is the precursor to fibrous capsule formation. Small blood vessels are formed by budding or sprouting of preexisting vessels in a process known as neovascularization or angiogenesis. This process involves proliferation, maturation, and organization of endothelial cells into capillary tubes. Fibroblasts also proliferate in developing granulation tissue and are active in synthesizing collagen and proteoglycans. In the early stages of granulation tissue development, proteoglycans predominate; later, however, collagen, especially type I collagen, predominates and forms the fibrous capsule. Granulation tissue is distinctly different from granulomas, which are small collections of modified macrophages called epithelioid cells. Foreign body giant cells may surround non-phagocytosable particulate materials in granulomas. Foreign body giant cells are formed by the fusion of monocytes/macrophages in an attempt to phagocytose the material.

Foreign-body reaction is composed of foreign body giant cells and the components of granulation tissue, which consist of macrophages, fibroblasts, and capillaries in varying amounts, depending upon the form and topography of the implanted material. Foreign-body giant cells develop from circulating blood monocyte to tissue macrophage as demonstrated in Figure 2.3. With biocompatible materials, the composition of the foreign body reaction in the implant site may be controlled by the surface properties of the biomaterial, the form of the implant, and the relationship between the surface area of the biomaterial and the volume of the implant. For example, high surface-to-volume implants such as fabrics or porous

materials will have higher ratios of macrophages and foreign body giant cells in the implant site than will smooth-surface implants, which will have fibrosis as a significant component of the implant site.

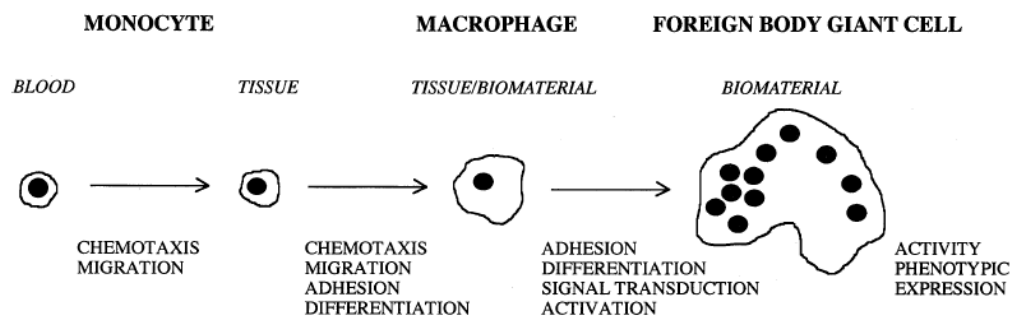


Figure 2.3 *In vivo* transition from blood-borne monocyte to biomaterial adherent monocyte/macrophage to foreign body giant cell at tissue/biomaterial interface [10]

Fibrosis or fibrous encapsulation is the end-stage healing response to biomaterials. The regeneration is the replacement of injured tissue by parenchymal cells of the same type, or replacement by connective tissue that constitutes the fibrous capsule.

2.1.2 Evaluation of the biomaterial-tissue interactions as following ISO10993-6 [7].

This part specifies methods for the assessment of the local effects after implantation of biomaterials intended for use in medical devices. The implanted tissue region is allowed to heal, explant and examine for macroscopic and microscopic tissue responses. Responses of the test implant sites are generally compared with the responses of similar sites implanted with control materials for using in medical devices which have been established. The test sample shall be implanted into various tissues such as subcutaneous, muscle and bone to the suitable field of application as shown in Table 2.3.

Table 2.3 Principle for various implant sites [7].

Implantation sites	Principle	Size of implanted sample
Subcutaneous	Compare the effect of different surface textures or modifications of a material	Diameter : 10-12 mm Thickness : 0.3-1.00 mm
Muscle	Compare the biological response to implant of implanted test sample with the biological response to implant of control sample.	Diameter : 10 mm Thickness : 1-3 mm (for rabbit paravertebral muscle)
Bone	Compare the biological response to implant of test samples with the biological response to implant of control sample.	Diameter : 2 mm Thickness : 6 mm (for rabbit bone)

2.1.2.1 Test periods

The test period shall be determined by the likely clinical exposure time or beyond a steady state has been reached with respect to the biological response.

For non-degradable and non-resorbable materials the short-term response are normally assessed from 1 week up to 4 weeks and the long-term responses in tests exceeding 12 weeks.

For degradable/resorbable materials the test period shall be related to the estimated degradation time of the test product. Before starting with animal studies and determining the time points for sample evaluation, an estimation of the degradation time shall be made. This can be done *in vitro* by real-time or accelerated degradation studies.

2.1.2.2 Evaluation

The explant sites, both test and control, are evaluated for macroscopic and microscopic tissue responses.

Macroscopic assessment

Each implant site shall be examined for alterations of the normal

structure. This should include assessment of the regional draining lymph nodes. Use of a lens with magnification is recommended. Record the nature and extent of any tissue reaction observed such as haematoma, oedema, encapsulation and additional gross findings. Macro photography shall be used for documentation. In addition to the inspection of the implant site, whenever an animal has shown signs of ill health or reactions to the implant, a gross necropsy as appropriate shall be conducted.

Microscopic assessment

The scoring system used for the histological evaluation shall take into account the extent of the area affected either quantitatively or semi-quantitatively. The biological response parameters, which shall be assessed and recorded, include :

- the extent of fibrosis/fibrous capsule and inflammation.
- the degeneration as determined by changes in tissue morphology.
- the number and distribution as a function of distance from the material/tissue interface of the inflammatory cell types, namely polymorph nuclear neutrophil leukocytes, lymphocytes, plasma cells, eosinophils, macrophages and multinucleated cells.
- the presence, extent and type of necrosis.
- other tissue alternations such as vascularization, fatty infiltration, granuloma formation and bone formation.
- the material parameters such as fragmentation and debris presence.
- the quality and quantity of tissue ingrowth.

2.1.3 Characteristic and function of inflammatory cell types [12,13]

White cells are responsible for the defense of the organism. In the blood, they are much less numerous than red cells. The density of the leukocytes in the blood is 5000-7000 /mm³. Five types of leukocyte are normally present in the circulation. These are traditionally divided into two main groups based on their nuclear shape and cytoplasmic granules : granulocytes and lymphoid cells or agranulocytes. Each type of leukocyte is presented in the blood in different proportions as shown in Table 2.4.

Table 2.4 Approximate percentages of leukocytes in adult human blood [12]

Leukocyte type	Concentration in blood (%)
Neutrophil	62.00 %
Eosinophil	2.30 %
Basophil	0.40 %
Lymphocyte	30.00 %
Monocyte	5.30 %

2.1.3.1 Type of white blood cells

- Granulocytes

The granulocytes have a single multilobed nucleus which may assume many morphological shapes leading to use of the term polymorphonuclear leukocytes (PMNs) as a synonym for the term granulocytes. Granulocytes are the only white blood cells to be formed in the bone marrow. There are three types of granulocytes identified as neutrophils, eosinophils and basophils. In the different types of granulocytes, the granules are different and help us to distinguish them.

Neutrophil : Neutrophils are the more common leukocytes. The diameter is around 12-15 micrometers. The average half-life of neutrophil in the circulation is about 12 hours.

Characteristics of neutrophils on hematoxylin and eosin : Their nucleus is



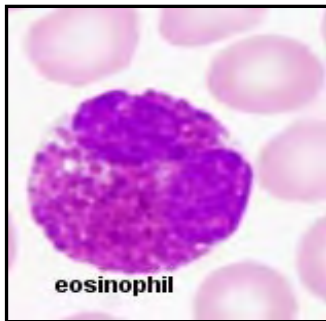
divided into 2 - 5 lobes connected by a fine nuclear strand or filament as in Fig 2.4. The cytoplasm is transparent because its granules are small and faintly pink colored. Immature neutrophils have a band-shaped or horseshoe-shaped nucleus and are known as band cells.

Figure 2.4 Neutrophil [13].

Function : Their principal function is in the acute inflammation response to tissue injury. Neutrophils quickly congregate at a focus of infection, attracted by cytokines expressed by activated endothelium, mast cells and macrophages. Neutrophils are phagocytes, capable of ingesting microorganisms or particles, particularly bacteria.

Eosinophil : Eosinophils are quite rare in the blood. Eosinophils are about 12-17 micrometers in size. Eosinophils develop and mature in bone marrow. After maturation, eosinophils circulate in blood and migrate to inflammatory sites in tissues. The lifespan of eosinophils is unknown.

Characteristics of eosinophils on hematoxylin and eosin : Eosinophils are



large, bright, pink granules that fill the cytoplasm. These cells are eosinophilic or 'acid-loving' normally transparent. They appear brick-red when stained with eosin. The specific granules within the cellular cytoplasm contain many chemical mediators such as histamines and proteins. The nucleus is typically bilobed, but small, third lobe

Figure 2.5 Eosinophil [13] may be present.

Function : Eosinophils function specifically as phagocytes to destroy larvae of parasites that have invaded tissues i.e. in trichinosis, schistosomiasis. Eosinophils appear to play a role in allergic responses. Other functions of eosinophils include phagocytosis of antigen antibody complexes.

Basophil : Basophils are the least common of the granulocytes and constitute less than 1% of leukocytes. Basophils are about 14-16 micrometers in size. Basophils are intermediate in size between neutrophils and eosinophils. The lifespan of basophils is unknown.

Characteristics of basophils on hematoxylin and eosin : Basophils are more



variable in size. The nucleus is not markedly lobulated and stains pale basophilic. The cytoplasm is full of dark purple specific granules.

Figure 2.6 Basophil [13]

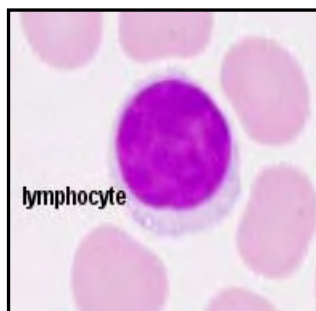
Function : Basophils are also phagocytic, but function largely like mast cells. These granules contain histamine and heparin which play an important role in initiation of the acute inflammatory response.

- Agranulocytes

Agranulocytes have non-lobulated nuclei and were described as mononuclear leukocytes. There are two types of agranulocytes identified as lymphocytes and monocyte.

Lymphocytes : Lymphocytes are about 9 to 14 micrometers in size. They are the smallest cells in the white cell series. There are actually two functional types of lymphocytes, one responsible for cell mediated immune reactions (T-cells) and the other for humoral immunity (B-cells). Both T and B cells are derived from stem cells in the bone marrow. Immature T lymphocytes migrate from the bone marrow to the thymus where they develop into mature T.

Characteristics of lymphocytes on hematoxylin and eosin : Lymphocytes look



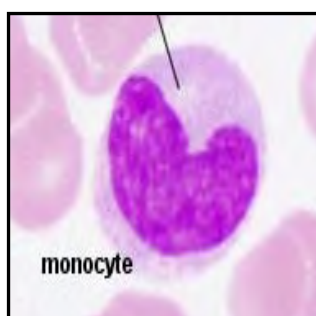
like little cells with a compact round nucleus which occupies nearly all the cellular volume. T and B lymphocytes are morphologically indistinguishable.

Figure 2.7 Lymphocyte [13]

Function : Lymphocytes are a defense against the attack of pathogenic microorganisms such as viruses, bacteria, fungi and protista.

Monocyte : Monocytes are about 12 to 20 micrometers in size. They migrate into the connective tissue, where they become macrophages or dendritic cell.

Characteristics of monocytes on hematoxylin and eosin : This large cell has a lightly



stained nucleus that often appears horseshoe or kidney shaped. The cytoplasm of the monocyte will stain a blue-gray color.

Figure 2.8 Monocyte [13]

Function : Monocytes are responsible for phagocytosis (ingestion) of foreign substances in the body. Monocytes can perform phagocytosis using intermediary (opsonising) proteins such as antibodies or complement that coat the pathogen.

2.2 Biomaterials

2.2.1 Silk

There are two types of silk [14]

- Mulberry silks (*Bombyx mori*)

The silkworm is the larva of *Bombyx mori* which is the domesticated silkworm. The silkworms are fed on a diet exclusively of mulberry leaves. Mulberry silk fibers are finer and softer than wild silk fibers.

- Wild silks

A variety of wild silks have been known and used in China, India, and Europe. The most common type of wild silks is Tussah Silk. Silkworms live on oak leaves instead of mulberry leaves consumed by cultivated species. Wild silks have a tan color derived from the tannin in the oak leaves, coarse in texture and cannot be bleached.

Thai silk is a *Bombyx mori* type. Thai silk cocoons are different from other *Bombyx mori*. Thai cocoons are yellow and contain more sericin than other domesticated cocoons. In this research, Nangnoi-Srisaket 1 was used to fabricate the silk fibroin scaffolds because this specie exhibits the good properties which passed to elect from department of agriculture on 19 December 1988 [15,16].

Structure and properties of silk [2,3,4]

- Structure of silk

Silk is generally defined as protein polymer fiber. Normally, silk fiber consists of two types of self-assembled proteins: fibroin and sericin. The core fibroins are encased in a coat of sericin, a family of hydrophilic proteins which holds two fibroin fibers together as shown in Figure 2.9. The structure of silk fiber was shown in

Table 2.5. Silk fibroin consists of two protein components: a light chain and a heavy chain, which are present in a 1:1 ratio and linked by a single disulphide bond.

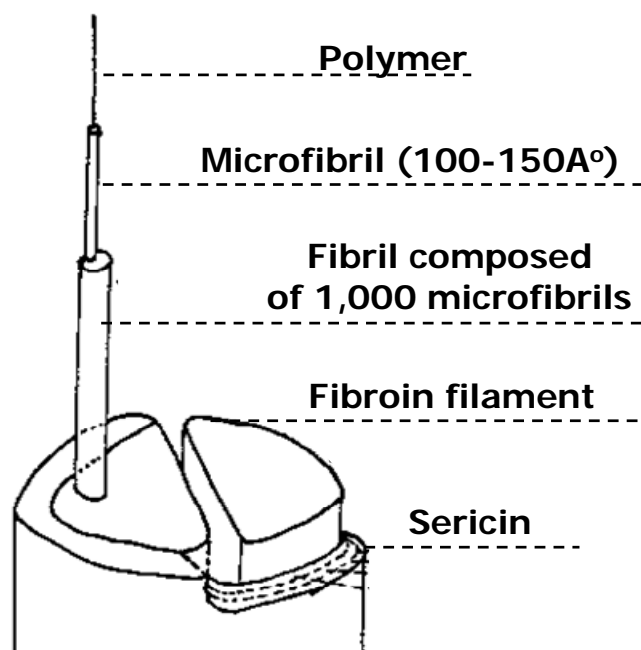


Figure 2.9 Structure of raw silk fiber [17]

Table 2.5 Structure of silk fiber [18]

Silk fiber	Silk fibroin (72-81%)		Silk sericin (19-58%)
	Heavy chain	Light chain	a glue-like protein
Molecular Weight	325 kDa	25 kDa	~300 kDa
Polarity	Hydrophobic		Hydrophilic
Structure	Silk I (random coil-or unordered structure)		
	Silk II (crystalline structure)		non-crystalline-structure

Silk fibroin fibers are about 10-25 micron in diameter. Silk fibroins are characterized as natural block copolymer composed of hydrophobic blocks with short side-chain amino acids such as glycine and alanine, and hydrophilic blocks with

larger side chain at the chain ends are present as shown in Figure 2.10. The former blocks lead to β -sheets or crystals through hydrogen bonding. The two main distinct structures in silk fibroin are Silk I and Silk II. The structure of Silk I contains random-coil and amorphous regions. The Silk II structural form of the silk fibroins has been characterized as an antiparallel β -sheet structure (Figure 2.11).

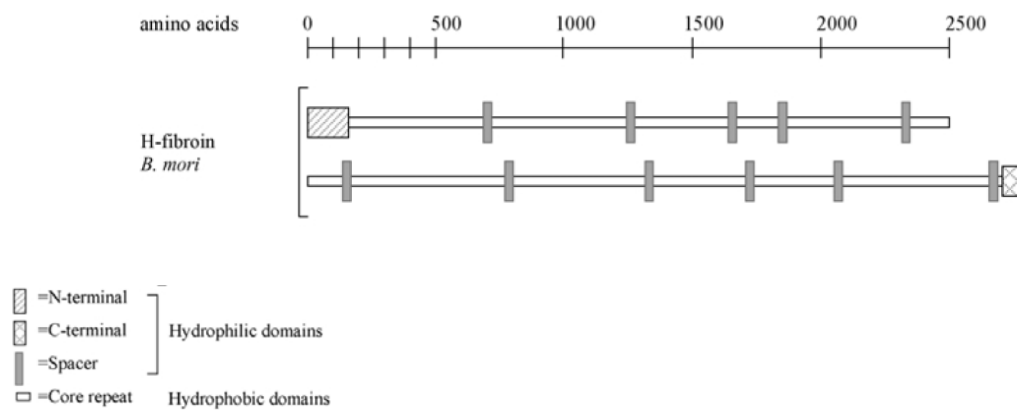


Figure 2.10 Organization of hydrophilic and hydrophobic domains in fibroin [19].

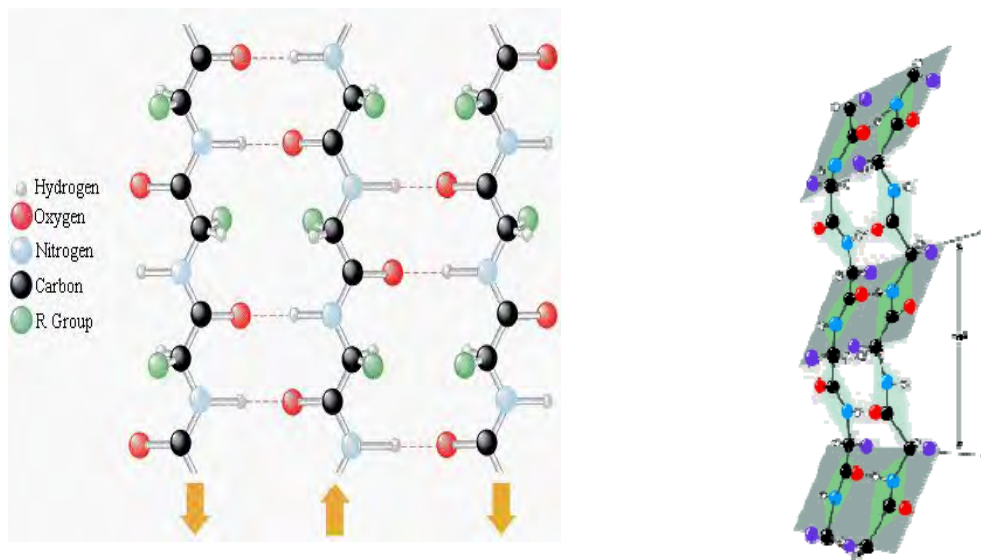


Figure 2.11 Structure of antiparalle β -sheet [20]

- Properties of silk

- Silk provides an excellent combination of lightweight (1.3 g/cm^3).
- Silk has high tensile strength.
(up to 4.8 GPa as the strongest natural fibers)
- Silk has remarkable toughness and elasticity (up to 35%).
- Silk is thermally stable up to about 250°C .

Silk fibroin fibers are insoluble in most solvents such as water, ethanol, dilute acids and bases which are soluble in highly concentrated sulfuric acid, formic acid, hexafluoroisopropanol (HFIP), calcium nitrate or LiBr solutions.

Silk sericin is soluble in water. Virgin silk (fibroin containing sericin gum) is potential allergen but degummed silk in which sericin is removed is biocompatible. The process of degumming can be achieved by dissolving in sodium carbonate for 20 min.

Silk fibroin scaffold fabrication for bone tissue engineering.

Silk fibroin material can be fabricated in various forms for bone tissue engineering e.g. hydrogel [21], nanofiber [22], porous sponge [23].

Porous sponges formed using freeze drying, gas foaming and porogens (salt-leaching) methods for bone tissue engineering, can provide temporary mechanical strength to the affected area and contain a porous architecture to allow for vascularization and bone ingrowth. Recently, it was reported that compressive strength of fibroin scaffolds formed by gas foaming, salt leaching and freeze drying were 280 ± 4 , 175 ± 3 and 30 ± 2 kPa, respectively and compressive modulus of fibroin scaffolds were 900 ± 94 , 450 ± 94 and 100 ± 1 kPa, respectively. The gas foamed and salt leached scaffolds had a higher compressive strength and compressive modulus than the freeze dried scaffolds. So gas forming and salt leaching methods were used to form three-dimensional silk biomaterial for bone tissue engineering [24]. Salt-leached silk fibroin scaffolds were derived from regenerated *B.mori* silk fibroin solution using either all aqueous process or organic solvent (HFIP) process as shown in Figure 2.12.

For aqueous-derived silk fibroin scaffolds fabrication via salt-leaching, cocoons were boiled in an aqueous solution of Na_2CO_3 to remove sericin and then

rinsed thoroughly with deionized water. The obtained silk fibroin was dried and dissolved in 9.3M LiBr solution at 60°C for 4 h. This solution was dialyzed in deionized water (MWCO 3500, Pierce) for 2 days. The silk fibroin aqueous solution was filled in container and NaCl granular was added. When the silk solution stayed in the same system with NaCl granular, the salt ion extracted water in silk solution to coat the hydrophobic fibroin domains, promoting chain–chain interactions leading in β -sheet formation as shown in Figure 2.13 [25]. The container was left overnight at room temperature to let gelation from. After that, salt was rinsed out resulting in three-dimensional porous scaffolds.

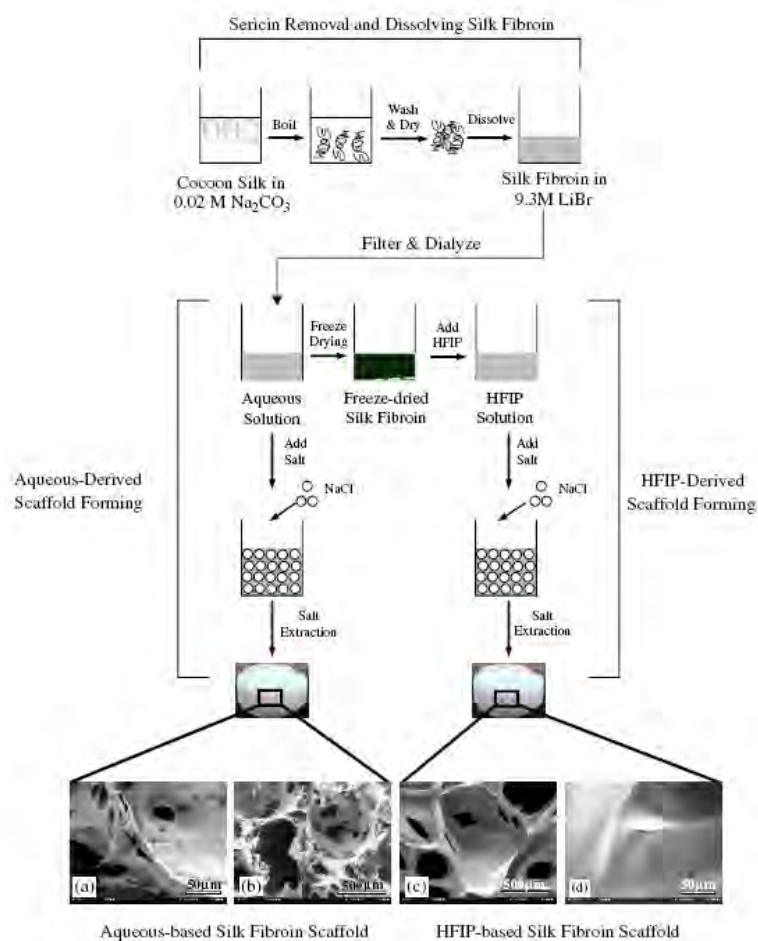


Figure 2.12 Processing silk fibroin into 3D porous scaffolds [3].

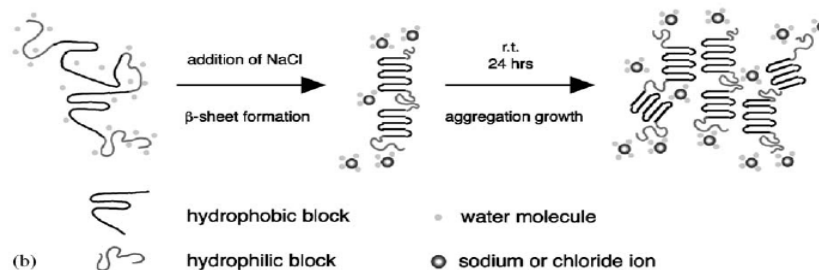


Figure 2.13 Structural silk fibroin transition from random coil to β -sheet structures [25]

For HFIP-derived silk fibroin scaffolds, the aqueous silk fibroin solution was freeze-dried prior to redissolve in HFIP. The salt-leached scaffolds from HFIP were obtained using the same procedures as in the case of aqueous derived scaffolds. Figure 2.12 showed that the aqueous-derived scaffolds have better pore interconnectivity, rougher and more hydrophilic surfaces than the HFIP-derived scaffolds.

2.2.2 Gelatin [26]

There are two types of gelatin as shown in Figure 2.14.

- Type A gelatin, with iso-electric point 9, is derived from acid processed materials and called basic gelatin. In the acid process, amide groups of collagen is hydrolyzed to obtain the iso-electric point of Type A gelatin similar to collagen.

- Type B gelatin, with iso-electric point of 5, is derived from alkaline or lime processed materials and called acid gelatin. In the alkaline process, amide groups of collagen is hydrolyzed into carboxyl groups which makes gelatin negatively charged.

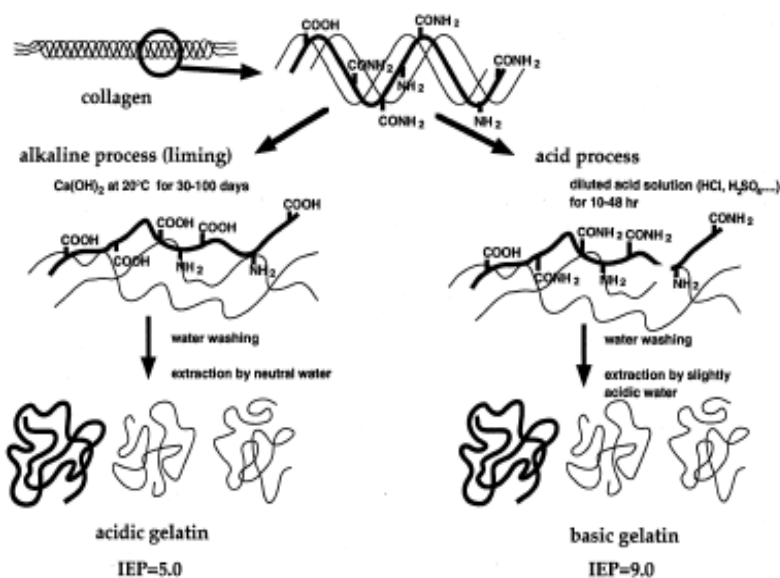


Figure 2.14 Preparation processes for acidic and basic gelatins from collagen [26].

Structure and properties of gelatin [27,28]

- Structure of gelatin

Gelatin is a denatured form of collagen. Gelatin is a heterogeneous mixture of single or multi-stranded polypeptides, each with extended left-handed proline helix conformation and containing between 300-4,000 amino acids. Gelatin contains many glycine (almost 1 in 3 residues, arranged every third residue), proline and 4-hydroxyproline (4-Hyp) residues. A typical structure is –Ala-Gly-Pro-Arg-Gly-Glu-4Hyp-Gly-Pro- as shown in Figure 2.15.

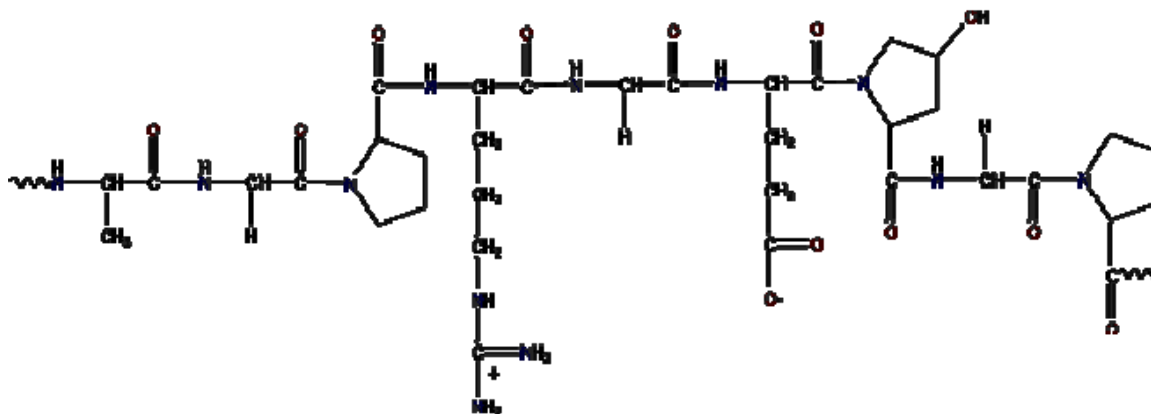


Figure 2.15 Structure of gelatin [26]

- Properties of gelatin

- Gelatin is yellowish.
- Gelatin is amphoteric. It is neither acidic nor alkali depending on the production process.
- Gelatin is soluble in hot water, glycerol, and acetic acid, and insoluble in organic solvents.
- Gelatin forms thermally reversible gels with water, and the gel melting temperature (<math><35^{\circ}\text{C}</math>) is below body temperature.

Since gelatin is water soluble, crosslinking process of gelatin is often necessary to improve the resistance against enzymatic degradation. Glutaraldehyde is one of a high effective reagent. However, the toxic effect of glutaraldehyde was its disadvantage as well known. The 1-ethyl-3-(3-dimethylaminopropyl) carbodiimide (EDC) and N-hydroxysuccinimide (NHS) reagent was introduced as an alternative crosslinking agent. The crosslinking reaction of gelatin crosslinked by EDC/NHS was illustrated in Figure 2.16. The carboxylic acid residues of glutamic and aspartic acid on gelatin chains are activated with EDC. The activated carboxylic acid groups can react with free amine groups to form an O-acylisourea intermediate. This intermediate may react with amine function to yield amine bond. However, the intermediate is also the susceptible to hydrolysis. The addition of NHS produces a more stable amine reactive, converting to an amine reactive NHS ester intermediate. The intermediate allows the carboxyl groups on one protein to remain unaltered.

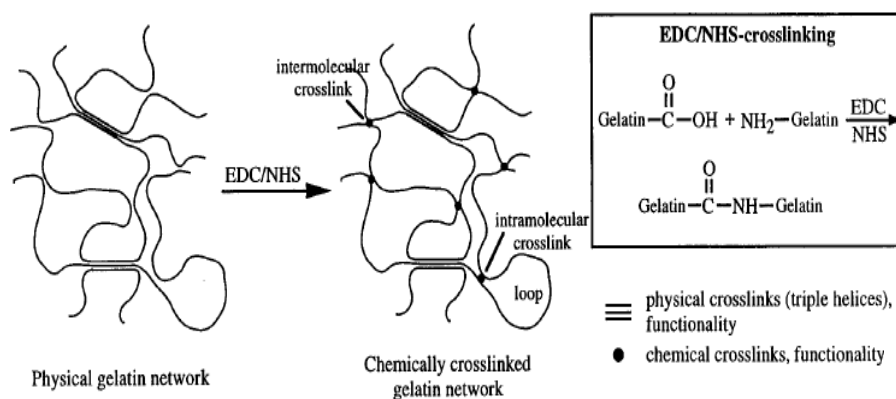


Figure 2.16 Reaction of chemically crosslinked gelatin network [29]

2.2.3 Hydroxyapatite [30, 31]

Hydroxyapatite ($\text{Ca}_{10}(\text{PO}_4)_6(\text{OH})_2$) is one of the implant materials for medical application. It is the major mineral component of natural bones with excellent biocompatibility, osteoconductivity and bioactivity. Pure hydroxyapatite has a theoretical Ca/P ratio of 1.67.

Structure and properties of hydroxyapatite [32,33]

- Structure of hydroxyapatite

The structure of hydroxyapatite (HAp) contains Ca^{2+} , PO_4^{3-} and OH^- as major components. Hydroxyapatite has two different structures in a hydroxyl arrangement; hexagonal and monoclinic structure as shown in Figure 2.17. Hexagonal hydroxyapatite (space group $P6_3/m$) has a disordered hydroxyl arrangement along c-axis and the hydroxyl ions are pointed in upper and lower directions. In contrast, monoclinic hydroxyapatite (space group $P2_1/b$) has an ordered hydroxyl arrangement along hydroxyl columns, and hydroxyl ions are aligned in the same direction.

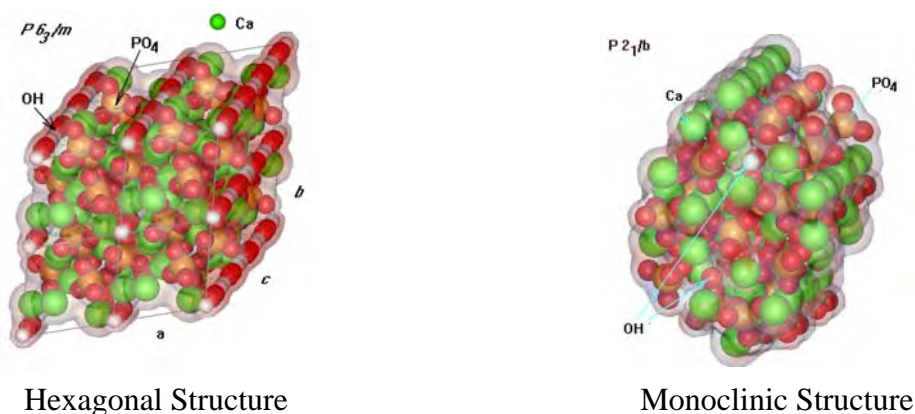


Figure 2.17 Structure of hydroxyapatite [31]

- Properties of hydroxyapatite

- Pure hydroxyapatite is white. Naturally occurring apatite has brown, yellow or green colorations.

- Hydroxyapatite has a specific gravity of 3.08. It is 5 on the Mohs hardness scale.
- Hydroxyapatite is a thermally unstable compound. It is decomposed at temperature about 800 - 1200°C depending on its stoichiometry.

Several fabrication processes of hydroxyapatite–polymer composites have been reported, i.e. biomimetic process, plasma spraying, and co-precipitation methods. Recently, Akashi *et al* developed a novel apatite formation process using an alternate soaking process to form large amounts of apatite in a remarkably short time [34]. An alternate soaking process was introduced to deposit hydroxyapatite on the substrate as shown in Figure 2.18. The substrates were immersed in calcium chloride solution and then were removed to immerse in disodium hydrogenphosphate solution. This is considered as one cycle of alternate soaking. The reaction of hydroxyapatite formation by alternate soaking process is as follows.

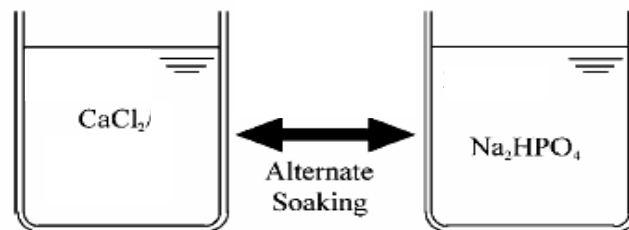
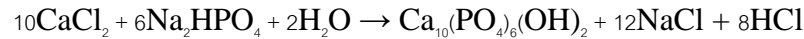


Figure 2.18 Alternate soaking process. [30]

2.3 Biodegradation of biomaterials [8, 11, 18]

The biodegradation of biomaterials is important in terms of restoring full tissue structure and function. The rate of scaffold degradation matches the rate of tissue ingrowths. Biodegradation is the chemical breakdown of materials by the action of living organism which leads to change in physical properties such as tensile strength and morphology. After polymers have been implanted and exposed to

chemical degradation *in vivo*. The analysis of chemically degraded polymers has always implicated either hydrolysis or oxidation process.

Hydrolysis is the scission of susceptible molecular functional groups by reaction with water. It may be catalyzed by acids, bases, salts, or enzymes. It is a single-step process of which the rate is directly proportional to the rate of reaction. A polymer's susceptibility to hydrolysis is the result of its chemical structure, its morphology, its dimension and the body's environment. In a commonly used category of hydrolysable polymeric biomaterials, functional groups consist of carbonyls bonded to heterochain elements (O, N, S). Examples include esters, amides and carbonates. Groups (Hydrocarbon, Halocarbon, Dimethylsiloxane and Sulfone) are normally very stable to hydrolysis. The rate of hydrolysis tends to increase with a high proportion of hydrolyzable groups in the main or side chain, other polar groups which enhance hydrophilicity, low crystallinity and low crosslink density.

Oxidation process induced by phagocyte is the result of oxidants produced by general foreign body responses. Both polymorphonuclear and macrophage metabolize oxygen to form a superoxide anion. Superoxide dismutase can catalyze the conversion of superoxide to hydrogen peroxide. Hydrogen peroxide is converted to hypochlorous acid (HOCl) by myeloperoxidase (MPO) derived from PMNs. Hypochlorite can oxidize free amine function to chloramines that can perform long-lived sources. Hypochlorite can oxidize other substituted nitrogen functional groups (amides, ureas, urethanes etc.) with potential chain cleavage of these groups. The direct oxidation focused primarily on acute implant periods in which bursts of PMNs activity followed by macrophage activity resolve within weeks.

Silk is classified as non-degradable according to the US Pharmacopeia's definition. However, from the literature, it can be considered as a degradable material. The reason may be connected to the fact that silk degradation behavior is usually mediated by a foreign body response. Different from synthetic materials, the degradable behavior of silk fibroins doesn't lead to an immunogenic response. Biodegradation is the breakdown of polymer materials into smaller compounds. The processes vary greatly, and the mechanisms are complex. Normally, they encompass physical, chemistry and biological factors. Depending on the mode of degradation, silk fibroins can be classified as enzymatically degradable polymers. Enzymes play a

significant role in the degradation of silk fibroins. Due to their enzymatic degradability, unique physic-chemical, mechanical and biological properties of silk fibroins have been extensively investigated. The enzymatic degradation of biomaterials is a two-step process. The first step is adsorption of the enzyme on the surface of the substrate through surface-binding domain and the second step is hydrolysis of the ester bond.

In vivo studies, silk material was implanted under the skin of rats *in vivo*. After 6 weeks post-implantation, 55% of silk tensile strength and 16% of elastic modulus were found to be lost. Silk fibers lose the majority of their tensile strength within 1 year *in vivo*, and fail to be recognized at the site within 2 years.

Some researchers have indicated that variable rates of silk absorption *in vivo* are dependent on the animal model and tissue implantation site (Table 2.6).

Table 2.6 Silk fibroin degradation *in vivo* [18]

Type of silk	Implantation site	Mechanism	Degree and measure of degradation
Black braided	Rat/Subcutaneous	Unknown/assumed Foreign body reaction	55% loss in tensile strength 6 weeks <i>in vivo</i>
Black braided	Rat/Subcutaneous	Unknown/assumed Foreign body reaction	83% loss in tensile strength 10 weeks <i>in vivo</i>
Black braided	Rat/abdominal wall muscle	Foreign body reaction	83% loss in tensile strength 10 weeks <i>in vivo</i>
Virgin silk wall muscle	Rabbit/abdominal wall muscle	Foreign body reaction	fragmentation following 4 weeks <i>in vivo</i>

Literature reviews

The literature reviews are summarized into four parts as follows:

1. *In vitro* degradation of silk fibroin
2. *In vivo* degradation of silk fibroin
3. Tissue responses to silk fibroin, gelatin and hydroxyapatite
4. Evaluation the tissue response to subcutaneously implantation or intramuscular implantation

***In vitro* degradation of silk fibroin**

Li M, *et al* [35]

In 2003, Li M *et al* investigated the degradation behavior of porous silk fibroin sheets in enzymatic solution; α -chymotrypsin, collagenase IA, and protease XIV. The silk fibroin sheets were immersed in various enzyme solution at 37°C for 1, 3, 6, 12 and 15 days. The weight of the fibroin sheets immersed in either protease XIV or collagenase IA extensively decreased as increasing the degradation time. After 15 days, the weight of the sheet immersed in both α -chymotrypsin and phosphate buffer was 68% of its starting weight. α -chymotrypsin did not digest the porous silk fibroin sheets because of the similarity of the digestion profile that of the phosphate buffer alone. X-ray diffraction studies suggested that the small amount of Silk II crystalline structure originally present in the porous silk fibroin sheet disappeared after degradation in protease XIV. Scanning electron micrographs of the porous silk fibroin sheets showed that the internal pore size in the sheet increased with increasing degradation time, until the sheet collapsed. The average molecular weight of the samples after degradation in three enzymes followed the order : protease XIV < collagenase IA < α -chymotrypsin.

Takayuki A, et al [36]

In 2004, Takayuki A *et al* investigated *in vitro* biodegradation behavior of *Bombyx mori* silk fibroin fibers and films that were incubated with proteolytic enzymes (collagenase type F, α -chymotrypsin type I-S, protease type XXI) from 1 to 17 days. It was found that both breaking load and elongation at break of silk fibers decreased with increasing contact time with enzyme as determined by tensile properties. Upon incubation with proteolytic enzymes, silk films exhibited a noticeable decrease of sample weight and degree of polymerization, the extent of which depended on the type of enzyme, on the enzyme-to-substrate ratio, and on the degradation time. Protease was more aggressive than α -chymotrypsin or collagenase. The biodegraded films indicated an enrichment in glycine and alanine sequences characteristic of the crystalline domains as determined from amino acid composition. FTIR measurements showed that the degree of crystallinity of biodegraded films increased. Biodegraded fibers showed an increase of surface roughness, while films displayed surface cracks and cavities with internal voids separated by fiber-like elements. Silk fibroin is susceptible to proteolytic attack but the extent of degradation depends on the structure and morphology of the substrate.

Horan RL, et al [37]

In 2005, Horan RL *et al* studied the degradation of *Bombyx mori* silk fibroin yarns *in vitro*. Silk fibroin yarns were incubated in 1 mg/ml Protease XIV at 37°C and harvested at designated time points up to 12 weeks to create an *in vitro* model system of proteolytic degradation. Negative control samples were incubated in phosphate-buffer saline. At designated time point, the morphology of samples was examined using scanning electron microscopy (SEM). SEM indicated increasing fragmentation of individual fibroin filaments from protease-digested samples with time of exposure to the enzyme. Particulate debris of silk fibroin was presented within 7 days of incubation. Gel electrophoresis indicated that both 325 kDa heavy chain and 25 kDa light chain were degraded with increased exposure time to protease. FTIR data indicated hydrolysis of the non crystalline domains.

Zhending S, et al [38]

In 2008, Zhending S *et al* studied the *in vitro* degradation of three-dimensional porous silk fibroin/chitosan (SFCS) scaffolds prepared by freeze-drying method. SFCS scaffolds were incubated in phosphate buffer saline solution at 37°C up to 8 weeks. The following properties of the scaffolds were measured as a function of degradation time: pore morphology, structure, weight loss, and wet/dry weight value. The pH value of the PBS solution during degradation was also detected. During the first 2 weeks, the pH value fluctuated in a narrow range from 6.53 to 6.93. SFCS scaffolds degraded much more quickly during the first 2 weeks, the structure change of silk fibroin from β -sheet to random coil form during the 6 weeks of degradation as determined by X-ray diffraction, and the weight loss reached 19.28 wt% after 8 weeks of degradation. SFCS scaffolds can maintain its porous structure till 6 weeks of degradation. Three-dimensional SFCS scaffolds have been proved to be a potential tissue engineering matrix with homogeneous porous structure, suitable pore size and mechanical properties.

In vivo degradation of silk fibroin**Wang Y, et al [39]**

In 2008, Wang Y *et al* systematically investigated the *in vivo* response to three-dimensional silk fibroin porous scaffolds with varying pore sizes, silk fibroin solution concentration and processing method (aqueous vs. organic solvent). The scaffold morphological changes and tissue ingrowth samples were analyzed by histology. The immune responses were examined by real-time RT-PCR and immunohistochemistry. Most scaffolds prepared from all-aqueous process degraded to completion between 2 and 6 months, while those prepared from organic solvent (hexafluoroisopropanol (HFIP)) process persisted beyond 1 year. In general, especially for the HFIP-derived scaffolds, a higher original silk fibroin concentration (e.g. 17%) and smaller pore size (e.g. 100–200 μ m) resulted in lower levels of tissue ingrowth and slower degradation. These results demonstrate that *in vivo* behavior of

the three-dimensional silk fibroin scaffolds is related to the morphological and structural features that resulted from different scaffold preparation processes.

Tissue responses to silk fibroin, gelatin and hydroxyapatite

- **Silk**

Meinel L, *et al* [2]

In 2005, Meinel L *et al* reported the biocompatibility of silk films (with or without covalently bound RGD) that were seeded with bone-marrow derived mesenchymal stem cells (MSC) and cultured *in vitro*. Silk films were seeded with autologous rat MSC and implanted *in vivo*. Controls for *in vitro* studies included tissue culture plastic (TCP) as negative control, TCP with lipopolysaccharide in the cell culture medium as positive control. Controls for *in vivo* studies included collagen and polylactic acid. Collagen as negative control is a FDA approved implant material to minimal tissue reaction after implantation. From *in vitro* test, overexpression of IL-1 β and COX-2 genes was observed after 9 h. The transcript level rapidly declined and reached the level of cells grown on tissue culture plastic. This result found that the expression of IL-1 β gene was stronger on collagens than silk or silk-RGD films. The same results were observed for the expression of COX-2 gene. More PGE₂ was produced by bone-marrow derived mesenchymal stem cells grown on collagen than on silk films. From *in vivo* test, silk film, collagen and polylactic acid were seeded with rat MSCs, implanted intramuscularly in rats and harvested after 6 weeks. Histological and immunohistochemical evaluation of silk film revealed the presence of oriented fibroblast, the collagen fibers around implant's surface and a small layer of macrophage. From histology, the surface reaction of implanted collagen films was stronger than silk. The strongest inflammatory response was elicited around polylactic acid with considerable numbers of giant cells present.

Gellynck K, et al [40]

In 2008, Gellynck K *et al* studied the biodegradation *in vitro* and *in vivo* of enzymatically spider egg sac silk (SpESS) cleaned. *In vitro* tests were performed to compare the rates of the decrease of the mechanical properties of spider egg sac silk, silkworm silk fiber (SWS) and Vicryl[®] after incubation in phosphate buffered saline at 37°C up to 12 weeks. Biodegradation of SpESS and SWS was insignificant compared to Vicryl[®]. *In vivo* tests, Spss fibers were treated with trypsin only or in combination with Proteinase K before subcutaneously implanted in Wistar rats. After 1, 4 and 7 weeks, the local reaction was compared to Vicryl[®] using the methods described in ISO 10993-6. The inflammatory reaction was compared to untreated SpESS and Vicryl[®] control samples. SpESS samples treated with trypsin only or in combination with a Proteinase K treatment induced less inflammatory reactions than untreated silk fibers. The enzymatical cleaning could diminish the tensile properties, but enhanced the biocompatibility of the SpESS fibers rendering them appropriate for use in biomaterial application where the slow biodegradability is an advantage.

• Gelatin**Burugapalli K, et al [41]**

In 2004, Burugapalli K *et al* studied full and semi-interpenetrating polymer networks (IPN) based on polyacrylic acid (AAc) and gelatin (Ge) crosslinked with N,N-methylene bisacrylamide and glutaraldehyde, respectively. IPNs with varying ratios of AAc and Ge were implanted subcutaneously in rats. Gentamicin sulfate (GS)-loaded IPN samples were also studied to evaluate the possible therapeutic use of these polymers. The site of implantation was biopsied and processed for light microscopy with image analysis for assessment of tissue reaction at 2-, 6-, and 12-week intervals. The degree of neutrophil, lymphocyte and macrophage infiltration, fibrosis, granuloma formation, integration with extracellular matrix, vascular proliferation, and damage of adjacent structures were assessed. Polymers with >66% crosslinked Ge showed persistence of acute inflammatory reaction till 3 months, with

marked tissue injury and fibrosis. On the other hand, high crosslinked AAc content showed chronic inflammatory reaction with high macrophage infiltration. Macrophages took active part in phagocytosis. The IPNs with acrylic acid and gelatin in the ratio of 1:1 showed least tissue reaction and thus appeared to be most biocompatible. The majority of the polymers showed integration with extracellular matrix and growth of capillaries in and around the polymer. GS loading showed no additional local or systemic reaction suggesting the potential usefulness of the hydrogels as carrier for drugs such as GS.

• Hydroxyapatite

Ye Q, *et al* [42]

In 2000, Ye Q *et al* evaluated the histological response of rat middle ear mucosa following implantation of Apaceram[®] granules, a synthetic dense hydroxyapatite [$\text{Ca}_{10}(\text{PO}_4)_6(\text{OH})_2$], prepared from commercially available synthetic auditory ossicle. The microscopic examination of mucosal tissue at various time points after implantation was assessed the precise histological response of the rat middle ear. Apaceram[®] granules were implanted in the temporal bulla of 32 rats. As control, sham surgery was performed in a group of ten rats. Bulla specimens were removed at 1, 3, 7, 14, and 30 days after surgery in the implant and control groups, and at 90, 180 and 300 days in the implant group. Specimens were decalcified, sectioned at a thickness of 6 mm, and stained with hematoxylin and eosin, and Mallory's azan for histological examination of mucosal tissue. Evidence of inflammatory reaction was slightly greater in the implant group than in controls. Lymphocyte and macrophage counts were higher in the implant group 1 day after surgery, but decreased to similar levels by day 3, and continued to decrease thereafter, and few were observed in the implant group at 300 days. Neutrophils observed at 1 day after surgery were not evident in either group at 3 days. Gradual fibrosis development continued in both groups over all time points studied. Foreign body giant cells were never observed in either group. No bony reaction was observed in any

specimen. The results of this study suggest that Apaceram[®] is biocompatible and suitable for reconstructive ear surgery.

Evaluation the tissue response to subcutaneously implantation or intramuscular implantation

- **Subcutaneous implantation**

Lehle K, *et al* [43]

In 2003, Lehle K *et al* evaluated the influence of titanium-coated polymers on the inflammatory response and remodeling of connective tissue during wound-healing processes. Discs of polyethyleneterephthalate (PET) and silicone as well as high-weight meshes of polypropylene (PP) were coated with a titaniumcarboxonitride layer by a plasma-assisted chemical vapor deposition process and implanted subcutaneously in the dorsal lumbar region of Wistar rats. Light microscopic and histological evaluation of capsule thickness, capsule quality, implant–tissue interface and collagen composition was performed 7, 14, 21 and 28 days post-operatively. All implants were surrounded by a fibrous capsule with decreasing thickness after 2–4 weeks post-implantation. Titaniumcarboxonitride-coated polymers showed no significant differences in capsule thickness and inflammatory cellular response. Ti-coating of polymers did not improve biocompatibility after subcutaneous implantation in rats. Material reduction to low-weight meshes and enlargement of pore size may demonstrate a benefit of Titanium-coated meshes with an increased biocompatibility.

Lickorish D, *et al* [44]

In 2004, Lickorish D *et al* studied the modulation of the rodent foreign body giant cell response to subcutaneously implanted, biodegradable poly(lactide-co-glycolide)/ calcium phosphate (PLGA/CaP) composites by application of a thin surface coat of calcium phosphate. Macroporous PLGA/CaP composite scaffolds, with interconnecting macroporosity, were half coated with a 3mm thick layer of CaP

by immersion in simulated body fluid. Half-coated scaffolds were implanted subcutaneously in the dorsum of male Wistar rats for 1, 4 and 8 weeks. Histomorphometry revealed that foreign body giant cells were in contact with 6% (\pm 3.5%) of the uncoated half, at 1 week, but no foreign body giant cells were seen on the coated half. By 4 weeks, foreign body giant cells were seen on both the uncoated and coated halves of the scaffolds with 87% (\pm 10%) and 36% (\pm 4%) FBGC/polymer contact respectively. By 8 weeks these foreign body giant cell contact percentages had risen to 97% (\pm 0.45%) in the case of the uncoated halves of scaffolds, but decreased to 22% (\pm 4%) in the case of the CaP-coated halves. Thus the CaP coating abrogated the foreign body giant cell response to the underlying polymer. Such a model may prove useful in providing an experimental system whereby both the mechanisms of biocompatibility and the transition from acute to chronic inflammation could be interrogated.

Macleoda TM, *et al* [45]

In 2005, Macleoda TM *et al* assessed the suitability of Permacole™ (a porcine derived, isocyanate crosslinked collagen based biomaterial) as an alternative to autologous tissue in soft tissue reconstruction. The Sprague–Dawley rat was used as a model for subcutaneous implantation over a 20 week period and comparison made with two other porcine biomaterials (small intestinal submucosa and glycerol treated ethylene oxide sterilised porcine dermis). Implants were scored histometrically on the degree of acute inflammation, chronic inflammation, fibrosis and stromal response. The vascularity and percentage composition of collagen within Permacole™ were assessed by stereology and seescan image analysis, respectively. In general terms, Permacole™ was well tolerated as a subcutaneous implant, with only a minor chronic inflammatory response remaining after a 20 week period of implantation. There was evidence of collagen degradation during this period and vascular ingrowth into Permacole™ was limited. Permacole™ has the potential for a broad range of applications in plastic surgery, but may benefit from modification to promote a more rapid degree of vascularisation.

Jong WH, *et al* [46]

In 2007, Jong WH *et al* compared two types of hydroxyethyl-methacrylated dextran (dex-HEMA) hydrogels difference in crosslink density for local tissue responses and degradation characteristics in mice and rats. Implants (1 mm thick, rat 10 mm diameter, mouse: 6 mm diameter) varying in degree of HEMA substitution (DS5 and DS13, meaning 5 or 13 HEMA groups per 100 glucose units of dextran) were subcutaneously implanted and tissue responses were evaluated at week 2, 6, and 13 after implantation. After 2 weeks in rats, a slight fibrous capsule was formed composing macrophages and fibroblasts sometimes accompanied by a minimal infiltrate. Small fragments, surrounded by macrophages and giant cells indicated hydrogel degradation. After 13 weeks, DS5 implants were resorbed while parts of the DS13 implants were still presented. In the mouse, a moderate to strong capsule formation was presented at 2 weeks accompanied by inflammatory cells (macrophages and polymorphonuclear granulocytes) and debris. Draining lymph node activation was observed. In the auxiliary and inguinal lymph nodes, a marked response was only observed at 2 weeks. This response was presented for both types of implants. At 6 and 13 weeks, this reaction was no longer present. Mice showed a more pronounced early inflammatory response compared with rats whereas the degradation was more complete in rats than in mice. Both in mice and rats, the DS5 hydrogels showed a faster degradation rate than the DS13 hydrogels. The resorption was found to be dependent on the degree of HEMA substitution of dextran used for the preparation of the hydrogels.

Satoa Y, *et al* [47]

In 2008, Satoa Y *et al* studied the *in vivo* implantation of rat of binder-free multi-walled carbon nanotube (MWCNT) blocks cross-linked by de-fluorination (de-F-MWCNT). The de-F-MWCNT blocks, MWCNT/resin blocks and poly(methyl methacrylate) materials were implanted in the subcutaneous tissue of rats for 1 week to compare a positive control which is pure Ni material. It found that the binder-free MWCNT blocks possess good biocompatibility, which were covered by thin

granulation tissue, 40– 70 μm in thickness, comprising a few lymphocytes, cell with large cytoplasmic spaces like fibroblasts and foreign-body giant cells. That is indicative of a slight inflammatory response than MWCNT/resin blocks and poly(methyl methacrylate). The inflammatory response to the pure Ni metal positive control was strong, as indicated by the many macrophages, neutrophils, necrosed tissue (no nuclei, light pink color) and diapedesis of red blood cells that were observed. The de-F-MWCNT material can potentially be employed as an alternative artificial hard tissue or internal bone plate that makes use of the properties of carbon nanotube.

Garrido G, *et al* [48]

In 2009, Garrido G *et al* investigated the biocompatibility of two experimental acetazolamide (AZ)-based pastes in the subcutaneous tissue of rats. Both pastes contained AZ as the main component in similar concentration. The vehicle in experimental paste 1 was saline, while experimental paste 2 was prepared with propylene glycol. Sixty polyethylene tubes were sealed at one end with gutta-percha (GP), which served as a control. The tubes were implanted in the subcutaneous tissue of 15 rats, being 4 tubes for each animal. The animals were killed 7, 15 and 45 days after surgery and the specimens were processed in laboratory. The histological sections were stained with hematoxylin and eosin and were analyzed by light microscopy. Scores were assigned to level of inflammatory process: 1- none; 2- mild; 3- moderate; 4- severe. Paste 1 produced an inflammatory process at 7 days. However, the intensity of this inflammation decreased with time and was nearly absent at 45 days. No statistically significant difference ($p>0.05$) was observed between the control (GP) and paste 1. However, paste 2 produced inflammatory response at all study periods and differed significantly ($p<0.05$) from the control. In conclusion, in the present study, the experimental AZ based paste 1 was considered as biocompatible as the control material (GP), while experimental paste 2 was irritating to rat subcutaneous tissue.

- **Intramuscular implantation**

Kotzara G, *et al* [49]

In 2002, Kotzara G *et al* proposed medical devices based on microelectromechanical systems (MEMS) platforms for a wide variety of implantable applications. However, biocompatibility data for typical MEMS materials of construction and processing, obtained from standard tests currently recognized by regulatory agencies, has not been published. Likewise, the effects of common sterilization techniques on MEMS material properties have not been reported. Medical device regulatory requirements dictate that materials that are biocompatibility tested be processed and sterilized in a manner equivalent to the final production device. Material, processing, and sterilization method can impact the final result. Six candidate materials for implantable MEMS devices, and one encapsulating material, were fabricated using typical MEMS processing techniques and sterilized. All seven materials were evaluated using a baseline battery of ISO 10993 physicochemical and biocompatibility tests. All seven materials were classified as non-irritants at 1- and 12-week rabbit muscle implantation.

Yang C, *et al* [50]

In 2003, Yang C *et al* evaluated a newly developed fiber optic micropressure sensor for biocompatibility using the International Organization for Standardization (ISO) test standard 10993-6. The test material and an inert control (fused silica glass) were tested in New Zealand white rabbits. Four test specimens were implanted in the paravertebral muscles on one side of the spine about 2-5 cm from the midline and parallel to the spinal column. Similarly, four control specimens were implanted on the opposite side. The implantation periods were 1, 4, and 12 weeks to ensure a steady state biological tissue response. Four animals were tested at each time period. Macroscopic and microscopic observations were performed to compare the biological reactions between the test and control materials. There was an inflammatory reaction at 1 week which subsided at 4 weeks. There was fibrous tissue growth near the

implant that also decreased over time. Most importantly, there was no significant difference in the biological response between the test and control materials. Therefore, we conclude that the pressure microsensor is biocompatible.

CHAPTER III

EXPERIMENTAL WORK

The experimental work can be divided into three main parts:

1. Raw materials and chemicals
2. Equipments
3. Experimental procedures

3.1 Raw materials and chemicals

Raw materials

- 3.1.1 *Bombyx mori* cocoon (Nangnoi Srisaket1 from Nakhonratchasima province, Thailand)
- 3.1.2 Type A gelatin powder (pI 9, Nitta Gelatin Inc., Japan)
- 3.1.3 Mined salt (particle size 600-710 μ m, Thai refined salt Co., Ltd., Nakhonratchasima, Thailand)

Chemicals

- 3.1.1 Sodium carbonate (Na_2CO_3 , Ajax Finechem, Australia)
- 3.1.2 Lithium bromide (LiBr, Sigma-Aldrich, Germany)
- 3.1.3 1-ethyl-3-(3-dimethylaminopropyl) carbodiimide hydrochloride (EDC, Nacalai Tesque, Inc., Japan)
- 3.1.4 N-hydroxysuccinimide (NHS, Nacalai Tesque, Inc., Japan)
- 3.1.5 Calcium chloride (CaCl_2 , Ajax Finechem, Australia)
- 3.1.6 Sodium phosphate dibasic heptahydrate ($\text{Na}_2\text{HPO}_4 \cdot 7\text{H}_2\text{O}$, Sigma-Aldrich, Germany)
- 3.1.7 Collagenase from *Clostridium histolyticum* (2.69 units/ml, Fluka, Biochemika, USA)

- 3.1.8 Phosphate buffer saline without calcium, and magnesium (PBS, Hyclone, USA)
- 3.1.9 Sodium Azide (Labchem, APS, Austraria)
- 3.1.10 Betadine
- 3.1.11 Ethanol (99.7-100%, VWR International Ltd., UK)
- 3.1.12 Sodium thiopental
- 3.1.13 Hexamethyldisilazan (Fluka, Germany)

3.2 Equipments

- 3.2.1 Seamless cellulose tubing (Molecular weight cut off 12,000-16,000, Viskase Companies, Inc., Japan)
- 3.2.2 Autopitte (1,000-5,000 ul with tips (Eppendorf, Germany)
- 3.2.3 Stirrer (MSH-10, Daihan Scientific Ltd., WiseStir)
- 3.2.4 -40°C freezer (Heto, PowerDry LL3000, USA)
- 3.2.5 Refrigerator 4oC (PT203, Italy)
- 3.2.6 Lyophilizer (Chaist)
- 3.2.7 Autclave (HVE-25/50, Hiclave)
- 3.2.8 Vacuum drying oven and pump (VD23, Binder, Germany)
- 3.2.9 Scanning Electron Microscope (JSM-5400, JEOL Ltd., Japan)
- 3.2.10 Sputter coater (SCD 040, Balzer, Lichtenstein)
- 3.2.11 X-ray diffractometer (D5000, Siemens, Germany)
- 3.2.12 CO₂ incubator (Model No. 490-1CE, Barnstead International, USA)
- 3.2.13 Laminar Flow (HWS Series 254473, Australia)
- 3.2.14 Centrifuge (5810R, Eppendorf)
- 3.2.15 Purelab Ultra (Elga)
- 3.2.16 Waterbath (SUB6, Grant, England)
- 3.2.17 Pump (DOA-P504-BN, Gast, USA)
- 3.2.18 Disposable syringe insulin 27GX1/2” (Nipro, Thailand)
- 3.2.19 Surgical blade stainless No.10 (Feather, Janpan)
- 3.2.20 Prolene 6-0 suture (Ethicon)
- 3.2.21 Forceps

3.2.22 Conical Tube 10 and 50 ml (Corning, Mexico)

3.2.23 Plastic tube 10, 25 ml

3.2.24 Light Microscope (DS-Fi1, Nikon)

3.3 Experimental procedures

The flowchart in Figure 3.1 illustrated all research procedures performed in this study. An experimental procedures can be divided into four main parts: preparation of four types of scaffolds, *in vitro* biodegradation, *in vivo* biodegradation and *in vivo* tissue response.

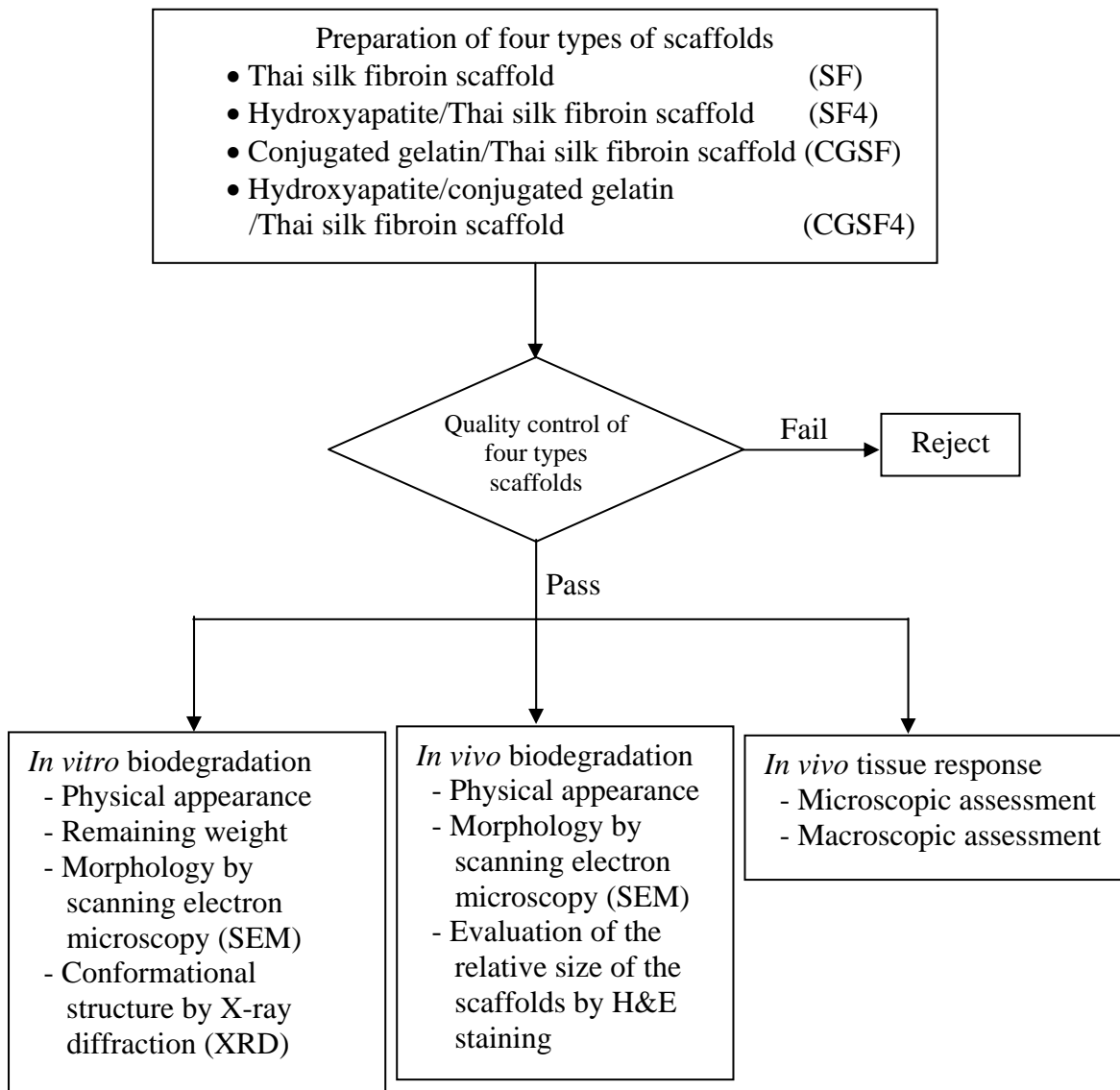


Figure 3.1 Flowchart of experimental procedures

3.3.1 Preparation of four types of Thai silk fibroin-based scaffolds

3.3.1.1 Preparation of Thai silk fibroin scaffolds (SF)

Thai silk fibroin scaffolds were prepared using salt leaching method as described by Kim *et al* [25]. The cocoons were boiled in 0.02 M Na₂CO₃ solution for 20 min and rinsed with water to extract sericin and other contaminating proteins. The silk fibroin fiber was dissolved in 9.3M LiBr solution at 60°C for 4 h and dialyzed against deionized water for 2 days to obtain 6.5 wt% silk fibroin solution as determined by weighing the remaining solid after drying. The silk fibroin scaffold was prepared by adding 7.2 g of 600-710 µm granular NaCl into 3 ml of silk fibroin solution in a plastic container. The container was covered and left at room temperature for 24 h to allow the gelation of silk fibroin. Then, the container was immersed in deionized water to leach out salt for 2 days. The silk scaffold was taken out from the container and washed under stirring for 1 day. After that, the silk scaffold was left to be dried overnight. The silk scaffold was punched into 11mm in diameter and 2 mm in thickness.

3.3.1.2 Preparation of conjugated type A gelatin/Thai silk fibroin scaffolds (CGSF)

Conjugated gelatin/Thai silk fibroin scaffolds were prepared following the method described by Chamchongkaset *et al* [6]. Thai silk fibroin scaffold obtained from salt leaching method was immersed in 0.5 wt% gelatin solution under vacuum for 2 h and then freeze dried. The ratio of weight of silk fibroin scaffold to gelatin solution was 1.5mg:1ml. Silk fibroin scaffold coated with gelatin was crosslinked by dehydrothermal (at 140°C for 48 h) and the conjugated using carbodiimide solution (14mM 1-ethyl-3-(3-dimethylaminopropyl) carbodiimide hydrochloride (EDC) and 5.5mM N-hydroxy-succinimide (NHS)) at room temperature under vacuum for 2 h. Conjugated scaffolds were rinsed three times with deionized water to remove excess EDC and NHS for 30 min in each cycle time. The obtained scaffolds were left to be dried at room temperature.

3.3.1.3 Preparation of hydroxyapatite/Thai silk fibroin scaffolds (SF4)

Hydroxyapatite/Thai silk fibroin scaffolds were prepared using alternate soaking method [51]. Thai silk fibroin scaffold was soaked in 0.2 M CaCl_2 solution under vacuum for 30 min and washed in deionized water (1.5 mg of silk fibroin scaffold per ml of CaCl_2 solution). Thai silk fibroin scaffold was transferred to 0.12 M Na_2HPO_4 solution and soaked under vacuum for 30 min and washed in deionized water (1.5 mg of silk fibroin scaffold per ml of CaCl_2 solution). This was considered as one cycle of alternate soaking. Soaking process was performed for 4 cycles to allow deposited hydroxyapatite onto the surface of Thai silk fibroin scaffold. The hydroxyapatite/Thai silk fibroin scaffold was left to be dried at room temperature.

3.3.1.4 Preparation of hydroxyapatite/conjugated gelatin/Thai silk fibroin scaffolds (CGSF4)

The conjugated gelatin/Thai silk fibroin scaffold was taken to deposit hydroxyapatite by alternate soaking process using the same procedure as described in the case of SF4.

3.3.2 Quality control of four types of Thai silk fibroin-based scaffolds

To control the quality of the prepared scaffolds, the characteristics of each type of scaffolds were inspected as follows. After salt-leached Thai silk fibroin scaffold preparation, the density and morphology of Thai silk fibroin scaffolds were examined from one-third of randomly sampling scaffolds. The density of scaffold was measured from the ratio of dried weight to volume of scaffold. The acceptable value of density was 0.06-0.09 mg/mm^3 . The morphology and interconnectivity of scaffolds were characterized by scanning electron microscopy (SEM) technique. The pore size of scaffold was measured using Image J software (n=5). The interconnectivity was identified from the open pore connected throughout the whole piece of scaffold.

Table 3.1 Quality control of Thai silk fibroin scaffolds

Characteristics	Results	Analysis		Acceptable criteria	Remark
		Pass	Fail		
Density (mg/mm ³)				0.06-0.09 mg/mm ³	
Morphology				Pore size = 580±40µm	
Interconnectivity				Porous interconnectivity	

After Thai silk fibroin scaffolds were obtained, they were further modified by gelatin conjugation and hydroxyapatite deposition. The increased weight of scaffolds after each step was determined and used to calculate the amount of gelatin and hydroxyapatite incorporated in the scaffolds. The weight percentage of silk, gelatin and hydroxyapatite in four types of scaffolds was controlled as presented in Table 3.2

Table 3.2 Weight percentage of silk, gelatin and hydroxyapatite in four types of scaffolds

Type of scaffolds	Abbreviation	Weight percentage		
		silk	gelatin	hydroxyapatite
Thai silk fibroin scaffold	SF	100	0	0
Hydroxyapatite/Thai silk fibroin scaffold	SF4	51.62±0.73	0	48.38±0.73
Conjugated gelatin/Thai silk fibroin scaffold	CGSF	92.15±0.85	7.85±0.85	0
Hydroxyapatite/conjugated gelatin/Thai silk fibroin scaffold	CGSF4	50.58±0.67	4.83±0.47	44.59±0.40

Remark : The number “4” in the abbreviated names represented the number of alternate soaking cycles employed to deposit the hydroxyapatite into the scaffolds.

3.3.3 *In vitro* biodegradation of Thai silk fibroin-based scaffolds

Four types of scaffolds were sterilized with ethylene oxide and left at room temperature for a few days prior to further investigation. To perform *in vitro* biodegradation test, Thai silk fibroin-based scaffolds were incubated at 37°C, pH 7.4 in 1.5 ml solution of 1 U/ml collagenase [52] and sodium azide 0.01% w/v [53] for 1, 7, 14, 21 and 28 days. The solution was changed every 2 days. After each time interval, the Thai silk fibroin-based scaffolds were taken out from the solution, rinsed with deionized water, centrifuged at 5,000 rpm (3,214 g) for 15 min and freeze dried. The characteristics of all scaffolds including remaining weight, morphology and conformational structure were examined and compared to the ones before *in vitro* biodegradation test.

3.3.3.1 Remaining weight of Thai silk fibroin-based scaffolds

The weight of scaffolds before and after *in vitro* biodegradation test were measured. The remaining weight of the scaffolds was calculated using the following equation.

$$\text{Remaining weight (\%)} = \frac{W_t}{W_0} \times 100$$

where W_0 was the initial weight of scaffold and W_t was the remaining weight of the scaffold after biodegradation in collagenase. The reported values were the mean±standard deviation (n=3).

3.3.3.2 Morphological observation of Thai silk fibroin-based scaffolds

Changes in the physical appearance and morphology of the scaffolds before and after biodegradation were observed and compared. The physical appearance (macrostructure) of scaffolds before and after biodegradation was explored using a digital camera. The microstructure of scaffolds before and after

biodegradation was examined using a scanning electron microscope (SEM, JEOL JSM 5410LV). Before observation, the samples were sputter-coated with a thin gold layer in order to provide sample conductivity.

3.3.3.3 Conformational structure of Thai silk fibroin-based scaffolds

Before and after *in vitro* biodegradation, the X-ray diffraction patterns of scaffolds were analyzed using a X-ray diffractometer (XRD, Siemens D5000) with CuK_α radiation. The voltage of the X-ray source was 30 kV at 30 mA. The scan speed used was 2.0 sec/step with the step size of 0.04° and the scanning region of $2\theta = 15^\circ$ - 40° .

3.3.4 *In vivo* biodegradation of Thai silk fibroin-based scaffolds

After sterilization, four types of scaffolds were tested for *in vivo* biodegradability. All *in vivo* procedures were approved by the Ethics Committee of the Faculty of Medicine, Chulalongkorn University (No.09/52). The animal experiment was performed according to Chulalongkorn University Animal Care and Use Committee (CU-ACUC). The size of the scaffold was 11 mm in diameter and 2 mm in thickness. The samples were implanted in the subcutaneous tissue of female wistar rats (8 weeks old and 200–300g). The rats were anaesthetized by an intraperitoneal injection of thiopental sodium (60 mg/kg body weight) [43]. Animals were shaved and cleaned with betadine solution and then ethanol at lumbar region. Using sterilized technique, the skin incision was made about 1 cm. to create four pockets in subcutaneous tissue. The skin was closed with 6-0 prolene suture and cleaned with betadine solution. The surgery method was shown in Figure 3.2

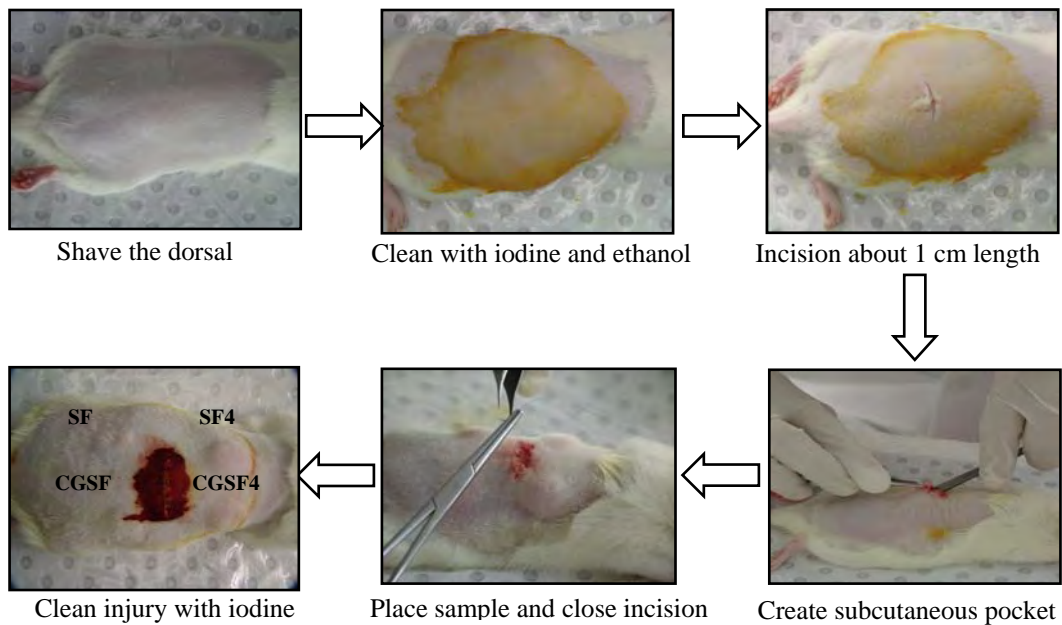


Figure 3.2 Method of subcutaneous implantation

A total of 28 scaffolds were implanted in 7 female rats (4 scaffolds per rat). The total of 7 female rats used in the experiment were divided into 3 groups of evaluation period as shown in Figure 3.3. After 2, 4, and 12 weeks of implantation, the animals were sacrificed by an overdose of thiopental sodium. The scaffolds and surrounding tissue were retrieved. The physical appearance, morphology and sizes of scaffolds were evaluated.

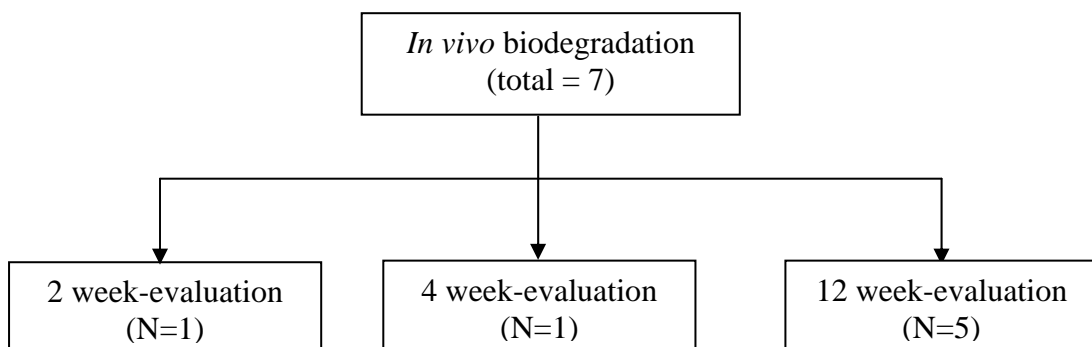


Figure 3.3 The group and the number of Wistar rats used to evaluate *in vivo* biodegradation

3.3.4.1 Physical appearance

After sacrificing the rats, the dorsal skin of the rats, where the samples were placed, was removed for photographing.

3.3.4.2 Morphological observation by scanning electron microscope

After 2, 4 and 12 weeks of implantation, the scaffolds and surrounding tissue were removed and fixed in formalin for 1 day. Then, the samples and tissue were dehydrated with a concentration series of ethanol, 30%, 50%, 70%, 80%, 90%, 95%, and 100%, for 10 min at each concentration. Finally, samples were treated with hexamethyldisilazane under fume hood and air dried naturally [54, 55]. Cross-section of dried samples were mounted onto a stab, sputtering-coated with gold and observed under SEM.

3.3.4.3 Evaluation of the relative size of the scaffolds

The cross-section of scaffolds was embedded in paraffin for H&E staining. All stained H&E slides were examined using a Nikon DS-Fi1 light microscope. Photographs of the entire scaffold were captured with the light microscope at 4X. The images at 4X did not cover the whole piece of scaffolds therefore a series of photographs were taken. All photographs were placed together to get the whole image of scaffold using photomerge in photoshop program. The scaffold area including extracellular matrix was calculated using Image J program. The steps of area evaluation using Image J program are explained in Appendix A. The report values were the mean±standard deviation (n=4).

3.3.5 Evaluation of the tissue response (local effects) of Thai silk fibroin-based scaffolds following ISO10993-6

The surgery method was performed using the same procedure as described in section 3.3.4. For each rat, the sample and the control were placed into the left and the right sides of the back of rat as shown in Figure 3.4. The control sample was Gelfoam[®] which is a medical device used as a hemostatic material for bleeding surfaces. (Details on Gelfoam[®] was included in appendix B)

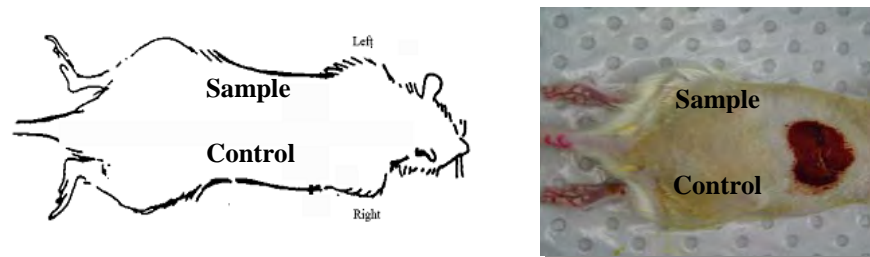


Figure 3.4 Implanted sites of Wistar rat

A total of 32 female rats used in the experiment were divided into 2 groups of evaluation period as shown in Figure 3.5. The total of 32 scaffolds were implanted in 32 female rats. After 2 and 4 weeks of implantation, the animals were sacrificed by an overdose of thiopental sodium. Scaffolds and surrounding tissue were retrieved, paraffin-embedded, cross-sectioned for histology, and stained with hematoxylin and eosin (H&E). The macroscopic and microscopic assessments were examined.

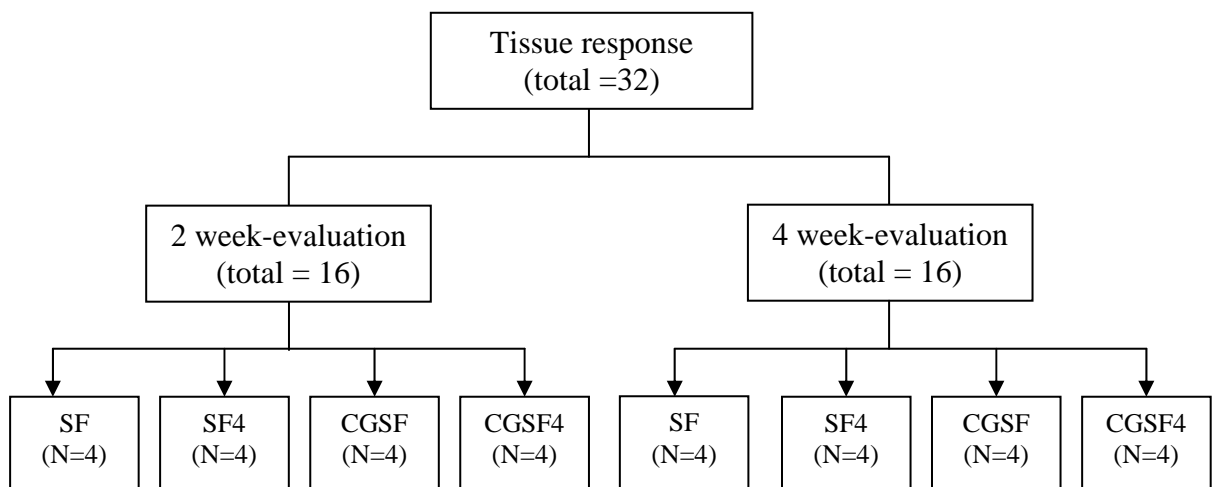


Figure 3.5 The group and the number of Wistar rats used to evaluate *in vivo* tissue response

3.3.5.1 Macroscopic assessment

The ordinary symptoms of inflammatory in animals which were redness (rubor), swelling (tumor), pain (dolor) and heat (calor) were observed weekly. At the time of sacrificing, the gross appearance of cross-section of retrieved material were examined.

3.3.5.2 Microscopic assessment

The H&E slides were semi-quantitatively scored following the ISO10993-6. Inflammatory cell types, neovascularisation, fibrosis and fatty infiltrate were evaluated and scored by a single pathologist at two different time using the criteria shown in Table 3.3 and 3.4. A scale of 0-4 was used to evaluate the presence of inflammatory cell type: 0=not observed, 1=rare, 2=minimal, 3=heavily infiltrate, and 4 packed infiltrate. The neovascularisation, fibrosis and fatty infiltrate were scored using a scale from 0 to 4 as illustrated in Table 3.4.

Table 3.3 Scoring systems used for biological evaluation-Cell types [7]

Cell type/response	Score				
	0	1	2	3	4
Polymorphonuclear cells	0	Rare, 1-4/phf ^a	5-10/phf	Heavy infiltrate	Packed
Lymphocytes	0	Rare, 1-4/phf ^a	5-10/phf	Heavy infiltrate	Packed
Plasma cells	0	Rare, 1-4/phf ^a	5-10/phf	Heavy infiltrate	Packed
Macrophages	0	Rare, 1-4/phf ^a	5-10/phf	Heavy infiltrate	Packed
Giant cells	0	Rare, 1-4/phf ^a	5-10/phf	Heavy infiltrate	Packed
Necrosis	0	Rare, 1-4/phf ^a	5-10/phf	Heavy infiltrate	Packed

^a phf = per high powered (400X) field.

Table 3.4 Scoring systems used for biological evaluation-Response [7]

Response	Score				
	0	1	2	3	4
Neovascularisation	0	Minimal capillary proliferation, focal, 1-3 buds	Groups of 4-7 capillaries with supporting fibroblastic structures	Broad band of capillaries with supporting structures	Extensive band of capillaries with supporting fibroblastic structures
Fibrosis	0	Narrow band	Moderately thick band	Thick band	Extensive band
Fatty infiltrate	0	Minimal amount of fat associated with fibrosis	Several layers of fat and fibrosis	Elongated and broad accumulation of fat cells about the implant site	Extensive fat completely surrounding the implant

Scoring cell types and response were recorded in the evaluation form presented in Table 3.5. The level of irritation is evaluated and compared to the control (Gelfoam[®]). The difference in the scores of test sample and control was classified as follows:

- 1) 0.0 up to 2.9- sample is non-irritant.
- 2) 3.0 up to 8.9-sample is slight-irritant.
- 3) 9.0 up to 15-sample is moderate-irritant.
- 4) More than 15-sample is severe-irritant.

Table 3.5 Semi-quantitative evaluation system [7]

Test sample :	Implantation interval.....weeks							
Animal number :	N=1		N=2		N=3		N=4	
	Test	Control	Test	Control	Test	Control	Test	Control
Polymorphonuclear								
Lymphocytes								
Plasma cells								
Macrophages								
Giant cells								
Necrosis								
SUB-TOTAL (X2)								
Neovascularisation								
Fibrosis								
Fatty infiltrate								
SUB-TOTAL								
TOTAL								
Test-Control								
Ranking of irritation								

3.3.6 Ethic issues

All *in vivo* procedures were approved by the Ethics Committee of the Faculty of Medicine, Chulalongkorn University (No.09/52). The animal experiment was performed according to Chulalongkorn University Animal Care and Use Committee (CU-ACUC).

3.3.7 Statistical analysis

The significant levels of data were determined by an independent two-sample t-test. All statistical calculations were performed on the SPSS system for Windows. P-values of <0.05 was significantly considered.

CHAPTER IV

RESULTS AND DISCUSSION

Four types of Thai silk fibroin-based scaffolds containing silk fibroin, gelatin and hydroxyapatite were fabricated as described in the previous chapter. The results on *in vitro* biodegradation, *in vivo* biodegradation, and *in vivo* tissue response of all Thai silk fibroin-based scaffolds were presented and discussed in this chapter.

4.1 *In vitro* biodegradation of Thai silk fibroin-based scaffolds

4.1.1 Physical appearance of Thai silk fibroin-based scaffolds

Physical appearance of four types of Thai silk fibroin based-scaffolds before and after degradation in collagenase for 1, 7, 14, 21 and 28 days was presented in Figure 4.1. The original SF and CGSF scaffolds before degradation test were light yellow while SF4 and CGSF4 scaffolds were white due to the hydroxyapatite particles deposited on the surface of the porous scaffolds from alternate soaking process. After 1 day of incubation in collagenase, SF and CGSF scaffold still remained as a whole piece. For SF4 and CGSF4 scaffolds, some small pieces of scaffolds were separated out from the main piece of scaffolds. These small pieces were the hydroxyapatite deposited on the scaffold surface. After 7 days of incubation, SF and SF4 scaffolds could not keep its original structure while CGSF and CGSF4 scaffolds still remained as a whole piece. After 14 days of incubation, the particle debris of SF, SF4 and CGSF4 were presented. The whole piece of CGSF with smaller diameter was observed, compared to before biodegradation test. Considering the debris lost from SF, SF4 and CGSF4 scaffolds, their sizes after 21 and 28 days of incubation were smaller than those after 14 days of incubation. In addition, small debris of CGSF scaffold was found after 21 and 28 days of incubation. From the physical appearance

noticed, SF, SF4 and CGSF4 scaffolds seemed to be easier to crack than CGSF scaffold.

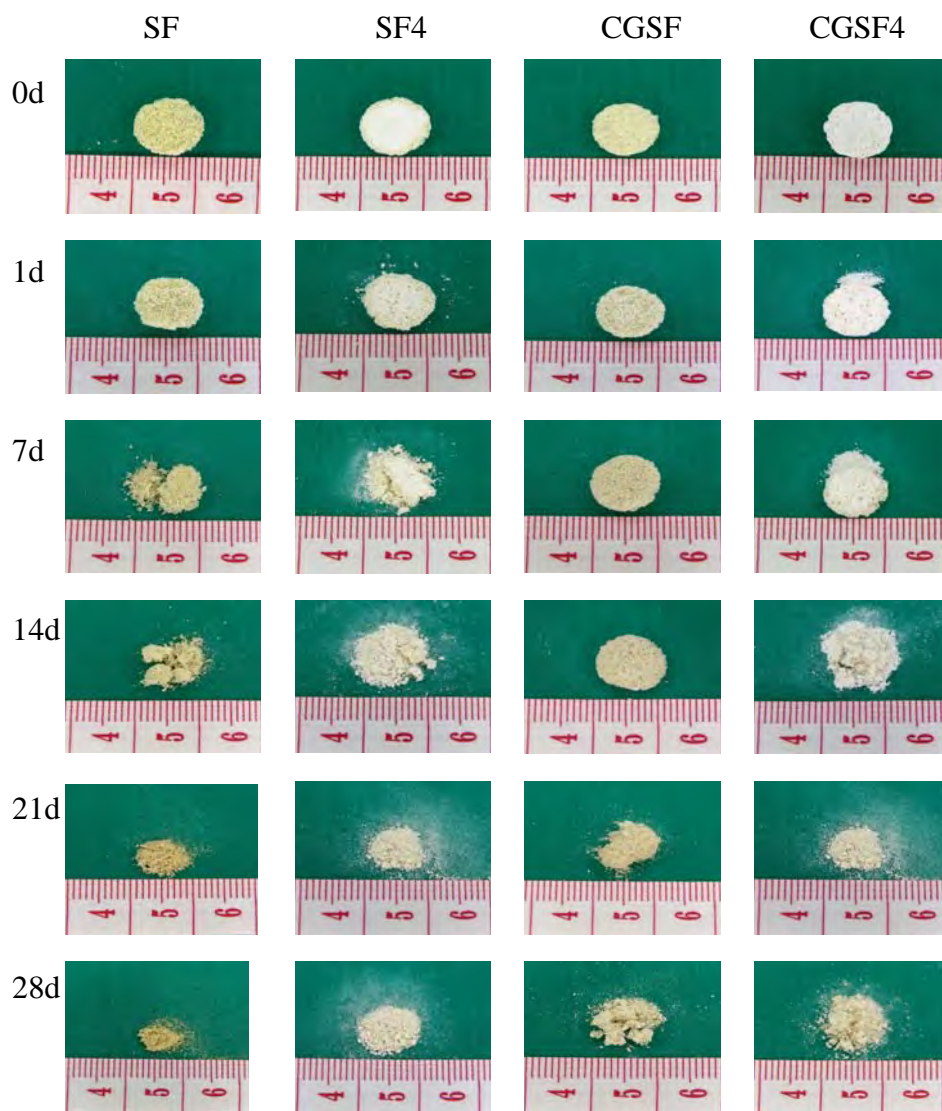


Figure 4.1 Physical appearances of SF, SF4, CGSF, CGSF4 scaffolds after incubation in 1 U/ml collagenase for 1, 7, 14, 21 and 28 days.

4.1.2 Remaining weight of Thai silk fibroin-based scaffolds

Figure 4.2 illustrated the remaining weight of four types of Thai silk fibroin-based scaffolds after incubation in collagenase solution at various time periods. After 1 day of incubation, the remaining weights of all scaffolds were around 93-97%. After 7 days of incubation, it was noticed that the remaining weights of SF, SF4 and CGSF4 scaffolds were lower significantly than those of the CGSF scaffolds. The lower remaining weight of scaffolds containing hydroxyapatite was the result of the degradation of protein portion in collagenase enzyme. Because hydroxyapatite crystals deposited into the porous surface of scaffold were dropped off from surface so collagenase solution could penetrate inside the scaffolds, leading more rapid degradation of protein contents, especially gelatin. After 14 and 21 days of incubation, the remaining weights of SF, SF4 and CGSF scaffold decreased significantly compared to CGSF scaffold. The half weight containing hydroxyapatite (SF4, CGSF4) and pure silk fibroin (SF) was noticed to be after 21 and 28 days, respectively after incubation in collagenase solution, while that of the CGSF scaffold is longer than 28 days. This could be considered as 50% of scaffold degradation. After 28 days of incubation, the remaining weights of scaffolds were in the order of CGSF>SF>SF4~CGSF4. The *in vitro* biodegradation results suggested that among four types of scaffolds, CGSF scaffold showed the slowest degradability. This could be due to double crosslinking (dehydrothermal treatment followed by EDC/NHS crosslinking) of CGSF scaffold. Dehydrothermal treatment generated chemical bonding between the amino and carboxyl groups of gelatin and silk molecules due to thermal dehydration [56]. EDC/NHS treatment was further crosslinked activated carboxyl groups and amine groups of silk and conjugated gelatin molecules [57].

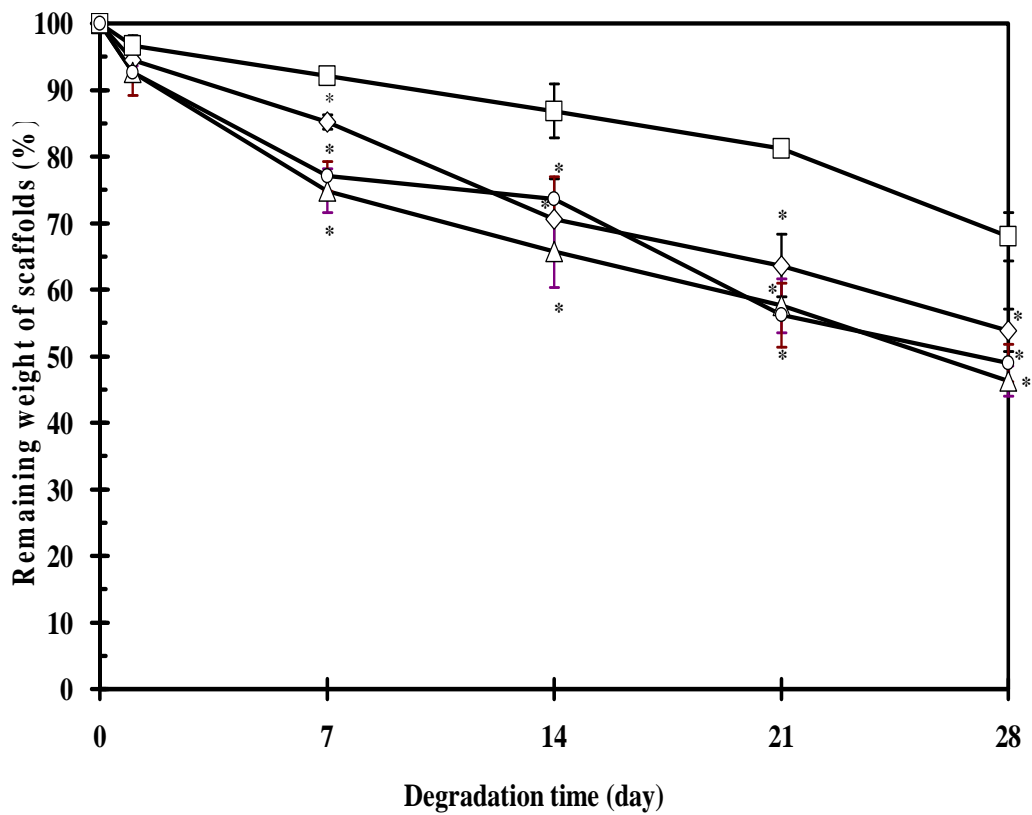


Figure 4.2 Remaining weight (%) of the scaffolds at each period of degradation time in collagenase : 1, 7, 14, 21 and 28 days : SF (◇), SF4 (Δ), CGSF (□) and CGSF4 (○) scaffolds.

* represented the significant difference ($p < 0.05$) relative to CGSF scaffolds in each periods.

4.1.3. Morphology of Thai silk fibroin-based scaffolds

The cross-sectional morphology of the original scaffolds before degradation was illustrated in Figure 4.3. Pore size of SF scaffold was around 580 ± 40 μm which was slightly smaller than the size of NaCl crystals used (600-710 μm). SF scaffold showed a smooth inner surface as shown in Figure 4.3. In the case of CGSF, conjugated gelatin fiber was formed inside the pore wall of silk fibroin scaffold. For the SF4 and CGSF4 scaffolds, pores were filled with the deposited hydroxyapatite crystals and the pore sizes were smaller than those of SF and CGSF scaffolds. In addition, the accumulated hydroxyapatite resulted in the rough surface of porous structure.

After incubation in collagenase, the morphology of four types of Thai silk fibroin-based scaffold at various incubation time in collagenase were shown in Figure 4.4-4.7. Figure 4.4 presented the morphology of SF scaffold after 1,7,14,21 and 28 days of incubation in collagenase. During the biodegradation test for 1 to 14 days, the pore size of scaffold increased gradually. In addition, the inner surface of Thai silk fibroin scaffold was found to be crack after 14 days of incubation. The small particulate debris was observed within 21 days of incubation. Figure 4.5 presented the morphology of SF4 scaffold after 1,7,14,21 and 28 days of incubation in collagenase. There were some holes observed on scaffold due to the loss of deposited hydroxyapatite after 1 to 7 days of incubation. After 21 days of incubation, only the small fragment of hydroxyapatite remained while the silk portion was degraded by enzymatic hydrolysis process. The morphology of CGSF scaffold after 1,7,14,21 and 28 days of incubation in collagenase was shown in Figure 4.6. The pores were poorly interconnected with increasing incubation time. In addition, gelatin fiber conjugated on silk scaffold could not be observed clearly in SEM micrograph after 14-day of incubation. The porous structure of CGSF scaffold could still be noticed at the 28th day of incubation. Figure 4.7 showed the SEM micrographs of CGSF4 scaffold after 1,7,14,21 and 28 days of incubation in collagenase. The degradability behavior of this scaffold was similar to the case of SF4 scaffold.

When comparing the morphology of four types of Thai silk fibroin-based scaffold before degradation to that after 21 days of degradation (Figure 4.8), it

was observed that the SF, SF4 and CGSF4 could not maintain their original structure. Only small particulate debris was found for these three scaffolds. In contrast, the porous morphology of CGSF scaffold was still observed. This implied that the gelatin conjugated on silk fibroin scaffold resist against the enzymatic degradation. This was because the gelatin conjugation by dehydrothermal and EDC/NHS treatments led to more stable amide formation of silk fibroin, resulting in scaffold slow degradation rate [56]. The morphology changes of four scaffolds corresponded to the results on remaining weight, i.e. the degradability of CGSF scaffolds was the slowest compared to other scaffolds.

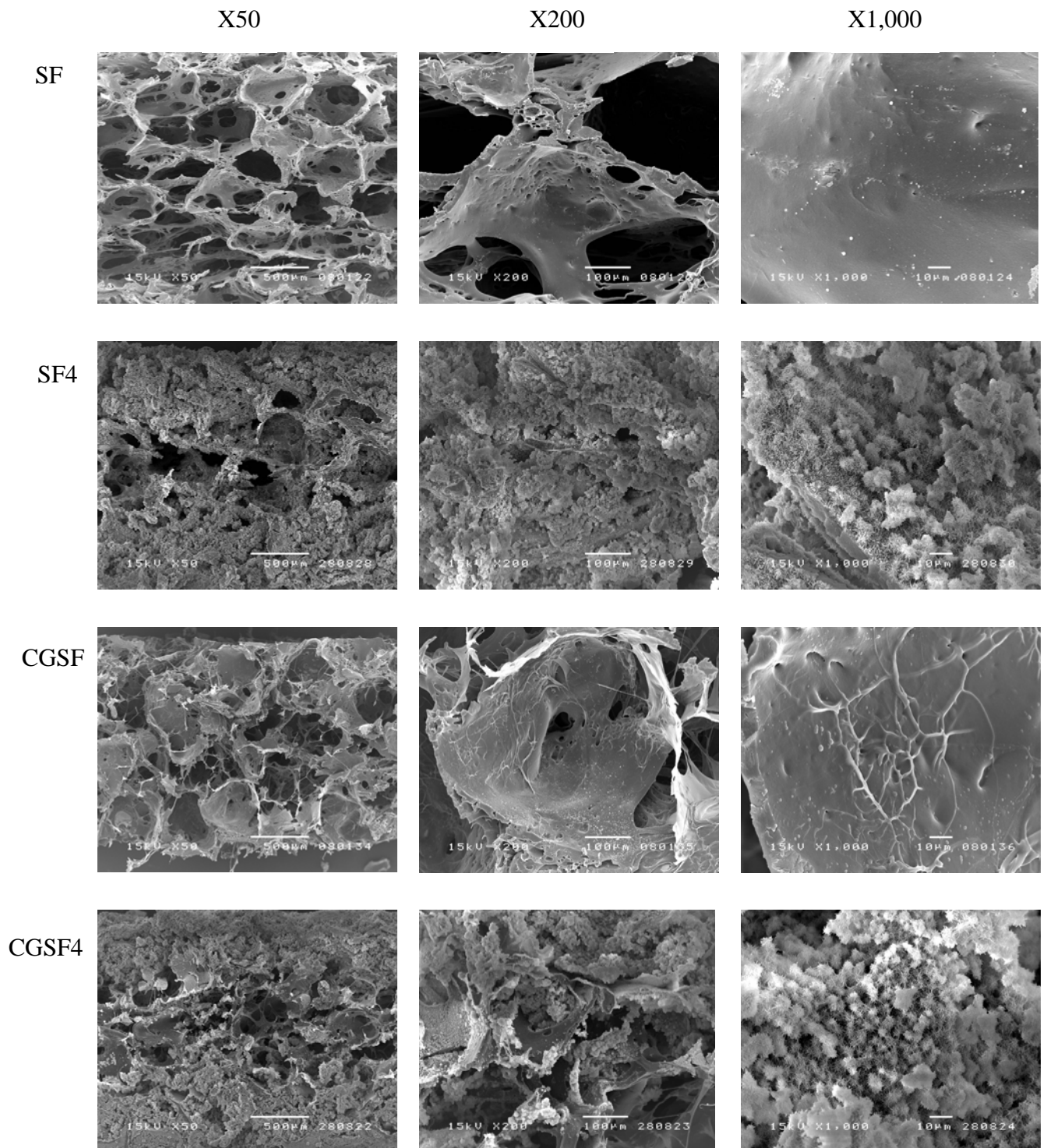


Figure 4.3 SEM micrographs of SF, SF4, CGSF and CGSF4 scaffolds before incubation in collagenase : X50, X200 and X1,000

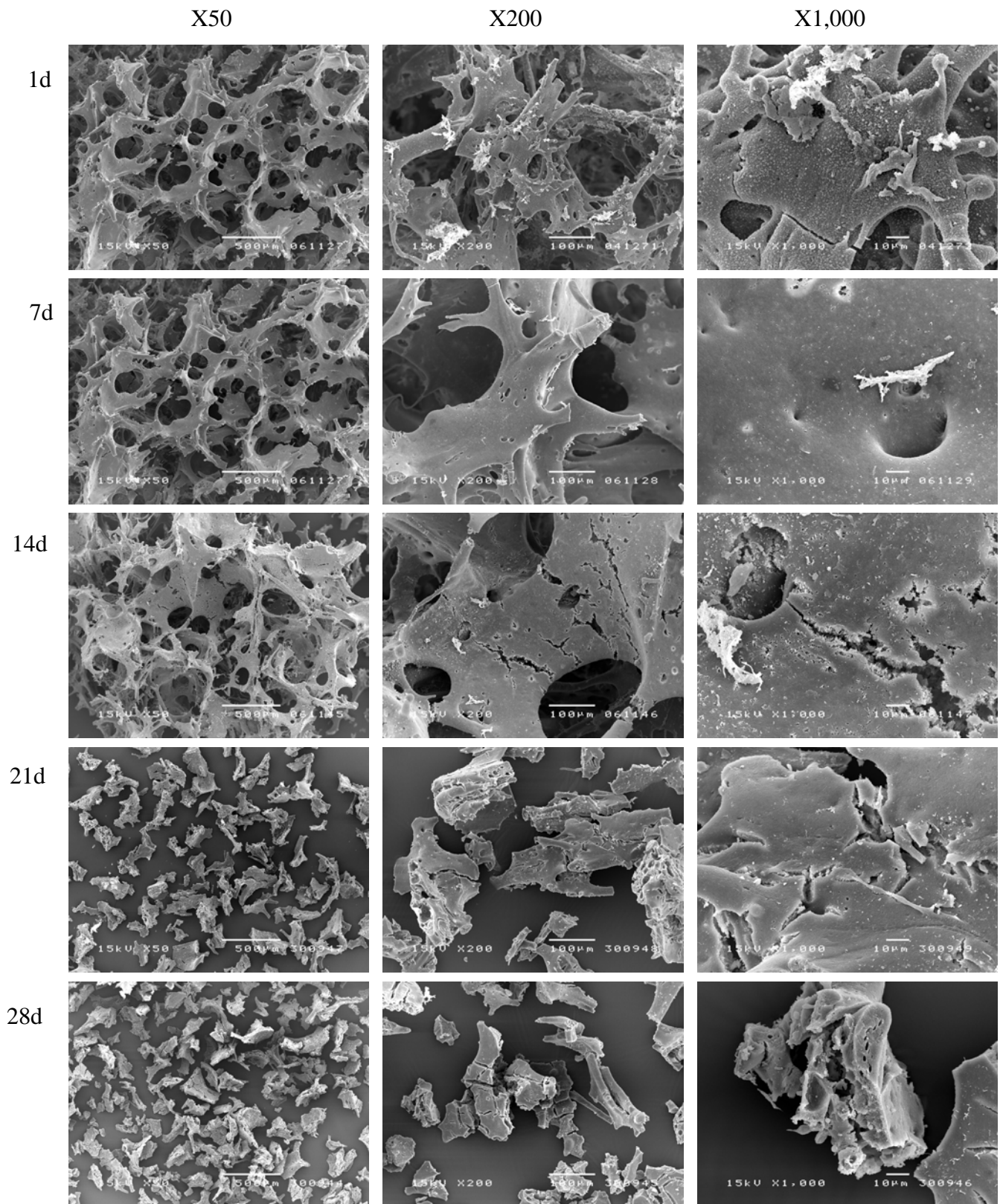


Figure 4.4 SEM micrographs of SF scaffold after incubation in collagenase for 1, 7, 14, 21 and 28 days : X50, X200 and X1,000

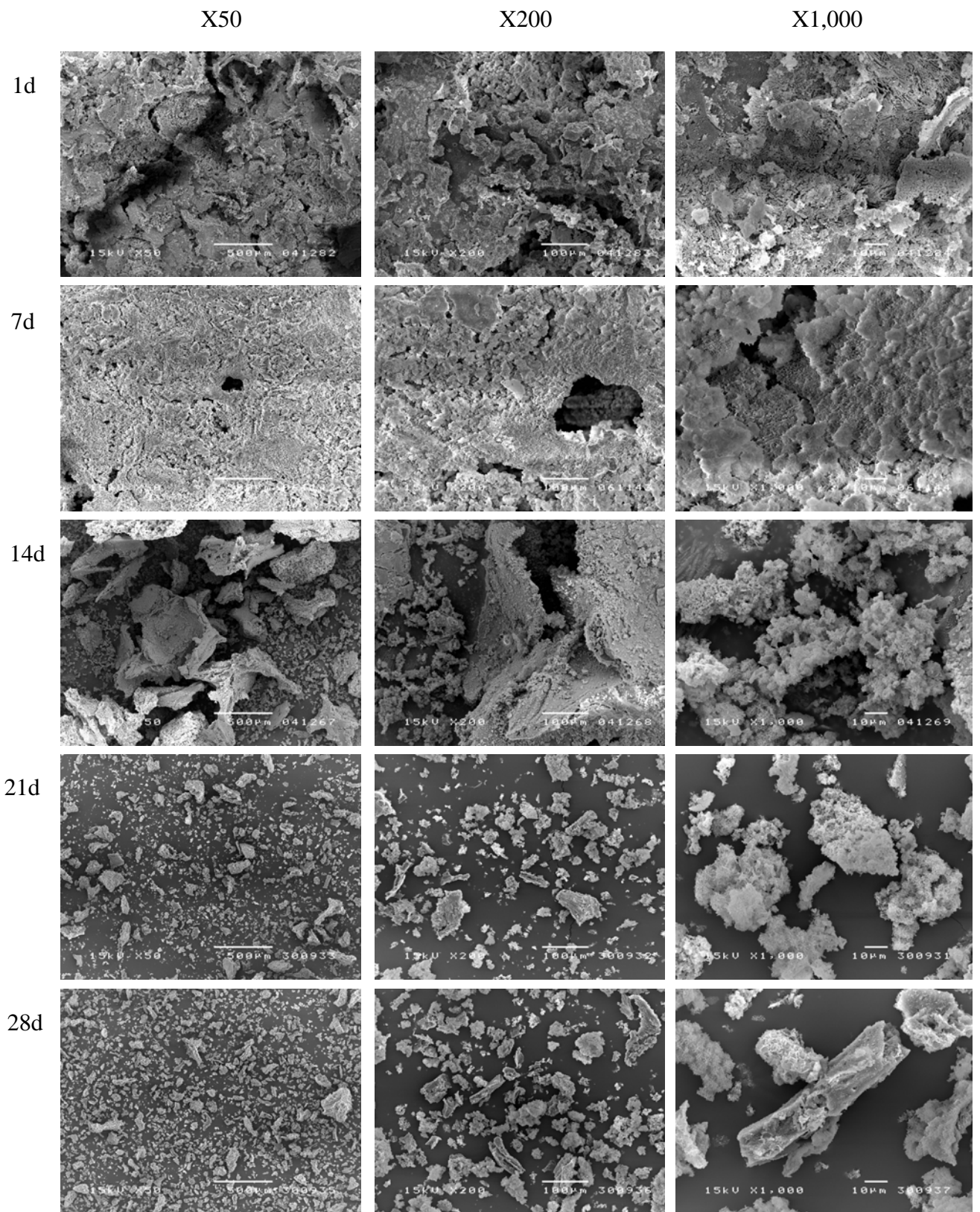


Figure 4.5 SEM micrographs of SF4 scaffolds after incubation for 1, 7, 14, 21 and 28 days :

X50, X200 and X1,000

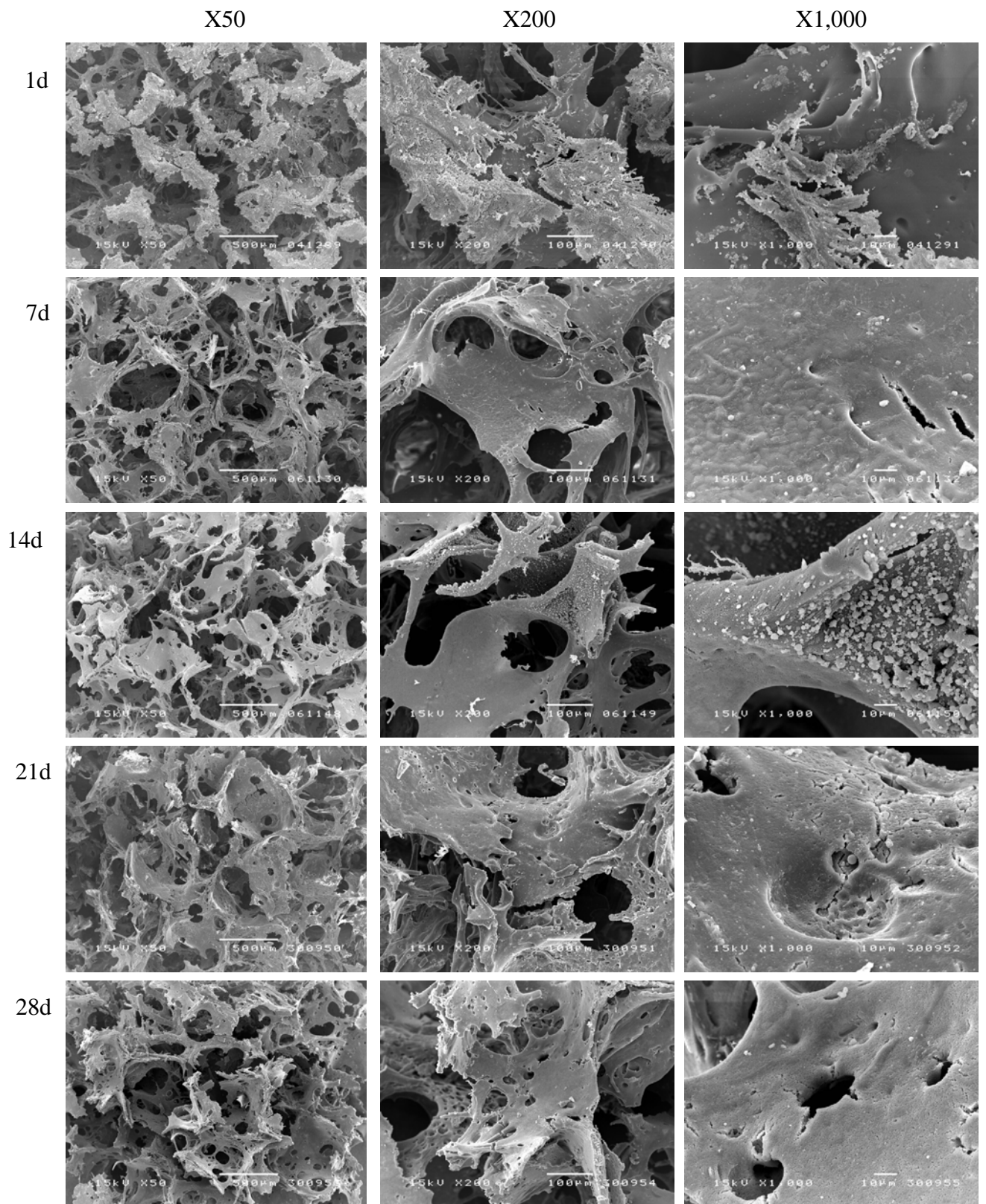


Figure 4.6 SEM micrographs of CGSF scaffold after incubation in collagenase for 1, 7, 14, 21 and 28 days : X50, X200 and X1,000

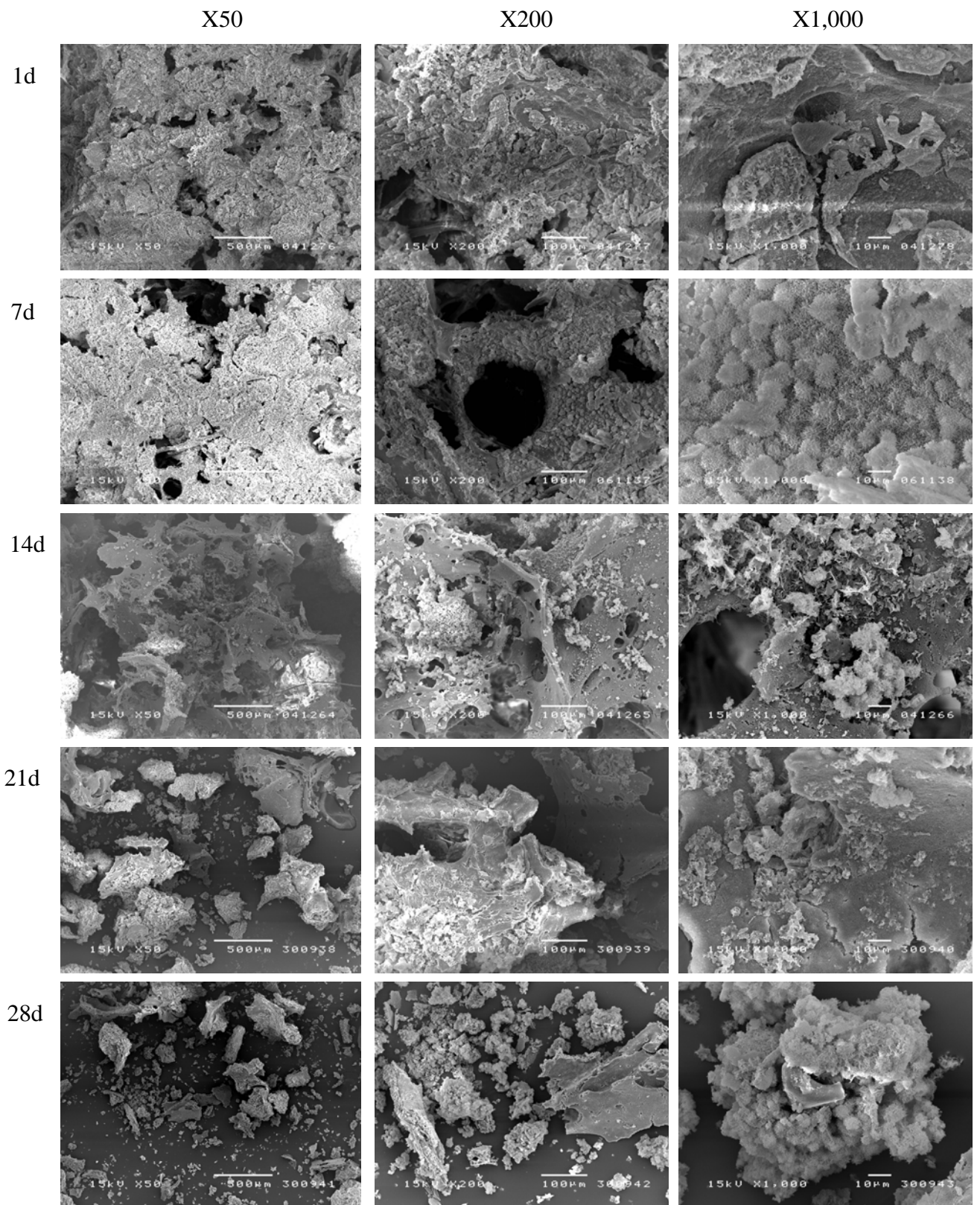


Figure 4.7 SEM micrographs of CGSF4 scaffolds after incubation in collagenase for 1, 7, 14, 21 and 28 days : X50, X200 and X1,000

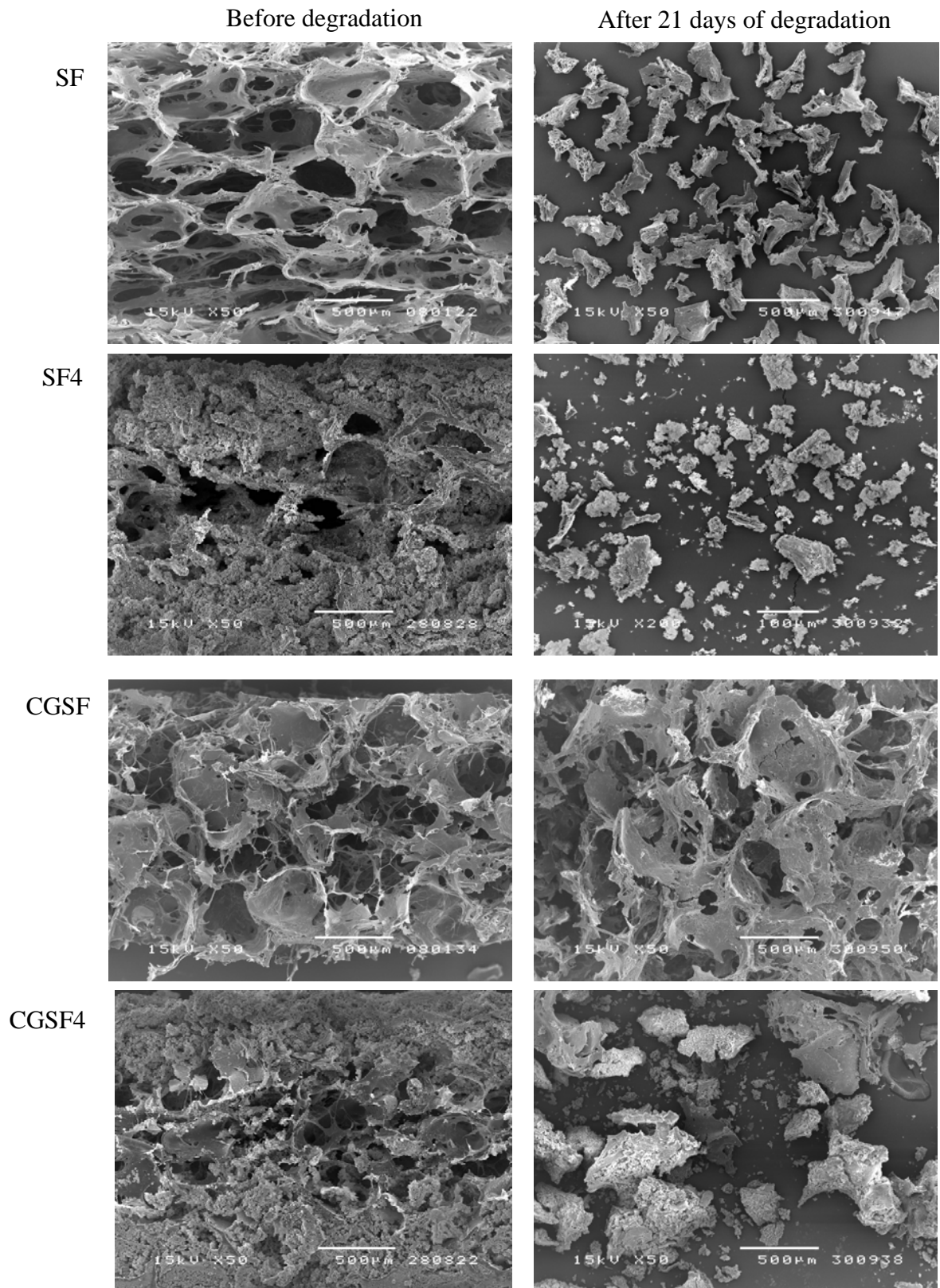


Figure 4.8 SEM micrographs of SF, SF4, CGSF and CGSF4 scaffolds before and after incubation in collagenase for 21 days : X50

4.1.4 Conformational structure of Thai silk fibroin-based scaffolds

The changes in the conformational structure of Thai silk fibroin-based scaffolds were determined by X-ray diffraction technique. The conformational structures of four types of Thai silk fibroin-based scaffolds before and after incubation in collagenase were shown in Figure 4.9-4.14.

4.1.4.1 XRD patterns of Thai silk fibroin-based scaffolds before degradation

X-ray diffraction patterns of four types of Thai silk fibroin-based scaffolds before degradation were presented in Figure 4.9. The broad diffraction peaks of SF scaffold were noticed at $2\theta=20.7^\circ$ and 24.6° (Figure 4.9). These peaks represented the β -sheet crystalline structure of protein [25, 52, 58]. This implied that Thai silk fibroin scaffold prepared using salt leaching method showed β -sheet crystalline structure. The other peak indicating the β -sheet crystalline structure ($2\theta=8.8^\circ$) was not observed in this result due to the limitation of the equipment. Generally, there are two crystalline forms of silk fibroin, Silk I and Silk II. The theoretical diffraction of Silk I crystal structure, representing α -helix conformation, is at $2\theta=19.7^\circ$ and 28.2° [58]. Silk II, a common β -sheet conformation found in the silk fibroin, is at $2\theta=8.5^\circ$, 20.8° and 24.6° which is essential in term of providing the outstanding mechanical properties [25, 52, 58].

After deposited hydroxyapatite on SF scaffold via alternate soaking process, the peaks of SF4 scaffold were observed at 21.8° , 26.7° and 32.5° as presented in Figure 4.9. The peak indicating β -sheet crystalline structure of silk fibroin in the SF4 scaffold (21.8°) were shifted from those in the SF scaffold. The other peaks at 25.8° and 31.8° were the hydroxyapatite crystal which were confirmed with the diffraction pattern of commercial hydroxyapatite particle as seen in Figure 4.10 (Fluka, Germany). The diffraction characteristic peaks at around 26° and 32° were assigned to the (002) and (211) plans of hydroxyapatite crystal [59, 60, 61]. However, peaks of deposited hydroxyapatite in SF4 scaffold was slightly broader and weaker as

compared to those of the commercial hydroxyapatite, implying low crystallinity and smaller crystal size of deposited hydroxyapatite. The XRD results of SF4 scaffold ensured the existing of crystallinity of hydroxyapatite and silk fibroin in SF4 scaffold.

Considering XRD pattern of CGSF scaffold in Figure 4.9, the broad diffraction peak appeared at $2\theta=22^\circ$ and the small diffraction peaks were found at $2\theta=31.4^\circ$ and 36.0° . These peaks represented the diffraction patterns of type A gelatin (Nitta, Japan), shown in Figure 4.10. The XRD pattern of CGSF scaffold revealed that type A gelatin conjugated was dominant.

X-ray diffraction pattern of CGSF4 scaffold showed in Figure 4.9 indicated that the hydroxyapatite component appeared dominantly as evidenced from the presence of two main reflection peaks, at around $2\theta=26^\circ$ and 32° . The crystalline peaks of deposited hydroxyapatite became slightly broader and weaker when compared with the peaks of commercial hydroxyapatite, implying low crystallinity and smaller crystal size of hydroxyapatite in CGSF4 scaffold. A small broad peak observed near $2\theta=21^\circ$ belonged to the characteristics of protein (silk fibroin and gelatin). The result on CGSF4 scaffold corresponded to the combination of the characteristic peaks of SF4 and CGSF scaffolds.

When comparing between hydroxyapatite peaks of the two scaffolds grown with hydroxyapatite (CGSF4 and SF4), it was found that the peak intensity of hydroxyapatite in CGSF4 scaffold was higher than that of SF4 scaffold, indicating higher crystallinity and higher crystal size of hydroxyapatite.

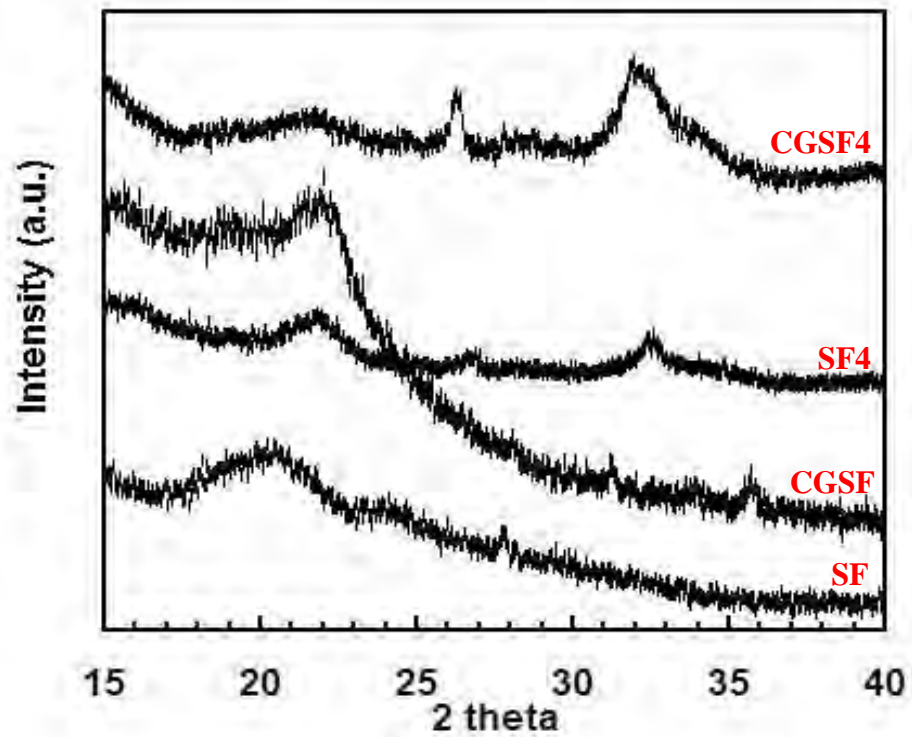


Figure 4.9 X-ray diffraction patterns of SF, SF4, CGSF and CGSF4 scaffolds before incubation in collagenase solution

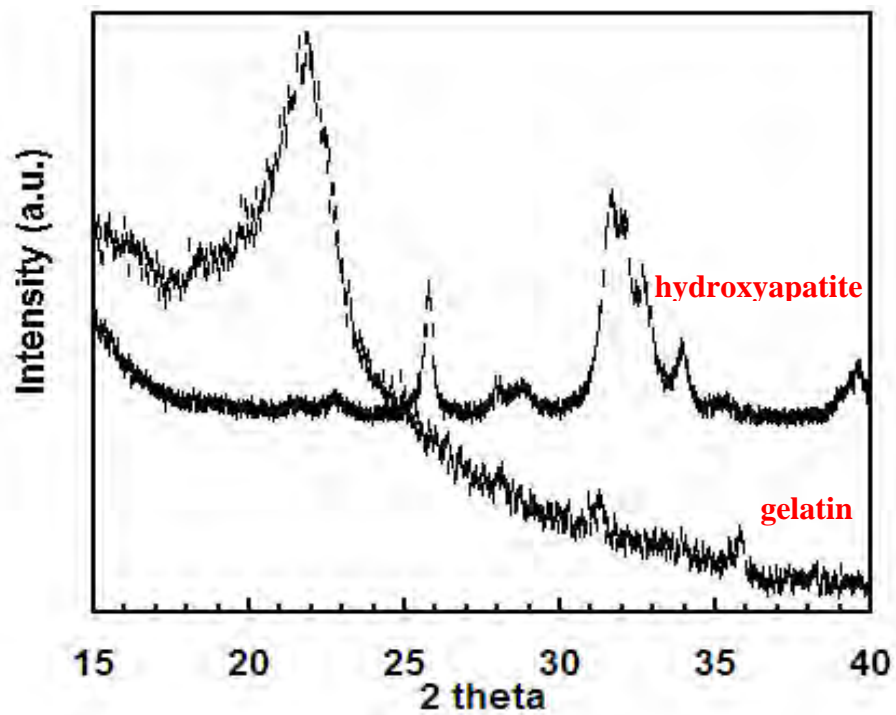


Figure 4.10 X-ray diffraction patterns of hydroxyapatite (Fluka, Germany) and Type A gelatin (Nitta, Japan)

4.1.4.2 XRD patterns of Thai silk fibroin-based scaffolds after degradation

The change in the conformational structure of four types of Thai silk fibroin-based scaffolds after degradation in collagenase for 1,7,14,21 and 28 days was shown in Figure 4.11-4.14. Figure 4.11 illustrated the XRD pattern of pure silk fibroin scaffold after degradation in collagenase. Conformational structure of SF scaffold after 1 day of degradation represented the similar pattern to its original structure. After 7 days of incubation and thereafter, Silk II crystalline structure ($2\theta=20.7^\circ$, 24.6°) disappeared but the peaks indicated Silk I crystalline structure ($2\theta=19.7^\circ$) appeared. XRD results indicated that the conformation structure of pure silk fibroin scaffold (SF) changed from β -sheet structure (Silk I) to random coil structure (Silk II) after 7-day of incubation in collagenase solution. This revealed that SF scaffold incubated in collagenase enzyme for 7-28 days was degraded, resulting in the change of conformational structure.

The XRD pattern of SF4 scaffold before and after degradation was presented in Figure 4.12. For the first 7 days of degradation, the main piece of scaffold was analyzed. After 1- and 7-day of degradation, the dominant peak at $2\theta=21^\circ$ which is the characteristic of silk fibroin and two small peaks at $2\theta=25.6^\circ$ and 31.5° indicating hydroxyapatite were noticed. It was noted that the peak of silk fibroin was clearly seen than the peak of hydroxyapatite compared to the XRD pattern of this scaffold before degradation. This was due to loss of hydroxyapatite from the scaffold surface. From 14-28 days of incubation as the scaffold was broken into small pieces, the structure of all small pieces of scaffolds exhibited only the characteristic peaks of hydroxyapatite. It seemed that the major constituent of residual scaffold was the hydroxyapatite portion while silk component disappeared. This implied that the silk fibroin portion completely degraded after 14 days of incubation.

Figure 4.13 showed the XRD pattern of CGSF scaffold before and after degradation. After 1-21 days of degradation, the conformational structure of the scaffolds was similar to that before degradation. This implied that the crystalline characteristics of the silk fibroin and gelatin constituents still existed until 21 days of biodegradation in collagenase. At the end of incubation, the peaks exhibited only the

β -sheet structure of silk fibroin ($2\theta = 20.2^\circ, 24.0^\circ$). This revealed that the conjugated gelatin on silk fibroin scaffold could remain till 21 days. After that only silk fibroin as the base material of scaffold could be noticed.

X-ray diffraction pattern of CGSF4 scaffold before and after degradation was illustrated in Figure 4.14. For the first 14 days of degradation, the main piece of scaffold were characterized. The peak at $2\theta = 21^\circ$ indicating the characteristic of conjugated gelatin on silk fibroin was dominant after incubation for 1 to 14 days. After 21-28 days of degradation, only small pieces of scaffolds was remained as residual. The residual of CGSF4 after 21 and 28 days of incubation indicated only the characteristic of hydroxyapatite. This implied that protein portion was degraded within 14 days of incubation in collagenase.

From the results on XRD analysis, it could be concluded that, among four types of scaffolds, CGSF scaffold had slowest biodegradability in collagenase solution. This corresponded to other results discussed previously.

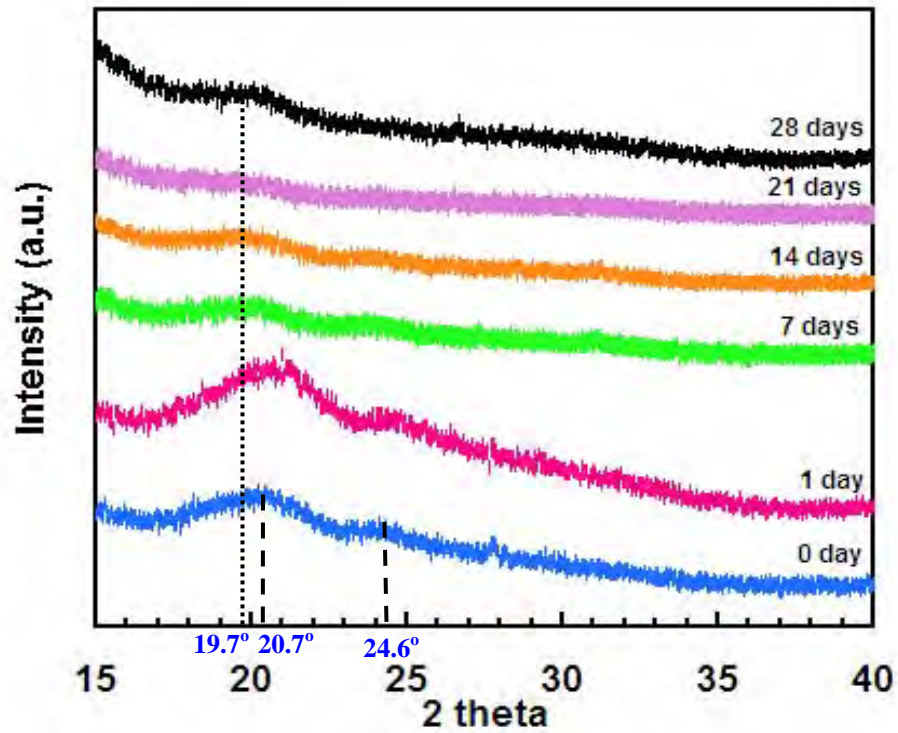


Figure 4.11 X-ray diffraction patterns of SF scaffold before and after incubation in collagenase solution for 0,1,7,14,21 and 28 days.

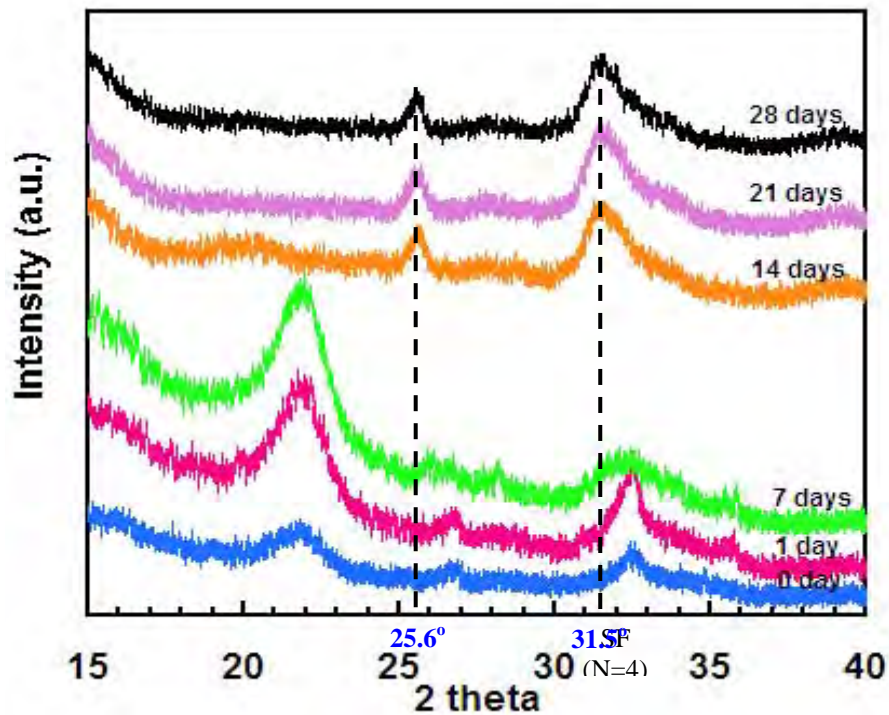


Figure 4.12 X-ray diffraction patterns of SF4 scaffold before and after incubation in collagenase solution for 0,1,7,14,21 and 28 days.

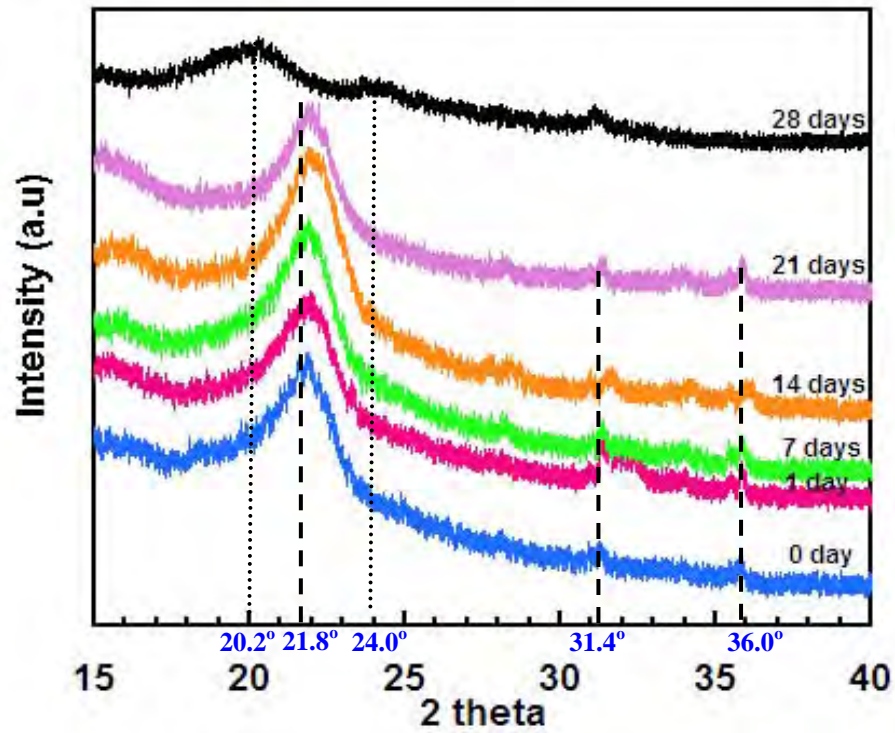


Figure 4.13 X-ray diffraction patterns of CGSF scaffold before and after incubation in collagenase solution for 0,1,7,14,21 and 28 days

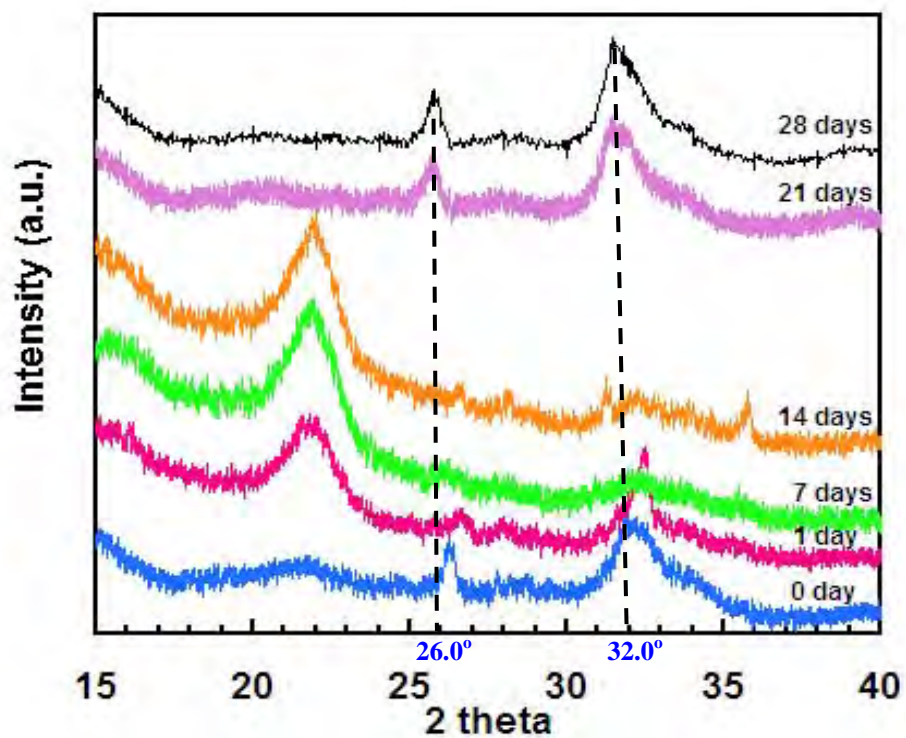


Figure 4.14 X-ray diffraction patterns of CGSF4 scaffold before and after incubation in collagenase solution for 0,1,7,14,21 and 28 days.

4.2 *In vivo* biodegradation of Thai silk fibroin-based scaffolds

In previous section, biodegradation behavior of four types of Thai silk fibroin-based scaffold was investigated *in vitro*, however the *in vitro* condition do not mimic the physiological situation. Then, to verify the degradation behavior of the scaffolds under living environment, the scaffolds were studied *in vivo* using implantation model. The degradation of scaffolds was evaluated in term of physical appearance, remaining area and morphology.

4.2.1 Physical appearance of Thai silk fibroin-based scaffolds

Physical appearance of four types of Thai silk fibroin-based scaffolds after 2, 4 and 12 weeks of implantation was showed in Figure 4.15 and 4.16. Comparing among four scaffold types, SF, SF4 and CGSF scaffolds seemed to degrade faster than CGSF4 scaffold, as seen from the thinner pieces of three scaffolds (SF, SF4 and CGSF). However, all scaffolds remained *in vivo* after 12 weeks of implantation. This might imply that all Thai silk fibroin-based scaffolds could be observed in subcutaneous tissue of Wistar rat after implantation longer than 12 weeks.

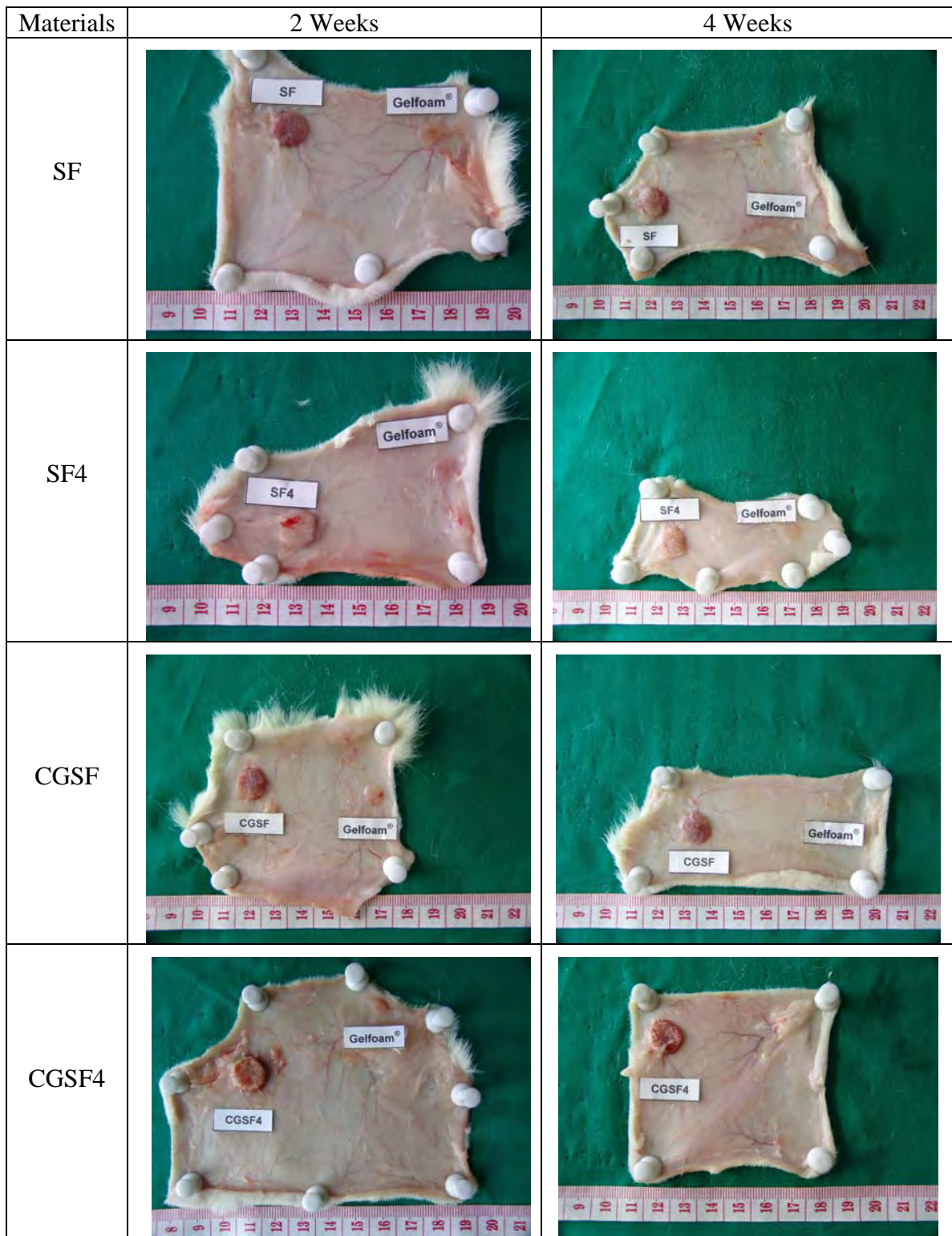


Figure 4.15 Physical appearances of Thai silk fibroin scaffold (SF), hydroxyapatite/Thai silk fibroin scaffold (SF4), conjugated gelatin/Thai silk fibroin scaffold (CGSF) and hydroxyapatite/conjugated gelatin/Thai silk fibroin scaffold (CGSF4) after 2 and 4 weeks of implantation

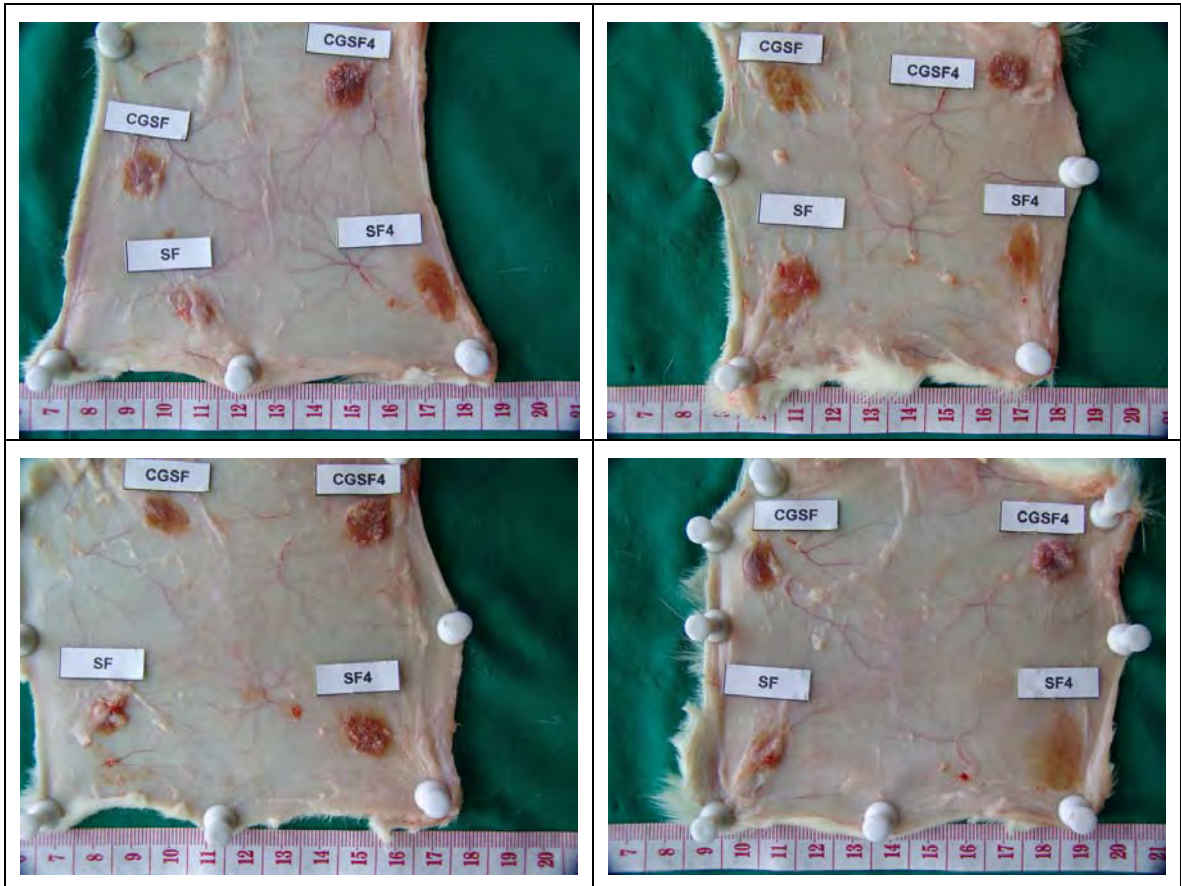


Figure 4.16 Physical appearances of Thai silk fibroin scaffold (SF), hydroxyapatite/Thai silk fibroin scaffold (SF4), conjugated gelatin/Thai silk fibroin scaffold (CGSF) and hydroxyapatite/conjugated gelatin/Thai silk fibroin scaffold (CGSF4) after 12 weeks of implantation

4.2.2 Remaining area of Thai silk fibroin-based scaffolds

At 2, 4 and 12 weeks after implantation, all scaffolds were retrieved from subcutaneous tissue in Wistar rats. The cross section of retrieved scaffolds was fixed in formalin, paraffin embedded and H&E stained. The remaining area of scaffolds was evaluated from H&E image based on the area occupied by scaffold. The histological image of the whole piece of scaffolds could be obtained by merging images as illustrated in appendix (Figure E1-E3). The boundary of the remaining scaffolds was marked and calculated using image J program. The calculated remaining area of all Thai silk fibroin-based scaffolds after 2, 4 and 12 weeks of implantation was compared in Figure 4.17. It was noted that, from histological photographs, the biodegradation of scaffold material was observed throughout the whole piece of scaffold, not only at the scaffold boundary. Therefore the remaining area presented could only be the guide for the relative biodegradability of scaffolds. Relatively, the largest remaining area of CGSF4 scaffold was observed among four types of scaffold after 12 weeks of implantation. Similar to the result after 4 weeks of implantation, the remaining area of CGSF4 scaffolds was largest compared to the other scaffolds (SF, SF4, CGSF). The results implied that the degradability of CGSF4 scaffolds seemed to be slowest which corresponded to the results of physical appearance observed after implantation in Figure 4.16. All Thai silk fibroin-based scaffolds still remained *in vivo* after 3 months of subcutaneous implantation in Wistar rats.

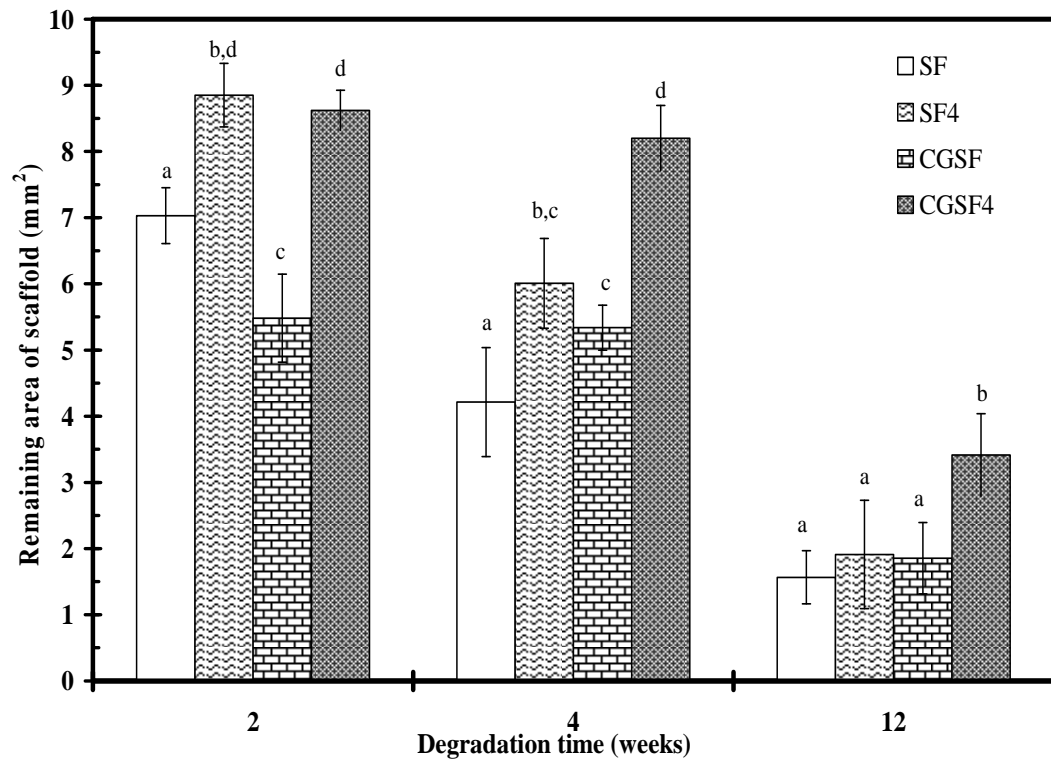


Figure 4.17 Remaining area of cross-sectioned SF, SF4, CGSF and CGSF4 scaffolds after 2, 4 and 12 weeks of subcutaneous implantation in Wistar rat. a, b, c and d represented the significant difference ($p < 0.05$) at each period of degradation time. The results with the same alphabet indicated that they are not significantly different.

4.2.3 Morphology of Thai silk fibroin-based scaffolds

The SEM micrographs of cross-sectional Thai silk fibroin-based scaffolds after 2, 4 and 12 weeks of implantation were presented in Figure 4.19, 4.20 and 4.21, respectively. After 2 weeks of implantation, it was observed that some inflammatory cells invaded into the SF scaffold and secreted the extracellular matrix. For CGSF scaffold, the wall of scaffold was fused. The deposited hydroxyapatite on SF4 scaffold was bioresorbable whereas the morphology of hydroxyapatite deposited on CGSF4 scaffold was similar to original morphology before degradation. After 4 weeks of implantation, a lot of inflammatory cells and blood cells invaded into SF scaffold, resulting in the fastest degradation. The fused morphology of CGSF scaffold was also observed as in the case of 2 weeks of implantation. It was also noticed that the deposited hydroxyapatite was resorbed faster on SF4 scaffold than that on CGSF4 scaffold. Bulk degradation of all scaffolds was observed after 12 weeks of degradation. The hydroxyapatite grown on SF4 and CGSF4 scaffolds was almost completely degraded. The result on morphology corresponded to the physical appearance and remaining area.

Comparing *in vitro* and *in vivo* biodegradation of Thai silk fibroin-based scaffolds, the CGSF scaffold showed the slowest *in vitro* degradation while *in vivo* the slowest degradation was observed in the case of CGSF4 scaffold. The double crosslinking of CGSF scaffold promoted the resistance against *in vitro* enzymatic degradation but this scaffold degraded faster *in vivo* environment due to inflammatory cell invasion. For CGSF4 scaffolds, the deposited hydroxyapatite from alternate soaking process dropped off from the surface scaffold when immersed in collagenase solution. In contrast, the hydroxyapatite deposition could prolong the *in vivo* degradability of Thai silk fibroin-based scaffolds compared to those without hydroxyapatite. Moreover, the hydroxyapatite grown on CGSF4 scaffold seemed to degrade much slower than that on SF4 scaffold. These difference could be due to the amide bond formation of the cross-linking reaction in CCSF4 scaffold. In general, pure hydroxyapatite could not degrade at all. However the degradation of hydroxyapatite depended on the fabrication method and complete degradation may

take several months or even many years [62]. In this study, the deposited hydroxyapatite particle appeared to be resorbed within 12 weeks of implantation.

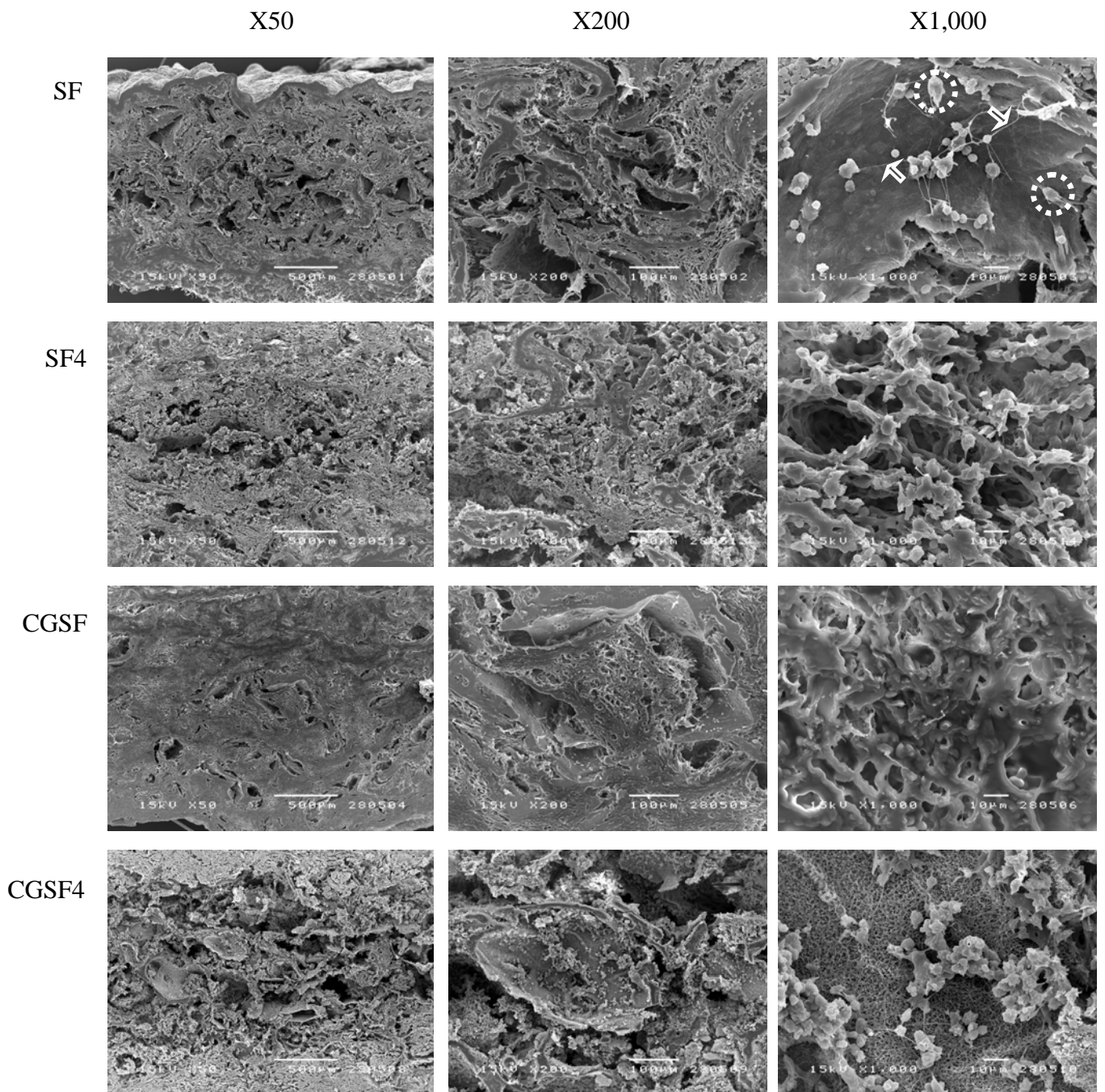


Figure 4.18 SEM micrographs of SF, SF4, CGSF and CGSF4 scaffolds after 2 weeks of implantation. Inflammatory cells=circle, extracellular matrix=arrow : X50, X200 and X1,000

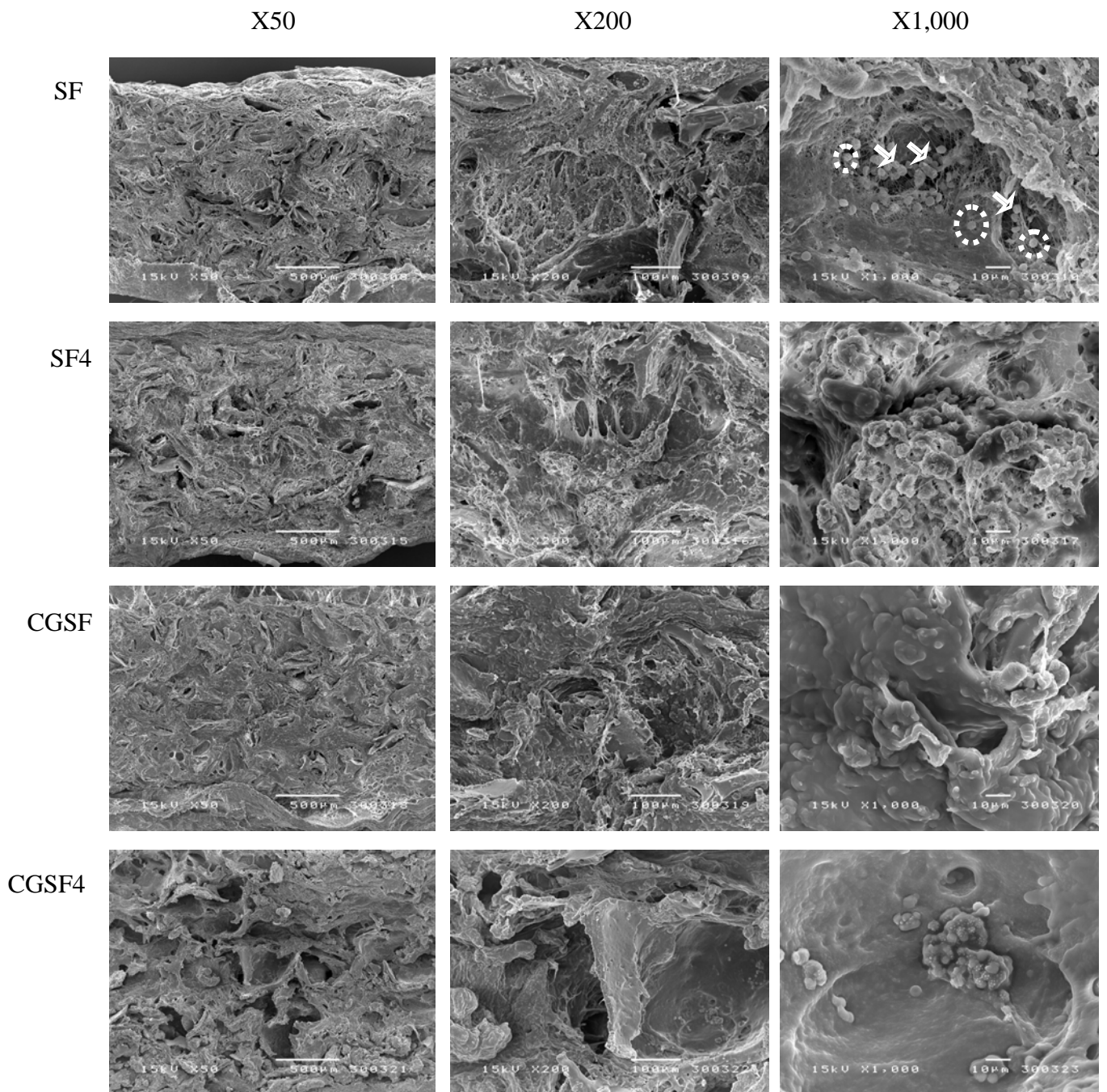


Figure 4.19 SEM micrographs of SF, SF4, CGSF and CGSF4 scaffolds after 4 weeks of implantation. Inflammatory cells=circle, blood cells=arrow
: X50, X200 and X1,000

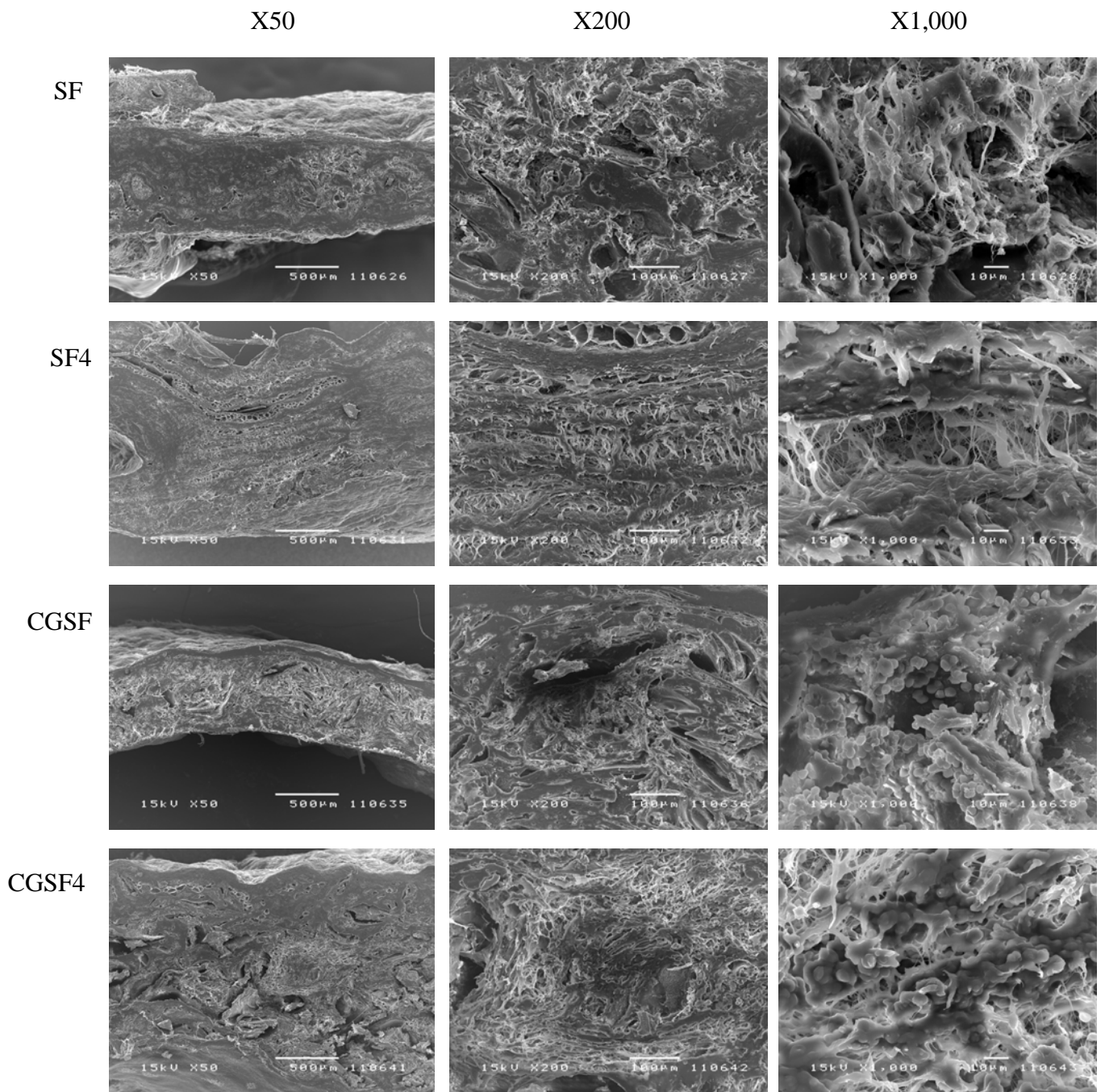


Figure 4.20 SEM micrographs of SF, SF4, CGSF and CGSF4 scaffolds after 12 weeks of implantation : X50, X200 and X1,000

4.3 Evaluation of the tissue response of Thai silk fibroin-based scaffolds following ISO10993-6.

4.3.1 Macroscopic assessment

Four types of Thai silk fibroin-based scaffolds were implanted in subcutaneous tissue of Wistar rats at 2 and 4 weeks. After implantation, Wistar rats appeared to be healthy throughout the implantation period as seen in Figure 4.21. There was no sign of inflammation such as redness, swelling, pain and heat along implantation period. After 2 and 4 weeks of implantation (Figure 4.22-4.23), the cross-section of retrieved SF and CGSF scaffolds were brownish yellow whereas that of SF4 and CGSF4 scaffolds were white and light yellow. There was no difference in the gross appearance of each scaffold. The abscess was not obviously found in all scaffolds during implantation period. In addition, no inflammatory reaction was seen around the implant sites.

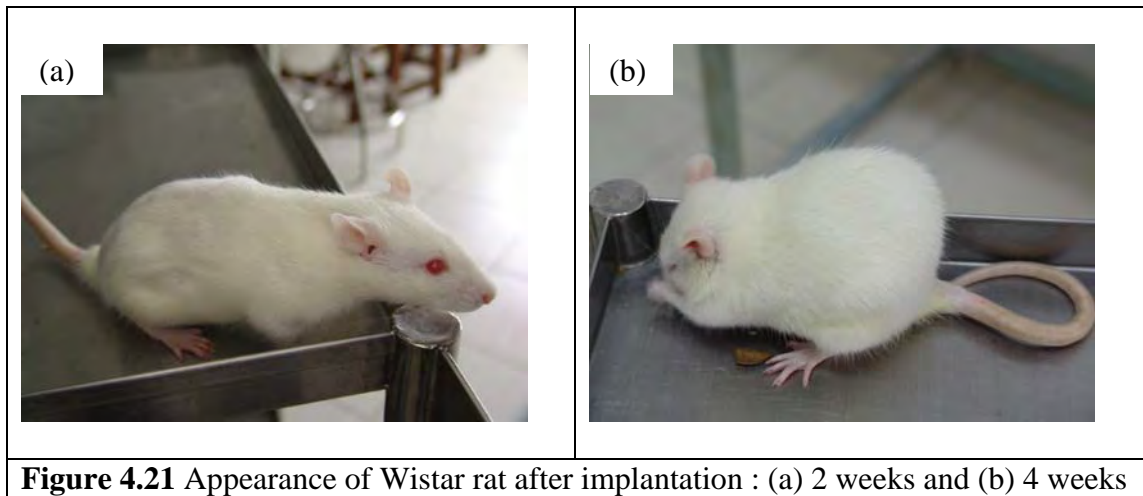


Figure 4.21 Appearance of Wistar rat after implantation : (a) 2 weeks and (b) 4 weeks

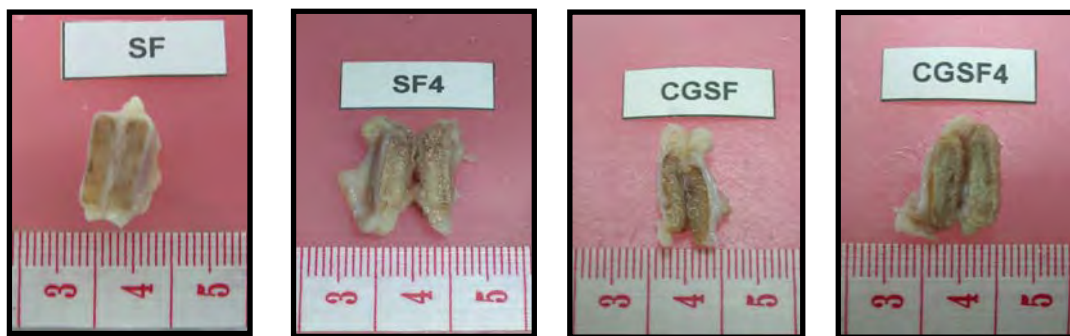


Figure 4.22 Gross appearance of cross-section of retrieved material after 2 weeks of implantation

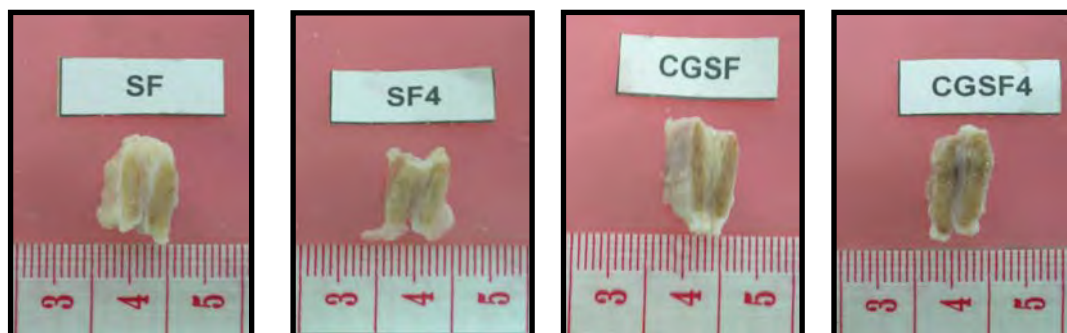


Figure 4.23 Gross appearance of cross-section of retrieved material after 4 weeks of implantation

4.3.2 Microscopic assessment

Inflammatory reactions at surrounding tissue for each type of scaffolds were investigated and compared to control material (Gelfoam[®]) after 2 and 4 weeks of implantation. The scoring of the histopathology of tissue reaction according to ISO10993-6, which was semi-quantitative evaluation system, was evaluated and presented in Table F in appendix. It was noted that the evaluation was performed twice (at two different time) by a pathologist. From the scoring, the level of irritation of all scaffolds after 2 and 4 weeks of implantation was shown in Table 4.1 -4.2. For the first evaluation at 2 weeks after implantation (Table 4.1), 2 out of 4 rats implanted with Thai silk fibroin scaffold (SF) were classified as “non-irritant” and the other rats were “slight irritant”. In case of SF4 and CGSF4 scaffolds, there was more than 50% rats showing as “non-irritant”. For CGSF scaffold, it was noticed that the control material implanted in the fourth rat could not be observed, resulting in no evaluation of this rat. For the second evaluation (Table 4.1), the results on the level of irritation was similar to the first evaluation. Figure 4.24-4.27 presented the surrounding tissue of Thai silk fibroin-based scaffolds after 2 weeks of implantation. Thai silk fibroin scaffolds showed minimal inflammatory response which consisted of rare macrophage and neovascularisation (Figure 4.24). In addition, in SF4, CGSF and CGSF4 scaffolds, rare macrophage, neovascularisation and giant cell, indicating a slight tissue response, was observed (Figure 4.25, 4.26, 4.27). Figure 4.28 displayed the tissue response of control sample, comprising rare macrophage. Comparing the surrounding tissue of Thai silk fibroin-based scaffolds to control (Gelfoam[®]) at the 2nd week of implantation, the tissue response of four Thai silk fibroin scaffold-based scaffold did not significantly different from the control. The results concluded that the level of irritation of all four types of scaffolds was “non-irritant” to “slight irritant” after 2 weeks of implantation.

Table 4.2 illustrated the level of irritation of scaffolds after 4 weeks of subcutaneous implantation. Similar to Table 4.1, the results on second evaluation was not significantly different from that on first evaluation. It was noted that the level of irritation of most scaffolds could not be evaluated because more than 50% of implanted control (Gelfoam[®]) was degraded completely. Considering the scores of

inflammatory cells and response (Table F-5-F-8), there was a decrease in inflammatory cells around SF, SF4 and CGSF4 scaffolds at the 4th week compared to at the 2nd week while CGSF scaffold still present the minimal macrophage, similar to the reaction at 2 weeks. Interestingly, no fibrosis and fatty infiltrate were observed in all scaffolds after 4 weeks of implantation. The surrounding tissue of all scaffolds and control after 4 weeks of implantation was shown in Figure 4.29-4.33. No significant difference in inflammatory cells and response was observed in all scaffolds compared to the control. It can be concluded that the tissue response to all Thai silk fibroin-based scaffolds after 4 weeks of implantation was less than that observed at the 2nd week.

Table 4.1 Level of irritation of scaffolds after 2 weeks of subcutaneous implantation

Types of material		Level of irritation	
		First evaluation	Second evaluation
SF	n=1	Non-irritant	Non-irritant
	n=2	Non-irritant	Non-irritant
	n=3	Slight irritant	Non-irritant
	n=4	Slight irritant	Non-irritant
SF4	n=1	Non-irritant	Non-irritant
	n=2	Non-irritant	Non-irritant
	n=3	Slight irritant	Slight irritant
	n=4	Non-irritant	Non-irritant
CGSF	n=1	Non-irritant	Non-irritant
	n=2	Non-irritant	Slight-irritant
	n=3	Slight irritant	Slight irritant
	n=4	N/A	N/A
CGSF4	n=1	Non-irritant	Non-irritant
	n=2	Non-irritant	Non-irritant
	n=3	Slight irritant	Slight irritant
	n=4	Non-irritant	Non-irritant

Remark : N/A no evaluation since control sample was completely degraded.

Table 4.2 Level of irritation of scaffolds after 4 weeks of subcutaneous implantation

Types of material		Level of irritation	
		First evaluation	Second evaluation
SF	n=1	Non-irritant	Non-irritant
	n=2	N/A	N/A
	n=3	N/A	N/A
	n=4	N/A	N/A
SF4	n=1	N/A	-
	n=2	N/A	-
	n=3	Slight irritant	Slight irritant
	n=4	N/A	-
CGSF	n=1	N/A	N/A
	n=2	Slight irritant	Slight irritant
	n=3	N/A	N/A
	n=4	N/A	N/A
CGSF4	n=1	N/A	N/A
	n=2	N/A	N/A
	n=3	N/A	N/A
	n=4	N/A	N/A

Remark : N/A no evaluation since control sample was completely degraded.

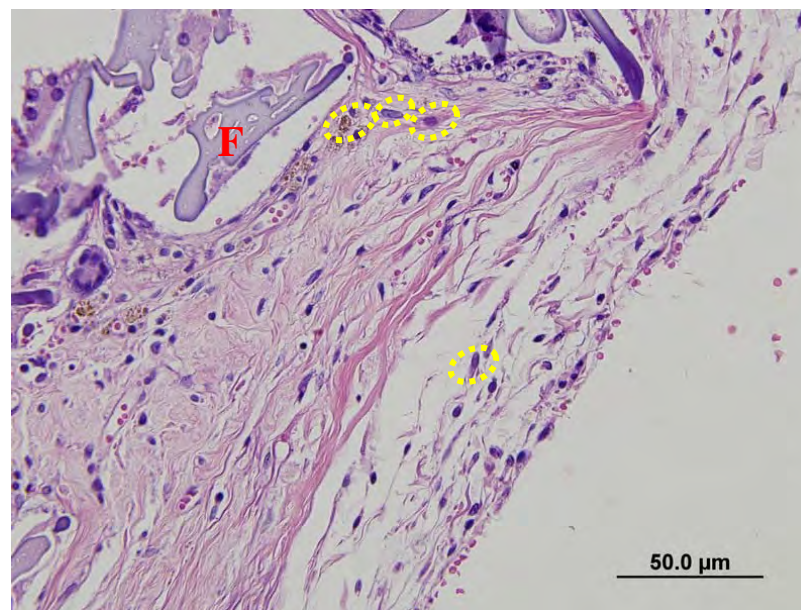


Figure 4.24 Histological section of subcutaneously implanted SF scaffold in Wistar rat after 2 weeks of implantation: yellow circle=macrophage, F=fragment of scaffold (magnification X400)

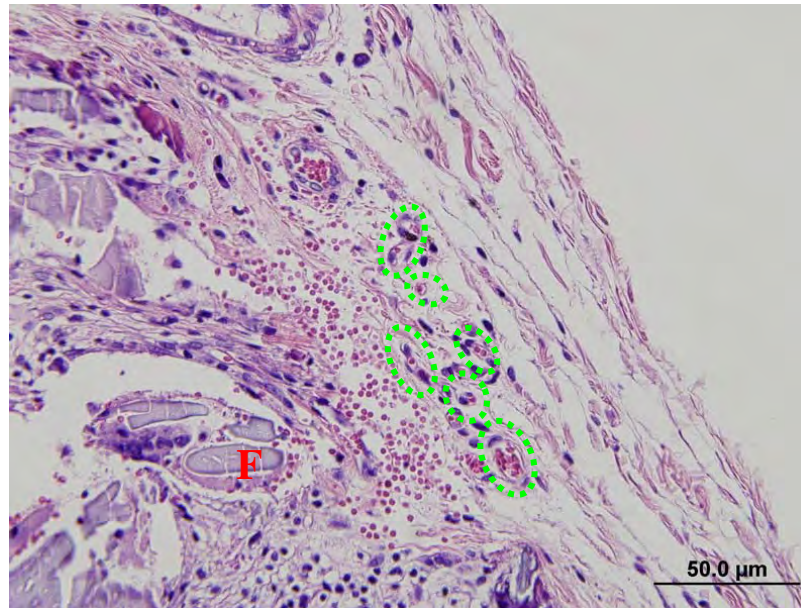


Figure 4.25 Histological section of subcutaneously implanted SF4 scaffold in Wistar rat after 2 weeks of implantation: green circle=neovascularisation, F=fragment of scaffold (magnification X400)

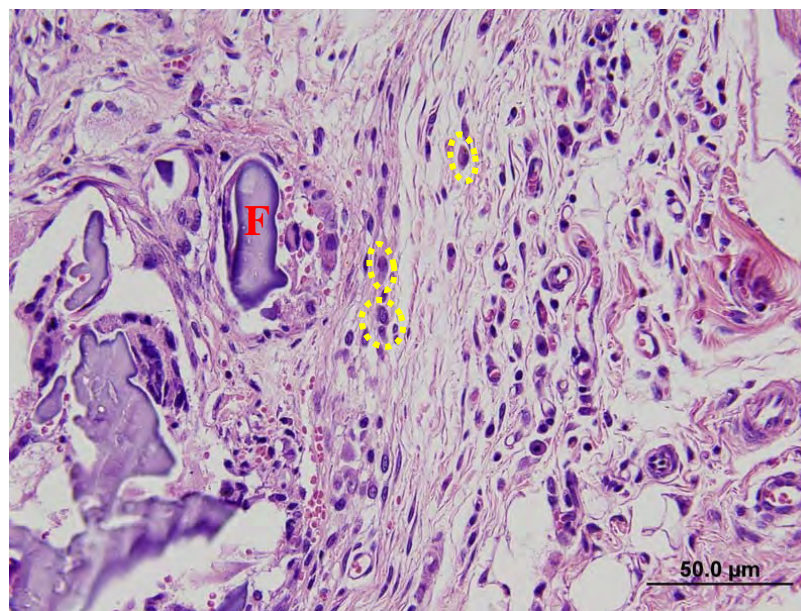


Figure 4.26 Histological section of subcutaneously implanted CGSF scaffold in Wistar rat after 2 weeks of implantation: yellow circle=macrophage, F=fragment of scaffold (magnification X400)

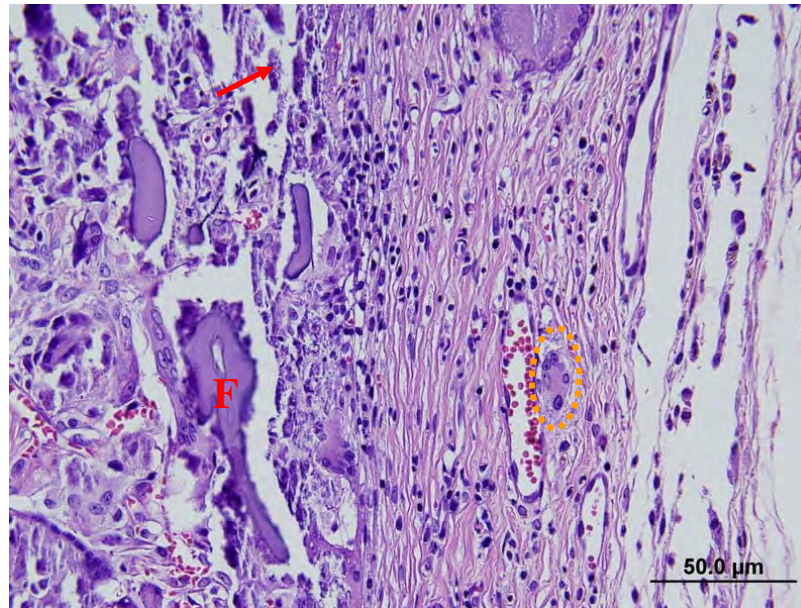


Figure 4.27 Histological section of subcutaneously implanted CGSF4 scaffold in Wistar rat after 2 weeks of implantation: orange circle=giant cell, F=fragment of scaffold and arrow= deposited calcium (magnification X400)

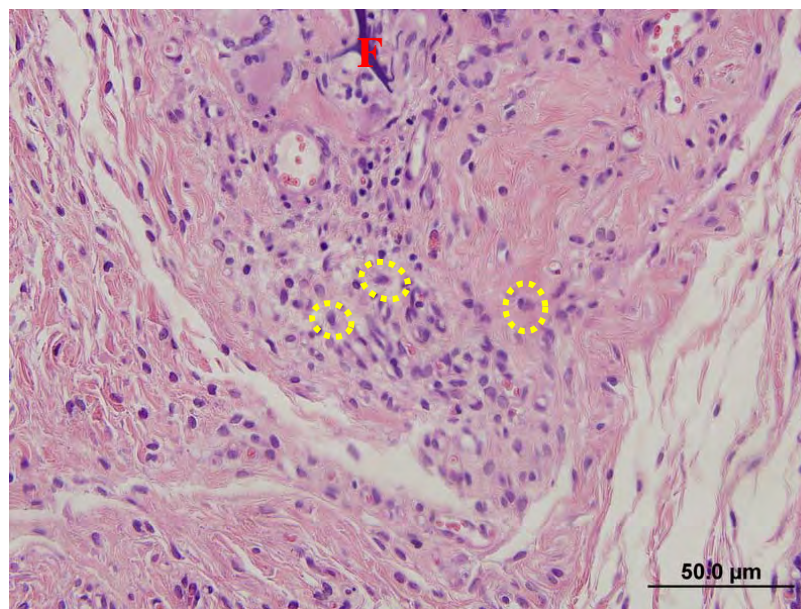


Figure 4.28 Histological section of subcutaneously implanted Gelfoam[®] in Wistar rat after 2 weeks of implantation: yellow circle=macrophage, F=fragment of scaffold (magnification X400)

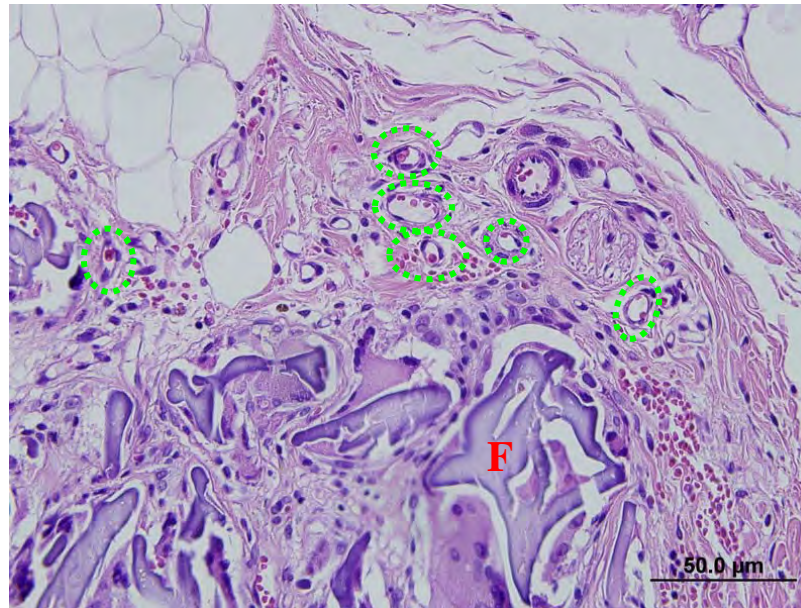


Figure 4.29 Histological section of subcutaneously implanted SF scaffold in Wistar rat after 4 weeks of implantation: green circle=neovascularisation, F=fragment of scaffold (magnification X400)

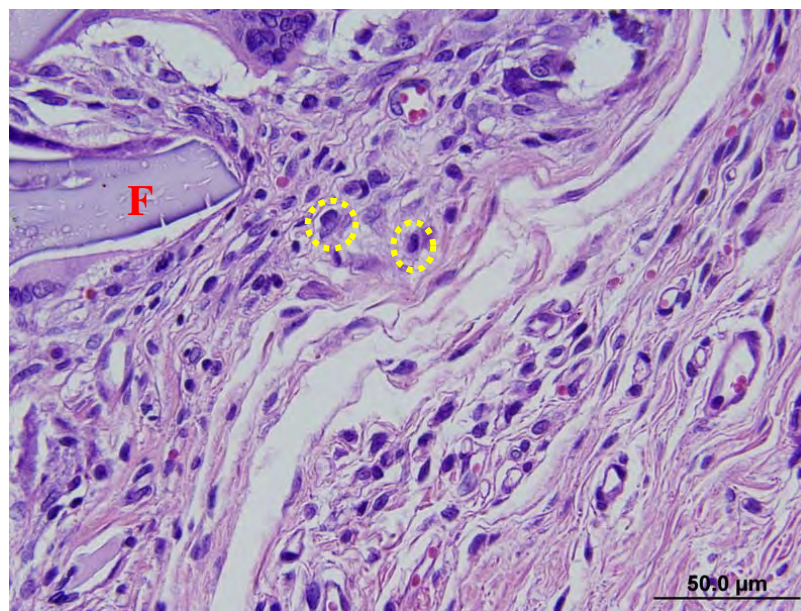


Figure 4.30 Histological section of subcutaneously implanted SF4 scaffold in Wistar rat after 4 weeks of implantation: yellow macrophage=circle, F=fragment of scaffold (magnification X400)

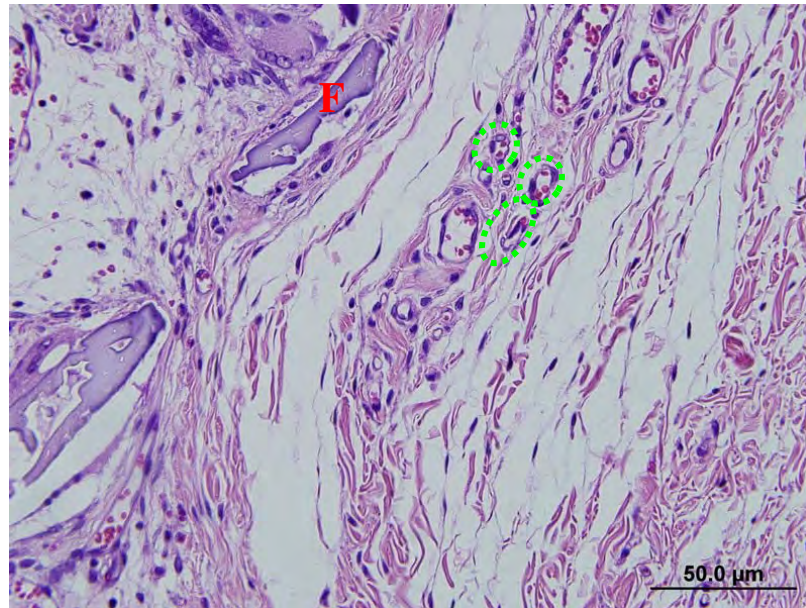


Figure 4.31 Histological section of subcutaneously implanted CGSF scaffold in Wistar rat after 4 weeks of implantation: green circle=neovascularisation
F=fragment of scaffold (magnification X400)

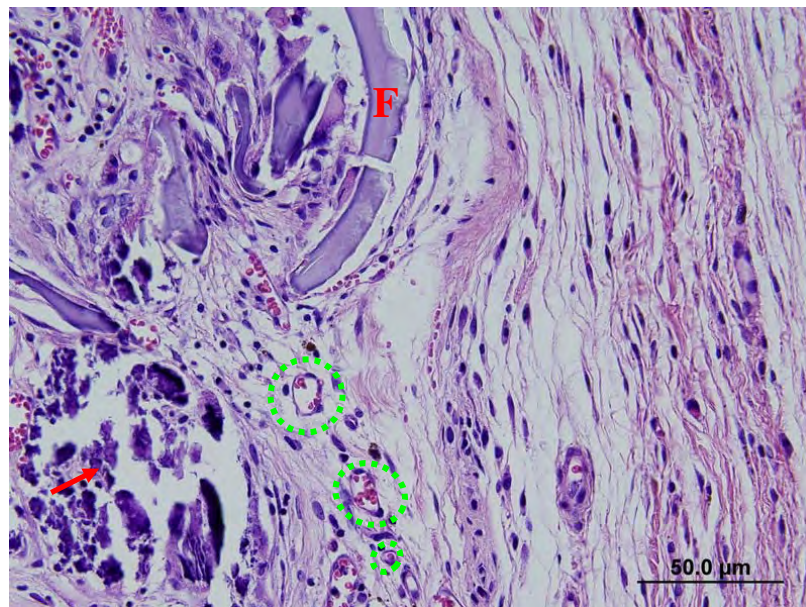


Figure 4.32 Histological section of subcutaneously implanted CGSF4 scaffold in Wistar rat after 4 weeks of implantation: green circle=neovascularisation
F=fragment of scaffold and arrow= deposited calcium (magnification X400)

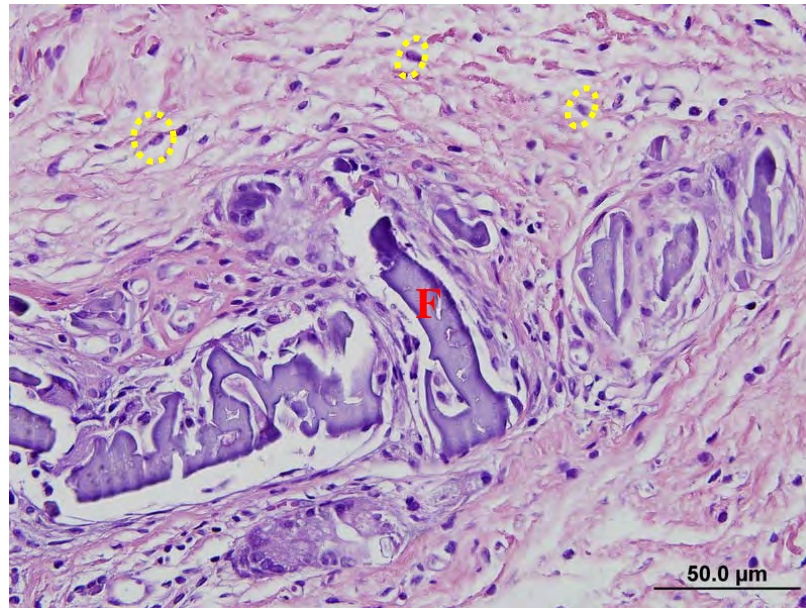


Figure 4.33 Histological section of subcutaneously implanted Gelfoam[®] in Wistar rat after 4 weeks of implantation: yellow circle =macrophage, F=fragment of scaffold (magnification X400)

CHAPTER V

CONCLUSIONS AND RECOMMENDATIONS

5.1 Conclusions

The biodegradation behaviors of four types of scaffolds were investigated *in vitro* (in collagenase solution) and *in vivo* (in a subcutaneous rat model). The physical appearance, remaining weight, scaffold morphology and conformational structure were examined *in vitro*. Among four types of scaffolds, the conjugated gelatin/Thai silk fibroin scaffold (CGSF) showed the slowest biodegradability in collagenase solution. This was because the gelatin conjugation by dehydrothermal and EDC/NHS treatments led to more stable amide formation of silk fibroin. The remaining weights of scaffolds after 28 days of incubation in collagenase solution were in the order of CGSF>SF>SF4~CGSF4. *In vivo* study demonstrated that all scaffolds remained *in vivo* after 12 weeks of subcutaneous implantation in Wistar rat. The biodegradability of CGSF4 scaffold was shown to be slowest compared to the other scaffolds (SF, CGSF, CGSF4) as evidenced by the physical appearance, remaining area and morphology. The hydroxyapatite deposition could prolong the *in vivo* biodegradability of Thai silk fibroin-based scaffolds compared to those scaffolds without hydroxyapatite. Comparing *in vitro* and *in vivo* biodegradation, the CGSF scaffold showed the slowest *in vitro* degradation while *in vivo*, the slowest degradation was observed in the case of CGSF4 scaffold.

The tissue response was evaluated according to International Standard Organization 10993-6: Biological evaluations of medical devices. All four types of scaffolds were classified as “non-irritant” to “slight irritant” after 2 weeks of subcutaneous implantation. After 4 weeks of implantation, the number of inflammatory cells decreased from those observed after 2 weeks of implantation.

In conclusion, four types of Thai silk fibroin-based scaffolds still remained after 12 weeks of subcutaneous implantation in Wistar rat. All implanted scaffolds at 2 and 4 weeks postoperatively showed the slight irritation as evaluated by ISO10993-6. The study indicated that Thai silk fibroin-based scaffolds were suitable to be further developed for tissue engineering applications that required slow biodegradation such as bone tissue engineering.

5.2 Recommendations

The tissue response and biodegradation of Thai silk fibroin-based scaffolds have been investigated in this work. In the attempt to apply Thai silk fibroin-based scaffolds in bone tissue engineering, there are some suggestions which should be further considered as follows:

1. Thai silk fibroin-based scaffolds should be tested in bone defect model.
2. Incorporation of growth factors and stem cells in Thai silk fibroin-based scaffolds may be useful to enhance bone ingrowth.

References

- [1] Meinel L, Fajardo R, Hofmann S, Langer R, Chen J, Snyder B, Novakovic GV, Kaplan DL. Silk implants for the healing of critical size bone defects. Bone 2005; 37: 688–698.
- [2] Meinel L, Hofmann S, Karageorgiou V, Heade CK, McCool J, Gronowicz G, Zichner L, Robert Langer R, Novakovic GV, Kaplan DL. The inflammatory responses to silk films in vitro and in vivo. Biomaterials 2005; 26: 147–155.
- [3] Wang Y, Kim HJ, Novakovic GV, Kaplan DL. Stem cell-based tissue engineering with silk biomaterials. Biomaterials 2006; 27 6064–6082.
- [4] Vepari C, Kaplan DL. Silk as a biomaterial. Progress in Polymer Science 2007; 32: 991–1007.
- [5] Kim HJ, Kima UJ, Novakovic GV, Min BH, Kaplan DL. Influence of macroporous protein scaffolds on bone tissue engineering from bone marrow stem cells. Biomaterials 2005; 26: 4442–4452
- [6] Chamchongkaset J. Development of three-dimensional gelatin/Thai silk fibroin scaffolds. Master Thesis. Department of Chemical Engineering. Chulalongkorn University 2007.
- [7] ISO10993-6, Biological evaluation of medical devices-Part 6: Tests for local effects after implantation.
- [8] Buddy DR, Allan SH. Biomaterials Science : An Introduction to Materials in Medicine. 2nd ed. The United States of America: Academic Press; 2004. Seminars in Immunology 2008; 20: 86–100.
- [9] James MA, Analiz R, David TC. Foreign body reaction to biomaterials. Anderson JM, Rodriguez A, Chang DT. Foreign body reaction to biomaterials. Seminars in Immunology 2008; 20: 86–100.
- [10] Anderson JM, Rodriguez A, Chang DT. Foreign body reaction to biomaterials. Seminars in Immunology 2008; 20: 86–100.
- [11] Anderson JM. Biological responses to materials. Annual Review of Material Research 2001; 31: 81–110.

- [12] Dee CK, Puleo AD, Bizios R, An Introduction to Tissue-Biomaterial Interactions. The United States of America: John Wiley & Sons, Inc; 2002.
- [13] Available from: http://www.tcd.ie/Genetics/staff/Miguel_DeArce_GE3095/Miguel_DeArce_GE3095/Aquired.html (8 July,2008).
- [14] Available from : http://www.themulberryleaf.com.au/about_us.htm (June 14, 2008).
- [15] Available from : http://210.246.186.28/pl_data/SILK/3var/var01.html (April 20, 2008).
- [16] Available from : <http://www.qthaisilk.com/thai/pages/menu31.htm> (April 20, 2008).
- [17] Available from : <http://www.fao.org/docrep/x2099E/x2099e03.htm> (March 8, 2008).
- [18] Cao Y, Wang B. Biodegradation of Silk Biomaterials. International Journal of Molecular Sciences 2009, 10: 1514-1524.
- [19] Bini E, David PK, Kaplan DL. Mapping Domain Structures in Silks from Insects and Spiders Related to Protein Assembly Journal of Molecular Biology 2004; 335: 27–40.
- [20] Available from : <http://chemed.chem.purdue.edu/genchem/topicreview/proteins4.html> (March 1, 2008).
- [21] Fini M, Motta A, Torricelli P, Giavaresi G, Nicoli Aldini N, Tschon M, Giardino R, Migliaresi C. The healing of confined critical size cancellous defects in the presence of silk fibroin hydrogel. Biomaterials 2005; 26 : 3527–3536.
- [22] Kim KH, Jeong L, Park HN, Shin SY, Park WH, Lee SC, Kim TI, Park YJ, Yang YJ, Lee YM, Ku Y, Rhyu IC, Han SB, Chung CP. Biological efficacy of silk fibroin nanofiber membranes for guided bone regeneration. Journal of Biotechnology 2005; 120 : 327–339.
- [23] Meinel L, Fajardo R, Hofmann S, Langer R, Chen J, Snyder B, Novakovic GV, Kaplan DL. Silk implants for the healing of critical size bone defects. Bone 2005; 37: 688–698.
- [24] Nazarov R, Jin HJ, Kaplan DJ. Porous 3-D Scaffolds from Regenerated Silk Fibroin. Biomacromolecules 2004; 5: 718-726.

- [25] Kim UJ, Park J, Kim HJ, Wada M, Kaplan DL. Three-dimensional aqueous-derived biomaterial scaffolds from silk fibroin. Biomaterials 2005; 26: 2775–2785.
- [26] Tabata Y, Ikada Y. Protein release from gelatin matrices. Advanced Drug Delivery Reviews 1998; 31: 287–301.
- [27] Available from : <http://www.lsbu.ac.uk/water/hygel.html> (August 29, 2008).
- [28] Available from : http://www.lakewoodconferences.com/catalog/98/197/food_additives.html (August 29, 2008).
- [29] Kuijpers AJ, Engbers GHM, Feijen J. Characterization of the Network Structure of Carbodiimide Cross-Linked Gelatin Gels. Macromolecules 1999, 32, 3325-3333.
- [30] Suzuki K, Yumura T, Mizuguchi M. Apatite-Silica gel composite materials prepared by alternate soaking process. Journal of Sol-Gel Science and Technology 2001; 21: 55–63.
- [31] Nagai H, Nishimura Y. Hydroxyapatite, ceramic material and process for preparing thereof. United States Patent 4448758.
- [32] Ikoma T, Yamazaki A. Preparation and dielectric property of sintered monoclinic hydroxyapatite. Journal of materials science letter 1999; 18: 1225-1228.
- [33] Available from : <http://www.impb.ru/downloads/hydroxyapatite.ppt> (August 29,2008).
- [34] Furuzono T, Taguchi T, Kishida A, Akashi M, Tamada Y. Preparation and characterization of apatite deposited on silk fabric using an alternate soaking process. John Wiley & Sons, Inc 2000; 346-352.
- [35] Li M., Ogiso M., Minoura N. Enzymatic degradation behavior of porous silk fibroin sheets. Biomaterials 2003; 24 357–365.
- [36] Takayuki A, Giuliano F, Riccardo I, Masuhiro T. Biodegradation of *Bombyx mori* silk fibroin fibers and films. Journal of Applied Polymer Science 2004; 91: 2383–2390.
- [37] Horan RL, Antle K, Collette AL, Wang Y, Huang J, Moreau JE, Volloch V, Kaplan DL, Altman GH. In vitro degradation of silk fibroin. Biomaterials 2005; 26: 3385–3393.

- [38] Zhending S, Bofeng Z, Chenrui J, Qingling F, Yingxin X. Preparation and *in vitro* degradation of porous three-dimensional silk fibroin/chitosan scaffold. Polymer Degradation and Stability 2008; 93: 1316-1322.
- [39] Wang Y, Rudym DD, Walsh A, Abrahamsen L, Kim HJ, Kim HS, Head CK, Kaplan DL. In vivo degradation of three-dimensional silk fibroin scaffolds. Biomaterials 2008; 29: 3415-3428.
- [40] Gellynck K, Verdonk P, Forsyth R, Almqvist KF, Nimmen EV, Gheysens T, Mertens J, Langenhove LV, Kiekens P, Verbruggen G. Biocompatibility and biodegradability of spider egg sac silk. Journal Material Science: Mater Med 2008; 19: 2963–2970.
- [41] Burugapalli K, Koul V, Dinda AK. Effect of composition of interpenetrating polymer network hydrogels based on poly(acrylic acid) and gelatin on tissue response: A quantitative in vivo study. Jouranl of Biomedical Materials Research 2004; 68A 210-218.
- [42] Ye Q, Ohsaki K, Li K, Li DJ, Zhu CS, Ogawa T, Tenshin S, Yamamoto TT. Histological reaction to hydroxyapatite in the middle ear of rats. International Journal of ORL&HNS 2008; 28: 131-136.
- [43] Lehle K, Lohn S, Reinerth GU, Schubert T, Preuner GJ, Birnbaum DE. Cytological evaluation of the tissue–implant reaction associated with subcutaneous implantation of polymers coated with titaniumcarboxonitride in vivo. Biomaterials 2004; 25: 5457–5466.
- [44] Lickorish D, Chan J, Song Jand Davies JE. An in-vivo model to interrogate the transition from acute to chronic inflammation. European Cells and Materials 2004; 8: 12 – 20.
- [45] Macleoda TM, Williamsb G, Sandersa R, Green CJ. Histological evaluation of Permacole as a subcutaneous implant over a 20-week period in the rat model British Journal of Plastic Surgery 2005; 58: 518–532.
- [46] Jong WH, A.M.A. Dormans J, Steenbergen M. Tissue response in the rat and the mouse to degradable dextran hydrogels. Journal of Biomedical Materials Research 2007; 83A 538–545.

- [47] Satoa Y, Yokoyamab A, Kasaib T, Hashiguchic S, Ootsuboa M, Oginoa SI, Sashidaa N, Namuraa M, Motomiyaa K, Jeyadevana B, Tohjia K. In vivo rat subcutaneous tissue response of binder-free multi-walled carbon nanotube blocks cross-linked by de-fluorination. Carbon 2008; 46: 1927-1934.
- [48] Garrido G, Gomes DI, Clapes D, Ribeiro L, Roberto W. Biocompatibility of actazolamide pastes in the subcutaneous tissue of rats. Brazilian Dental Journal 2009; 20(1): 17-21.
- [49] Kotzara G, Mark Freasa P, Abelb P, Fleischmanc A, Royc S, Zormand C, Morane JM, Melzak J. Evaluation of MEMS materials of construction for implantable medical devices. Biomaterials 2002; 23: 2737–2750.
- [50] Yang C, Zhao C, Wold L, Kenton R. Kaufman Biocompatibility of a physiological pressure sensor. Biosensors and Bioelectronics 2003; 19 51-58.
- [51] Taguchi, T. Kishida, A, and Akashi M. Hydroxyapatite Formation on/in poly(vinyl alcohol) hydrogel matrices using a novel alternate soaking process. Chemistry Letters 1998: 711-712.
- [52] Li M, Ogiso M, Minoura N. Enzymatic degradation behavior of porous silk fibroin sheets. Biomaterials 2003; 24: 357–365.
- [53] Petrini P, Parolari C, Tanzi MC. Silk fibroin-polyurethane scaffolds for tissue engineering. Journal of Materials Science: materials in medicine 2001; 12; 849-853.
- [54] Dykstra JM. A Manual of applied techniques for biological electron microscopy. Drying samples with hexamethyldisilazane, 109. New York, 1993.
- [55] Yuan YD, Jun J, Shao-hai W, Wei Y, Lei J, Zhong-yi W. Preparation of PLGA electrospun nanofibers for tissue engineering application. Journal of US-China Medical Science 2007; 4: 41-44.
- [56] Ozeki A, Tabata Y. *In vivo* degradability of hydrogels prepared from different gelatins by various crosslinking method. Journal of Biomaterials Science, Polymer Edition 2004.

- [57] Everaerts F, Torrianni M, Hendriks M, Feijen J. Biomechanical properties of carbodiimide crosslinked collagen: influence of the formation of ester crosslinks. Journal of Biomedical Materials Research Part A. 2008; 85(2): 547-55.
- [58] Kim HJ, Kim JU, Kim SH, Li C, Wada M, Leisk GG and Kaplan DL. Bone tissue engineering with premineralized silk scaffolds. Bone 2008; 42: 1226-1234.
- [59] Chunling D, Jun J, Yucheng L, Xiangdong Kong, Kemin W, Juming Y. Novel silk fibroin/hydroxyapatite composite films: Structure and properties. Materials Science and Engineering 2009; C29: 62–68.
- [60] Wang L, Nemoto R and Senna M. Microstructure and chemical states of hydroxyapatite/silk fibroin nanocomposites synthesized via a wet-mechanochemical route. Journal of Nanoparticle Research 2002; 4: 535–540.
- [61] Furuzono T, Taguchi T, Kishida A, Akashi M, Tamada Y. Preparation and characterization of apatite deposited on silk fabric using an alternate soaking process. Journal of Biomedical Materials Research 2000; 50: 344–352.
- [62] Ravaglioli A. and Krajewski A. Bioceramics: Material. Properties. Application. 1st ed. Faenza-Italy; 1992.

APPENDICES

A. Evaluation of scaffold area

- Opening an image program :

The image J window has a menu bar, tool bar and status bar as presented in Figure A-1.

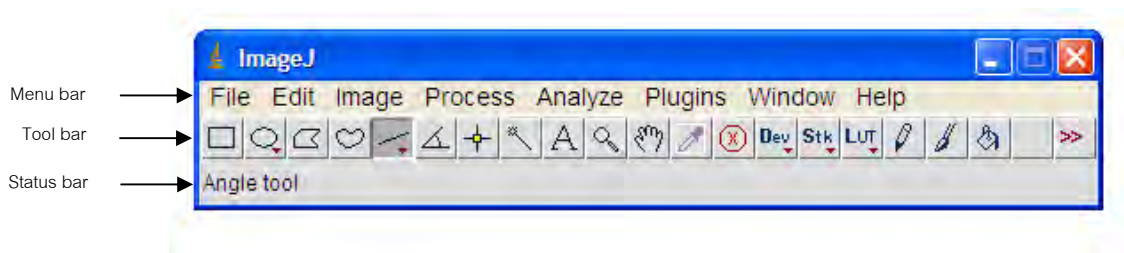


Figure A-1 Image J window

- Opening a stored image file : Select file → open from the menu bar

The opening image file was shown in Figure A-2.

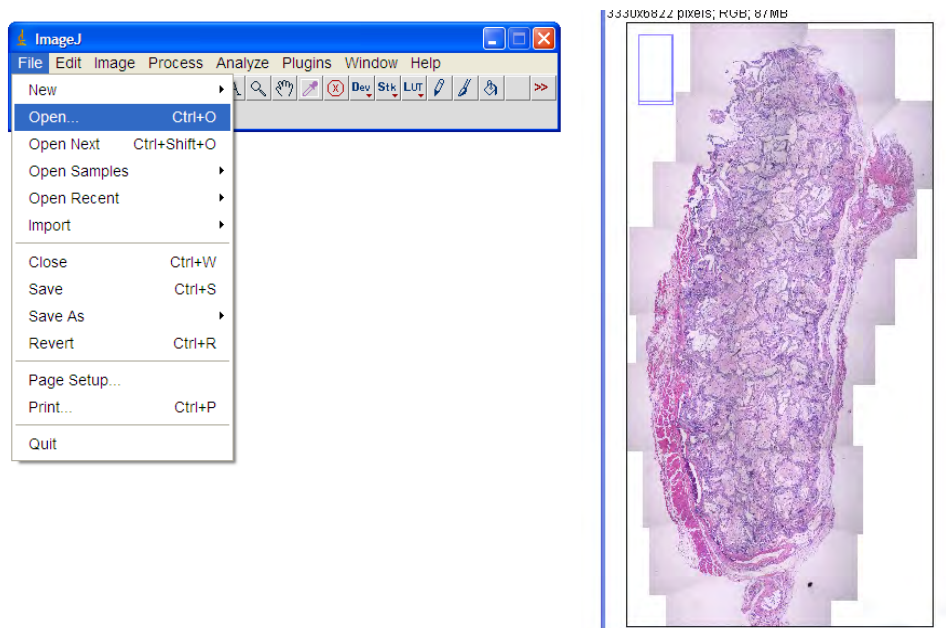


Figure A-2 Opening the image file

- Setting measurement scale as seen in Figure A-3 :

- 1) Select the straight line from toolbar and draw a straight line on scale bar as known distance in image
- 2) Go to analyze to set scale (Type known distance and unit of length)

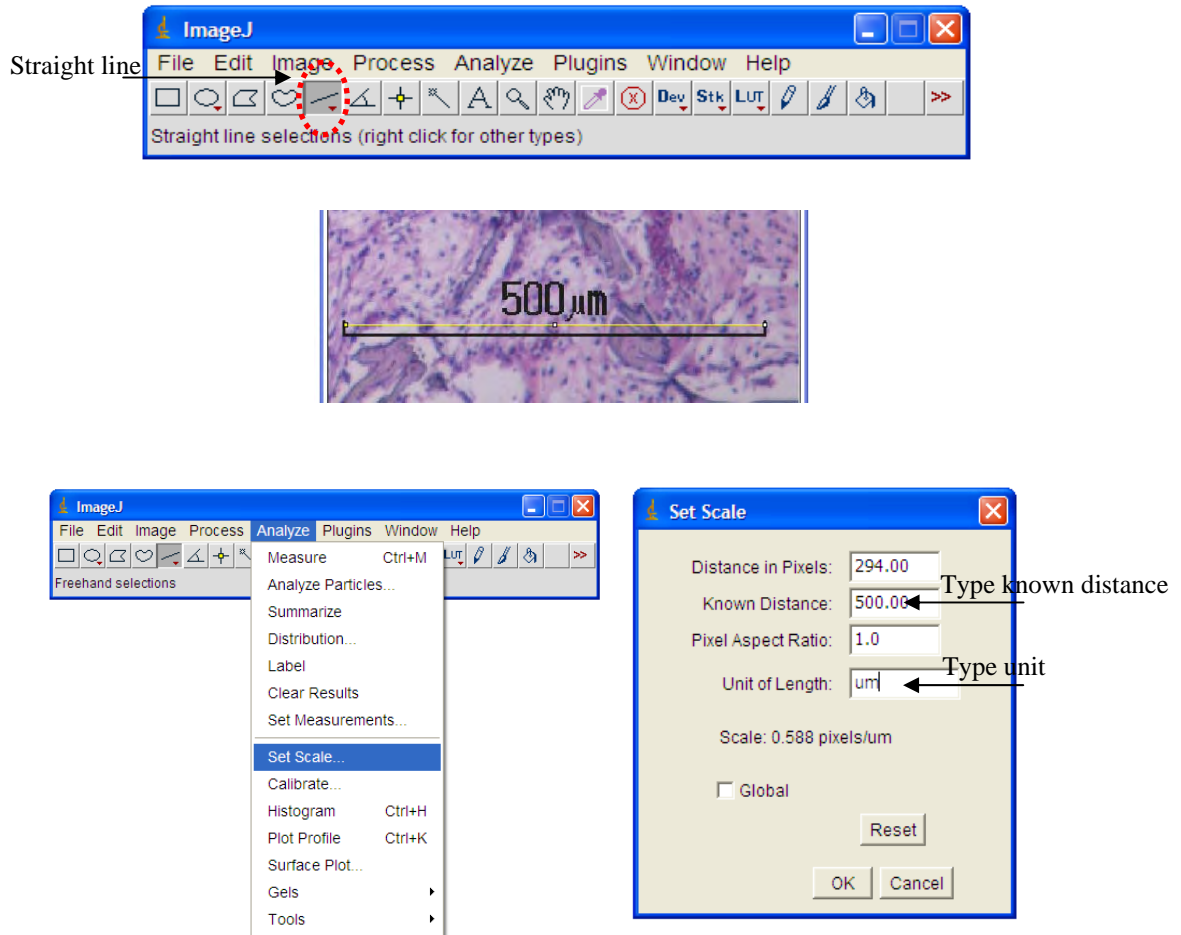


Figure A-3 Setting measurement scale

- Measuring area as presented in Figure A-4 :
 - 1) Select the polygonal shape from toolbar and surround a scaffold area
 - 2) Go to analyze to measurement area

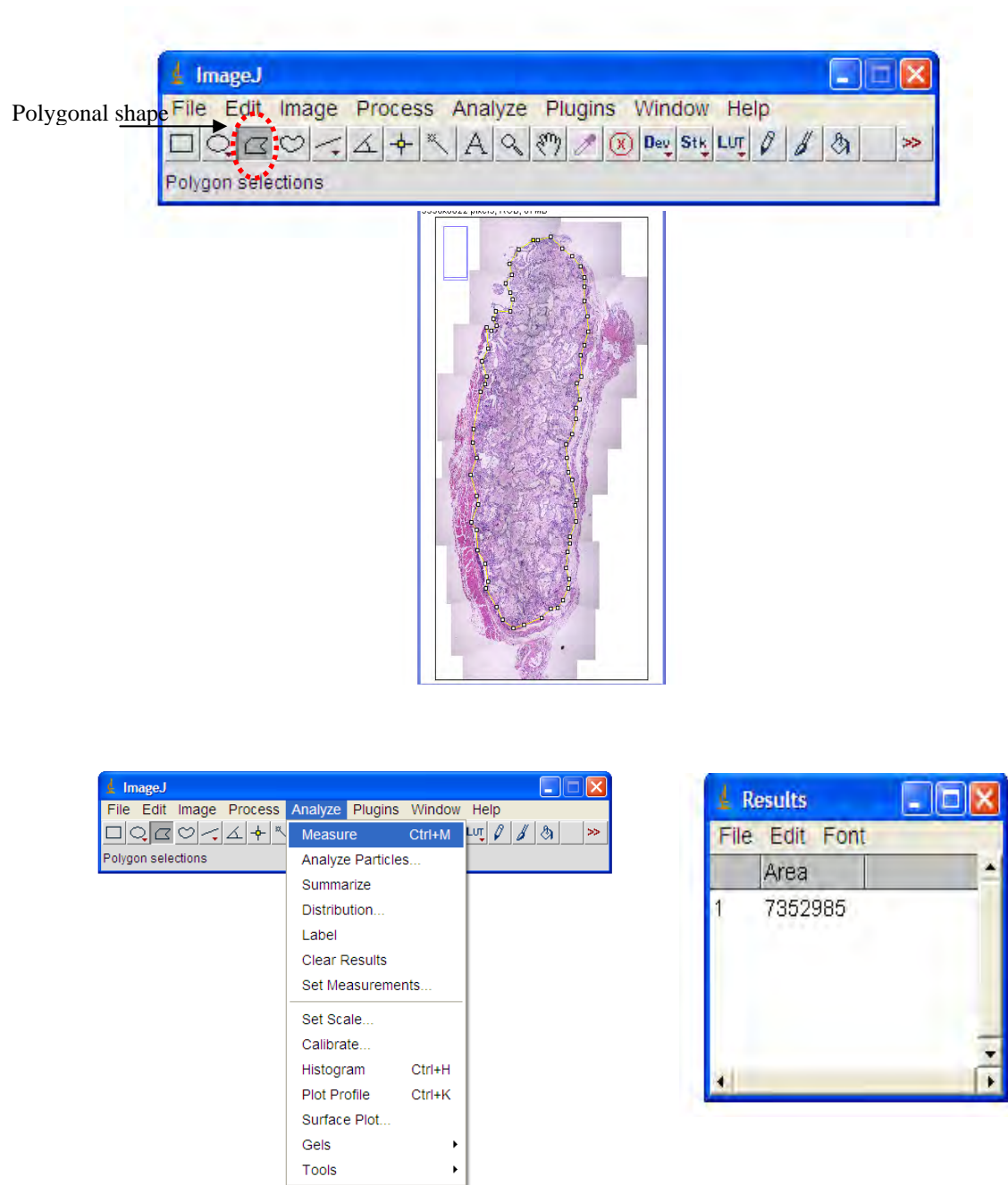


Figure A-4 Measuring area of scaffold

B. Gelfoam[®] (absorbable gelatin, compressed sponge, USP)**Description**

GELFOAM Sterile Compressed Sponge is a medical device intended for application to bleeding surfaces as a hemostatic. It is water-insoluble, off-white, nonelastic, porous, pliable product prepared from purified porcine Skin Gelatin USP Granulates and Water for Injection, USP. It may be cut without fraying and is able to absorb and hold within its interstices, many times its weight of blood and other fluids.

Actions

GELFOAM Sterile Compressed Sponge has hemostatic properties. While its mode of action is not fully understood, its effect appears to be more physical than the result of altering the blood clotting mechanism. When not used in excessive amounts, GELFOAM is absorbed completely, with little tissue reaction. This absorption is dependent on several factors, including the amount used, degree of saturation with blood or other fluids, and the site of use. When placed in soft tissues, GELFOAM is usually absorbed completely within four to six weeks, without inducing excessive scar tissue. When applied to bleeding nasal, rectal, or vaginal mucosa, it liquefies within two to five days.

Clinical studies

GELFOAM Sterile Sponge is a water-insoluble, hemostatic device prepared from purified porcine skin gelatin, and capable of absorbing up to 45 times its weight of whole blood.⁴ The absorptive capacity of GELFOAM is a function of its physical size, increasing as the size of the gelatin sponge increases.⁵ The mechanism of action of surface-mediated hemostatic devices is supportive and mechanical.⁵ Surface-acting devices, when applied directly to bleeding surfaces, arrest bleeding by the formation of an artificial clot and by producing a mechanical matrix that facilitates clotting.⁶ Jenkins et al⁷ have theorized that the clotting effect of GELFOAM may be due to release of thromboplastin from platelets, occurring when platelets entering the sponge become damaged by contact with the walls of its myriad of interstices. Thromboplastin interacts with prothrombin and calcium to produce thrombin, and this sequence of events initiates the clotting reaction. The authors suggest that the physiologic formation of thrombin in the sponge is sufficient to produce formation of a clot, by its action on the fibrinogen in blood.⁷ The spongy physical properties of the

gelatin sponge hasten clot formation and provide structural support for the forming clot.^{6,8} Several investigators have reported that GELFOAM becomes liquefied within a week or less and is completely absorbed in four to six weeks, without inducing excessive scar formation.^{4,7,9,10,11} Barnes¹⁰ reviewed experiences with GELFOAM in gynecologic surgery. No excessive scar tissue, attributable to the absorption of GELFOAM, could be palpated at postoperative examination.

Animal pharmacology

Surface-acting hemostatic devices, when applied directly to bleeding surfaces, arrest bleeding by providing a mechanical matrix that facilitates clotting.^{6,8,13,14} Due to their bulk, surface-acting hemostatic agents slow the flow of blood, protect the forming clot, and offer a framework for deposition of the cellular elements of blood. MacDonald and Mathews studied GELFOAM implants in canine kidneys and reported that it assisted in healing, with no marked inflammatory or foreign-body reactions. Jenkins and Janda studied the use of GELFOAM in canine liver resections and noted that the gelatin sponge appeared to offer a protective cover and provide structural support for the reparative process. Correll et al studied the histology of GELFOAM Sterile Sponge when implanted in rat muscle and reported no significant tissue reaction.

Indications

HEMOSTASIS: GELFOAM Sterile Compressed Sponge, used dry or saturated with sterile sodium chloride solution, is indicated in surgical procedures as a hemostatic device, when control of capillary, venous, and arteriolar bleeding by pressure, ligature, and other conventional procedures is either ineffective or impractical. Although not necessary, GELFOAM can be used either with or without thrombin to obtain hemostasis.

Directions for use

Sterile technique should always be used to remove GELFOAM Sterile Compressed Sponge from its packaging. Cut to the desired size, a piece of GELFOAM, either dry or saturated with sterile, isotonic sodium chloride solution (sterile saline), can be applied with pressure directly to the bleeding site. When applied dry, a single piece of GELFOAM should be manually applied to the bleeding site, and held in place with moderate pressure until hemostasis results. When used

with sterile saline, GELFOAM should be first immersed in the solution and then withdrawn, squeezed between gloved fingers to expel air bubbles, and then replaced in saline until needed. The GELFOAM sponge should promptly return to its original size, with slight expansion in thickness and shape in the solution. If it does not, it should be removed again and kneaded vigorously until all air is expelled and it does expand to its original size, with slight increases in thickness and shape when returned to the sterile saline. GELFOAM if used wet it may be blotted to dampness on gauze before application to the bleeding site. It should be held in place with moderate pressure, using a pledget of cotton or small gauze sponge until hemostasis results. Removal of the pledget or gauze is made easier by wetting it with a few drops of sterile saline, to prevent pulling up the GELFOAM which by then should enclose a firm clot. Use of suction applied over the pledget of cotton or gauze to draw blood into the GELFOAM is unnecessary, as GELFOAM will draw up sufficient blood by capillary action. The first application of GELFOAM will usually control bleeding, but if not, additional applications may be made. For additional applications, fresh pieces should be used, prepared as described above. Use only the minimum amount of GELFOAM, cut to appropriate size, necessary to produce hemostasis. The GELFOAM may be left in place at the bleeding site, when necessary. Since GELFOAM causes little more cellular reaction than does the blood clot, the wound may be closed over it. GELFOAM may be left in place when applied to mucosal surfaces until it liquefies. For use with thrombin, consult the thrombin insert for complete prescribing information and proper sample preparation.

Contraindications

GELFOAM Sterile Compressed Sponge should not be used in closure of skin incisions because it may interfere with the healing of skin edges. This is due to mechanical interposition of gelatin and is not secondary to intrinsic interference with wound healing. GELFOAM should not be placed in intravascular compartments, because of the risk of embolization. Do not use GELFOAM Compressed Sponge in patients with known allergies to porcine collagen.

Warnings

GELFOAM Sterile Compressed Sponge is not intended as a substitute for meticulous surgical technique and the proper application of ligatures, or other

conventional procedures for hemostasis. GELFOAM is supplied as a sterile product and cannot be resterilized. Unused, opened envelopes of GELFOAM should be discarded. Only the minimum amount of GELFOAM necessary to achieve hemostasis should be used. Once hemostasis is attained, excess GELFOAM should be carefully removed. The use of GELFOAM is not recommended in the presence of infection. GELFOAM should be used with caution in contaminated areas of the body. If signs of infection or abscess develop where GELFOAM has been positioned, reoperation may be necessary in order to remove the infected material and allow drainage. Although the safety and efficacy of the combined use of GELFOAM with other agents such as topical thrombin has not been evaluated in controlled clinical trials, if in the physician's judgment concurrent use of topical thrombin is medically advisable, the product literature for that agent should be consulted for complete prescribing information. While packing a cavity for hemostasis is sometimes surgically indicated, GELFOAM should not be used in this manner unless excess product not needed to maintain hemostasis is removed. Whenever possible, it should be removed after use in laminectomy procedures and from foramina in bone, once hemostasis is achieved. This is because GELFOAM may swell to its original size on absorbing fluids, and produce nerve damage by pressure within confined bony spaces. The packing or wadding of GELFOAM, particularly within bony cavities, should be avoided, since swelling to original size may interfere with normal function and/or possibly result in compression necrosis of surrounding tissues.

Precautions

Use only the minimum amount of GELFOAM Sterile Compressed Sponge needed for hemostasis, holding it at the site until bleeding stops, then removing the excess. GELFOAM should not be used for controlling postpartum bleeding or menorrhagia. It has been demonstrated that fragments of another hemostatic agent, microfibrillar collagen, pass through the 40 μ transfusion filters of blood scavenging systems. GELFOAM should not be used in conjunction with autologous blood salvage circuits since the safety of this use has not been evaluated in controlled clinical trials. Microfibrillar collagen has been reported to reduce the strength of methylmethacrylate

adhesives used to attach prosthetic devices to bone surfaces. As a precaution, GELFOAM should not be used in conjunction with such adhesives. GELFOAM is not recommended for the primary treatment of coagulation disorders. It is not recommended that GELFOAM be saturated with an antibiotic solution or dusted with antibiotic powder.

Adverse reactions

There have been reports of fever associated with the use of GELFOAM, without demonstrable infection. GELFOAM Sterile Compressed Sponge may form a nidus of infection and abscess formation, and has been reported to potentiate bacterial growth. Giant-cell granuloma has been reported at the implantation site of absorbable gelatin product in the brain, and compression of the brain and spinal cord resulting from an accumulation of sterile fluid has been reported following use of absorbable gelatin sponge in closed space. Foreign body reactions, "encapsulation" of fluid and hematoma have also been reported. When GELFOAM was used in laminectomy operations, multiple neurologic events were reported, including but not limited to cauda equina syndrome, spinal stenosis, meningitis, arachnoiditis, headaches, paresthesias, pain, bladder and bowel dysfunction, and impotence. Excessive fibrosis and prolonged fixation of a tendon have been reported when absorbable gelatin products were used in severed tendon repair. Toxic shock syndrome has been reported in association with the use of GELFOAM in nasal surgery. Fever, failure of absorption, and hearing loss have been reported in association with the use of GELFOAM during tympanoplasty.

Adverse reactions reported from unapproved use

GELFOAM is not recommended for use other than as an adjunct for hemostasis. While some adverse medical events following the unapproved use of GELFOAM have been reported (see ADVERSE REACTIONS), other hazards associated with such use may not have been reported. When GELFOAM has been used during intravascular catheterization for the purpose of producing vessel occlusion, the following adverse events have been reported; fever, duodenal and pancreatic infarct, embolization of lower extremity vessels, pulmonary embolization, splenic abscess, necrosis of specific anatomic areas, asterixis, and death. These adverse medical events have been associated with the use of GELFOAM for repair of

dural defects encountered during laminectomy and craniotomy operations: fever, infection, leg paresthesias, neck and back pain, bladder and bowel incontinence, cauda equina syndrome, neurogenic bladder, impotence, and paresis.

Dosage and administration

Sterile technique should always be used in removing the inner envelope containing the GELFOAM Sterile Sponge from the outer printed sealed envelope. The minimum amount of GELFOAM of appropriate size and shape should be applied (dry or wet, see DIRECTIONS FOR USE) to the bleeding site and held firmly in place until hemostasis is observed. Opened envelopes of unused GELFOAM should always be discarded.

How supplied

GELFOAM Sterile Compressed Sponge is supplied in an individual sterile envelope enclosed in an outer peelable envelope. Sterility of the product is assured unless the outer envelope has been damaged or opened. It is available as follows
Sponge-Size 100 Box of 6 09-0353-01 (100 sq cm (8X12.5 cm), 15 5/8 sq in (3 1/8 X 5 in)

Storage and handling

GELFOAM Sterile Compressed Sponge should be stored at 25°C (77°F); excursions permitted to 15-30°C (59-86°F) [see USP Controlled Room Temperature]. Once the package is opened, contents are subject to contamination. It is recommended that GELFOAM be used as soon as the package is opened and unused contents discarded.

Caution

Federal law restricts this device to sale by or on the order of a physician.

C. Quality control of Thai silk fibroin scaffold

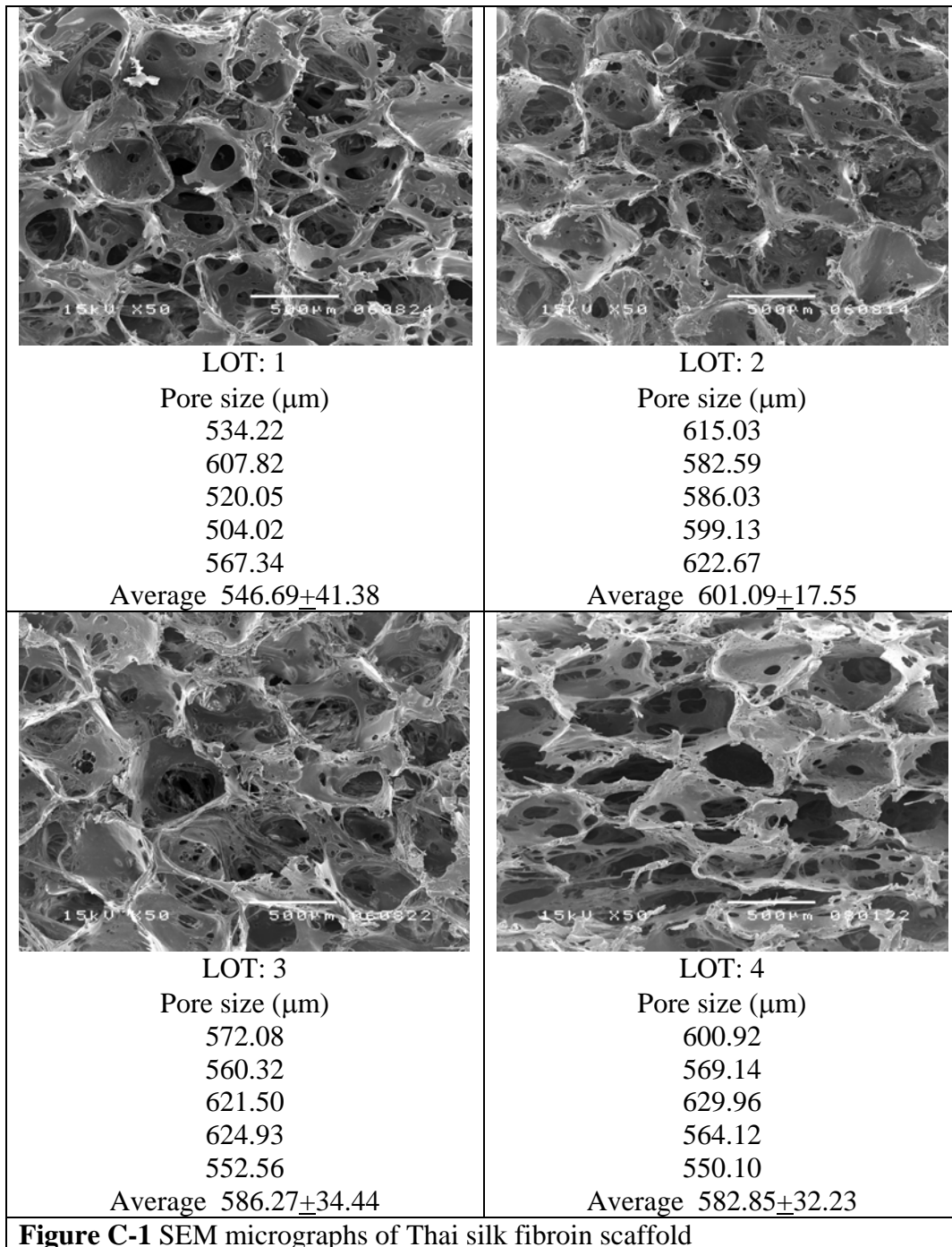
- Density

Table C-1 Density of Thai silk fibroin scaffold

LOT. Number	Weight (mg)	Thickness (mm)	Diameter (mm)	Volume (mm ³)	Density of scaffold (mg/mm ³)
LOT: 1	19.50	2.67	10.42	227.57	0.09
	19.60	2.67	10.58	234.61	0.08
	18.60	2.71	10.86	250.90	0.07
	17.90	2.34	10.78	213.46	0.08
	18.80	2.65	10.75	240.40	0.08
	19.70	2.83	10.77	257.68	0.08
	19.80	2.85	10.33	238.73	0.08
	19.70	2.79	10.48	240.55	0.08
	19.30	2.72	10.65	242.18	0.08
	16.10	2.85	10.67	254.71	0.06
	18.20	2.73	10.53	237.62	0.08
	19.00	2.69	10.63	238.61	0.08
LOT: 2	19.00	2.62	10.62	231.96	0.08
	16.90	2.71	10.06	215.30	0.08
	15.90	2.75	10.37	232.15	0.07
	19.00	2.76	10.62	244.36	0.08
	16.30	2.51	10.37	211.89	0.08
	17.80	2.54	10.67	227.00	0.08
	17.10	2.72	10.33	227.84	0.08
	17.30	2.77	10.43	236.55	0.07
	17.30	2.52	10.37	212.73	0.08
	18.60	2.55	10.47	219.43	0.08
	18.50	2.57	10.27	212.79	0.09
	17.00	2.31	10.51	200.30	0.08
LOT: 3	17.60	2.65	10.62	234.62	0.08
	18.00	2.46	10.31	205.27	0.09
	18.50	2.64	10.69	236.83	0.08
	17.10	2.52	10.52	218.93	0.08
	17.20	2.12	10.62	187.70	0.09
	18.40	2.63	10.49	227.18	0.08
	19.10	2.59	10.54	225.87	0.08
	20.20	2.61	10.35	219.48	0.09
	17.30	2.17	10.52	188.52	0.09
	19.60	2.51	10.80	229.82	0.09
	18.00	2.27	10.48	195.71	0.09
	15.90	2.33	10.46	200.12	0.08

LOT. Number	Weight (mg)	Thickness (mm)	Diameter (mm)	Volume (mm ³)	Density of scaffold (mg/mm ³)
LOT: 4	19.60	2.66	10.39	225.41	0.09
	18.00	2.76	10.22	226.30	0.08
	15.90	2.33	10.46	200.12	0.08
	19.60	2.66	10.39	225.41	0.09
	18.00	2.76	10.22	226.30	0.08
	17.90	2.57	10.27	212.79	0.08
	19.60	2.51	10.29	208.63	0.09
	20.00	2.54	10.64	225.73	0.09
	19.50	2.77	10.30	230.69	0.08
	18.70	2.66	10.74	240.86	0.08
	19.20	2.69	10.26	222.29	0.09
	19.50	2.51	10.70	225.59	0.09

- Pore size



D. Raw data of remaining weight

Table D-1 Remaining weight at various degradation time of Thai silk fibroin scaffolds (SF)

Types of scaffold	Degradation time(day)	Weight of scaffold (mg)	Remaining weight (mg)	% Remaining weight
SF	1	17.80	16.89	94.89
		19.70	18.60	94.42
		19.20	18.10	94.27
		Average	17.86	94.52
		S.D	0.88	0.32
	7	18.90	16.10	85.19
		19.60	16.90	86.22
		19.50	16.40	84.10
		Average	16.47	85.17
		S.D	0.40	1.06
	14	19.60	14.20	72.45
		20.00	15.10	75.50
		18.50	11.80	63.78
		Average	13.70	70.58
		S.D	1.71	6.08
	21	17.50	10.20	58.29
		18.10	12.20	67.40
		15.50	10.10	65.16
		Average	10.83	63.62
		S.D	1.18	4.75
28	18.70	9.50	50.80	
	18.10	9.70	53.59	
	19.40	11.10	57.22	
	Average	10.10	53.87	
	S.D	0.87	3.22	

Table D-2 Remaining weight at various degradation time of hydroxyapatite/Thai silk fibroin scaffolds (SF4)

Types of scaffold	Degradation time(day)	Weight of scaffold (mg)	Remaining weight (mg)	% Remaining weight
SF4	1	31.40	28.80	8.28
		32.20	29.80	7.45
		31.60	29.60	6.33
		Average	29.40	7.35
		S.D	0.53	0.98
	7	35.30	25.50	27.76
		34.00	26.70	21.47
		31.60	23.30	26.27
		Average	25.17	25.17
		S.D	1.72	3.29
	14	31.10	18.60	59.81
		33.70	22.60	67.08
		29.20	20.50	70.21
		Average	20.57	65.69
		S.D	2.00	5.33
	21	35.20	21.10	59.94
		34.10	20.40	59.82
		30.60	16.20	52.94
		Average	19.23	57.57
		S.D	2.65	4.01
28	26.70	12.40	46.44	
	32.80	15.90	48.48	
	32.80	14.40	43.90	
	Average	14.23	46.27	
	S.D	1.76	2.29	

Table D-3 Remaining weight at various degradation time of conjugated gelatin/
Thai silk fibroin scaffolds (CGSF)

Types of scaffold	Degradation time(day)	Weight of scaffold (mg)	Remaining weight (mg)	% Remaining weight
CGSF	1	16.30	15.50	95.09
		16.00	15.50	96.88
		21.20	20.80	98.11
		Average	17.27	96.69
		S.D	3.06	1.52
	7	17.90	16.30	91.06
		18.00	16.80	93.33
		18.40	16.90	91.85
		Average	16.67	92.08
		S.D	0.32	1.15
	14	15.70	13.99	89.17
		21.30	13.99	89.20
		18.50	15.20	82.16
		Average	14.39	86.85
		S.D	0.70	4.06
	21	13.30	10.80	81.20
		15.90	12.80	80.50
		16.10	13.20	81.99
		Average	12.27	81.23
		S.D	1.29	0.74
28	19.40	12.60	64.95	
	18.40	12.30	66.85	
	18.60	13.40	72.04	
	Average	12.77	67.95	
	S.D	0.57	3.67	

Table D-4 Remaining weight at various degradation time of hydroxyapatite/conjugated gelatin/Thai silk fibroin scaffolds (CGSF4)

Types of scaffold	Degradation time(day)	Weight of scaffold (mg)	Remaining weight (mg)	% Remaining weight
CGSF4	1	35.20	34.00	96.59
		39.90	35.80	89.72
		35.00	32.10	91.71
		Average	33.97	92.68
		S.D	1.85	3.53
	7	40.20	30.40	75.62
		33.30	26.50	79.58
		35.70	27.10	75.91
		Average	28.00	77.04
		S.D	2.10	2.21
	14	33.00	24.10	73.03
		33.00	23.30	70.61
		34.70	26.80	77.23
		Average	24.73	73.62
		S.D	1.83	3.35
	21	34.80	21.40	61.49
		33.60	18.50	55.06
		36.50	19.00	52.05
		Average	19.63	56.20
		S.D	1.55	4.82
28	41.10	20.10	48.91	
	29.30	15.20	51.88	
	34.80	16.10	46.26	
	Average	17.13	49.02	
	S.D	2.61	2.81	

E. Histological image

















Scaffolds	N =1	N =2	N =3	N =4
SF				
SF4				
CGSF				
CGSF4				

Figure E-1 Histological image of Thai silk fibroin scaffold (SF), hydroxyapatite/ Thai silk fibroin scaffold (SF4), conjugated gelatin/Thai silk fibroin scaffold (CGSF) and hydroxyapatite/conjugated gelatin/Thai silk fibroin scaffold (CGSF4) after 2 weeks of subcutaneous implantation in Wistar rat

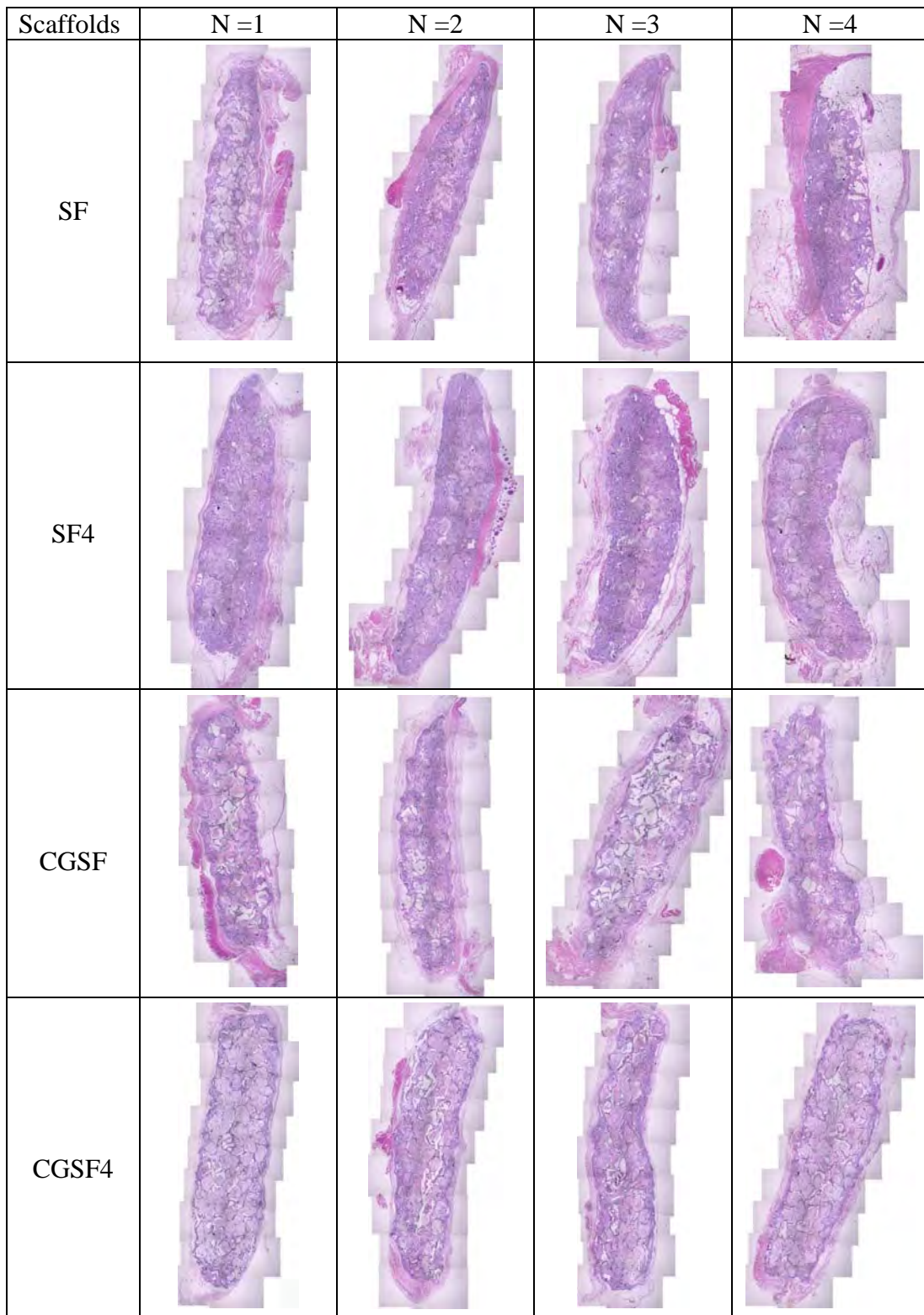


Figure E-2 Histological image of Thai silk fibroin scaffold (SF), hydroxyapatite/ Thai silk fibroin scaffold (SF4), conjugated gelatin/Thai silk fibroin scaffold (CGSF) and hydroxyapatite/conjugated gelatin/Thai silk fibroin scaffold (CGSF4) after 4 weeks of subcutaneous implantation in Wistar rat

















Scaffolds	N =1	N =2	N =3	N =4
SF				
SF4				
CGSF				
CGSF4				

Figure E-3 Histological image of Thai silk fibroin scaffold (SF), hydroxyapatite/ Thai silk fibroin scaffold (SF4), conjugated gelatin/Thai silk fibroin scaffold (CGSF) and hydroxyapatite/conjugated gelatin/Thai silk fibroin scaffold (CGSF4) after 12 weeks of subcutaneous implantation in Wistar rat

F: Semi-quantitative evaluation system according to ISO10993-6

Table F-1 Semi-quantitative evaluation of SF and SF4 scaffolds after 2 weeks of implantation (1st evaluation)

Test sample : SF,SF4	Implantation interval : 2 weeks															
Animal number :	N=1		N=2		N=3		N=4		N=1		N=2		N=3		N=4	
	SF	Gel	SF	Gel	SF	Gel	SF	Gel	SF4	Gel	SF4	Gel	SF4	Gel	SF4	Gel
Polymorphonuclear cell	0	0	0	0	0	0	0	0	0	0	0	0	0	0	0	0
Lymphocytes	0	0	1	1	0	1	1	2	0	1	0	0	0	0	2	2
Plasma cells	0	0	0	0	0	0	0	0	0	0	0	0	0	0	0	0
Macrophages	1	0	1	2	2	0	3	2	2	3	0	2	1	0	2	3
Giant cells	0	0	0	0	0	0	0	0	1	0	0	1	0	0	1	2
Necosis	0	0	0	0	0	0	0	0	0	0	0	0	0	0	0	0
Sub X2	2	0	4	6	4	2	8	8	6	8	0	6	2	0	10	14
Neovascularisation	0	0	1	3	2	0	3	0	2	3	2	3	1	0	2	2
Fibrosis	0	0	0	0	0	0	0	0	0	0	0	0	0	0	0	1
Fatty infiltrate	0	1	0	0	0	0	0	0	0	0	0	0	0	0	0	0
Sub-total	0	1	1	3	2	0	3	0	2	3	2	3	1	0	2	3
Total	2	1	5	9	6	2	11	8	8	11	2	9	3	0	12	17
Test-Control	1		-4		4		3		-3		-7		3		-5	
Ranking of irritant	Non-irritant		Non-irritant		Slight-irritant		Slight-irritant		Non-irritant		Non-irritant		Slight-irritant		Non-irritant	

Remarks

- SF - Thai silk fibroin scaffold
- SF4 - Hydroxyapatite/Thai silk fibroin scaffold
- CGSF - Conjugated gelatin/Thai silk fibroin scaffold
- CGSF4 - Hydroxyapatite/Conjugated gelatin/Thai silk fibroin scaffold
- Gel - Gelfoam®

Table F-2 Semi-quantitative evaluation system of CGSF and CGSF4 scaffolds after 2 weeks of implantation (1st evaluation)

Test sample : CGSF, CGSF4	Implantation interval : 2 weeks															
	N=1		N=2		N=3		N=4		N=1		N=2		N=3		N=4	
Animal number :	CGSF	Gel	CGSF	Gel	CGSF	Gel	CGSF	Gel	CGSF4	Gel	CGSF4	Gel	CGSF4	Gel	CGSF4	Gel
Polymorphonuclear cell	0	0	0	0	0	0	0	X	0	0	0	0	0	0	0	0
Lymphocytes	0	0	0	0	0	0	0	X	1	2	0	0	1	1	1	1
Plasma cells	0	0	0	0	0	0	0	X	1	0	0	0	0	0	0	0
Macrophages	0	2	0	0	2	0	2	X	2	2	0	2	2	1	3	3
Giant cells	0	1	0	0	0	0	0	X	1	0	0	0	1	1	0	1
Necrosis	0	0	0	0	0	0	0	X	0	0	0	0	0	0	0	0
Sub X2	0	6	0	0	4	0	4	X	10	8	0	4	8	6	8	10
Neovascularisation	0	2	3	1	1	0	1	X	2	1	0	2	2	0	1	0
Fibrosis	0	1	0	0	0	0	0	X	0	1	0	1	1	0	0	0
Fatty infiltrate	0	0	0	0	0	0	0	X	0	0	0	0	0	0	0	0
Sub-total	0	3	3	1	1	0	1	X	2	2	0	3	3	0	1	0
Total	0	9	3	1	5	0	5	X	12	10	0	7	11	6	9	10
Test-Control	-9		2		5		-		2		-7		5		-1	
Ranking of irritant	Non-irritant		Non-irritant		Slight-irritant		-		Non-irritant		Non-irritant		Slight-irritant		Non-irritant	

Remarks

- SF - Thai silk fibroin scaffold
SF4 - Hydroxyapatite/Thai silk fibroin scaffold
CGSF - Conjugated gelatin/Thai silk fibroin scaffold
CGSF4 - Hydroxyapatite/Conjugated gelatin/Thai silk fibroin scaffold
Gel - Gelfoam®
X - No control available

Table F-3 Semi-quantitative evaluation of SF and SF4 scaffolds after 2 weeks of implantation (2nd evaluation)

Test sample : SF,SF4	Implantation interval : 2 weeks															
	N=1		N=2		N=3		N=4		N=1		N=2		N=3		N=4	
	SF	Gel	SF	Gel	SF	Gel	SF	Gel	SF4	Gel	SF4	Gel	SF4	Gel	SF4	Gel
Polymorphonuclear cell	0	0	0	0	0	0	0	0	0	0	0	0	0	0	0	0
Lymphocytes	0	0	0	1	0	2	0	2	0	1	0	0	0	0	0	2
Plasma cells	0	0	0	0	0	0	0	0	0	0	0	0	0	0	0	0
Macrophages	1	0	1	2	1	2	2	2	2	2	0	2	1	0	2	2
Giant cells	0	0	0	0	0	0	0	0	0	0	0	1	0	0	0	0
Necosis	0	0	0	0	0	0	0	0	0	0	0	0	0	0	0	0
Sub X2	2	0	2	6	2	8	4	8	4	6	0	6	2	0	4	8
Neovascularisation	0	1	1	3	2	0	2	0	1	3	2	2	2	0	3	2
Fibrosis	0	0	1	2	0	0	0	0	0	0	0	0	0	0	0	0
Fatty infiltrate	0	0	0	0	0	0	0	0	0	0	0	0	0	0	0	0
Sub-total	0	1	2	5	2	0	2	0	1	3	2	2	2	0	3	2
Total	2	1	4	11	4	8	6	8	5	9	2	8	4	0	7	10
Test-Control	1		-7		-4		-2		-4		-6		4		-3	
Ranking of irritant	Non-irritant		Non-irritant		Non-irritant		Non-irritant		Non-irritant		Non-irritant		Slight irritant		Non-irritant	

Remarks

SF - Thai silk fibroin scaffold

SF4 - Hydroxyapatite/Thai silk fibroin scaffold

CGSF - Conjugated gelatin/Thai silk fibroin scaffold

CGSF4 - Hydroxyapatite/Conjugated gelatin/Thai silk fibroin scaffold

Gel - Gelfoam®

Table F-4 Semi-quantitative evaluation of CGSF and CGSF4 scaffolds after 2 weeks of implantation (2nd evaluation)

Test sample : CGSF, CGSF4	Implantation interval : 2 weeks															
	N=1		N=2		N=3		N=4		N=1		N=2		N=3		N=4	
	CGSF	Gel	CGSF	Gel	CGSF	Gel	CGSF	Gel	CGSF4	Gel	CGSF4	Gel	CGSF4	Gel	CGSF4	Gel
Polymorphonuclear cell	0	0	0	0	0	0	0	X	0	0	0	0	0	0	0	0
Lymphocytes	0	1	0	0	0	0	0	X	0	2	0	2	2	1	0	1
Plasma cells	0	0	0	0	0	0	0	X	0	0	0	0	0	0	0	0
Macrophages	2	2	1	0	1	0	2	X	2	2	0	1	2	1	2	2
Giant cells	0	0	0	0	0	0	0	X	0	0	0	0	0	0	0	0
Necrosis	0	0	0	0	0	0	0	X	0	0	0	0	0	0	0	0
Sub X2	4	6	2	0	2	0	4	X	4	8	0	6	8	4	4	6
Neovascularisation	2	2	2	1	1	0	1	X	1	2	0	2	1	0	0	0
Fibrosis	0	2	0	0	0	0	0	X	0	0	0	0	1	0	0	0
Fatty infiltrate	0	0	0	0	0	0	0	X	0	0	0	0	0	0	0	0
Sub-total	2	4	2	1	1	0	1	X	1	2	0	2	2	0	0	0
Total	6	10	4	1	3	0	5	X	5	10	0	8	10	4	4	6
Test-Control	-4		3		3		-		-5		-8		6		-2	
Ranking of irritant	Non-irritant		Slight irritant		Slight irritant		-		Non-irritant		Non-irritant		Slight irritant		Non-irritant	

Remarks

- SF - Thai silk fibroin scaffold
SF4 - Hydroxyapatite/Thai silk fibroin scaffold
CGSF - Conjugated gelatin/Thai silk fibroin scaffold
CGSF4 - Hydroxyapatite/Conjugated gelatin/Thai silk fibroin scaffold
Gel - Gelfoam®
X - No control available

Table F-5 Semi-quantitative evaluation of SF and SF4 scaffolds after 4 weeks of implantation (1st evaluation)

Test sample : SF,SF4	Implantation interval : 4 weeks															
	N=1		N=2		N=3		N=4		N=1		N=2		N=3		N=4	
	SF	Gel	SF	Gel	SF	Gel	SF	Gel	SF4	Gel	SF4	Gel	SF4	Gel	SF4	Gel
Polymorphonuclear cell	0	0	0	X	0	X	0	X	0	X	0	X	0	0	0	X
Lymphocytes	0	0	0	X	0	X	0	X	0	X	0	X	0	0	0	X
Plasma cells	0	0	0	X	0	X	0	X	0	X	0	X	0	0	0	X
Macrophages	0	1	0	X	0	X	0	X	0	X	1	X	1	0	0	X
Giant cells	0	0	0	X	0	X	0	X	0	X	0	X	0	0	0	X
Necrosis	0	0	0	X	0	X	0	X	0	X	0	X	0	0	0	X
Sub X2	0	2	0	X	0	X	0	X	0	X	2	X	2	0	0	X
Neovascularisation	1	0	1	X	1	X	0	X	2	X	1	X	1	0	0	X
Fibrosis	0	0	0	X	0	X	0	X	0	X	0	X	0	0	0	X
Fatty infiltrate	0	0	0	X	0	X	0	X	0	X	0	X	0	0	0	X
Sub-total	1	0	1	X	1	X	0	X	2	X	1	X	1	0	0	X
Total	1	2	1	X	1	X	0	X	2	X	3	X	3	0	0	X
Test-Control	-1		-		-		-		-		-		3		-	
Ranking of irritation	Non-irritant		-		-		-		-		-		Slight-irritant		-	

Remarks

SF - Thai silk fibroin scaffold

SF4 - Hydroxyapatite/Thai silk fibroin scaffold

CGSF - Conjugated gelatin/Thai silk fibroin scaffold

CGSF4 - Hydroxyapatite/Conjugated gelatin/Thai silk fibroin scaffold

Gel - Gelfoam®

X - No control available

Table F-6 Semi-quantitative evaluation of CGSF and CGSF4 scaffolds after 4 weeks of implantation (1st evaluation)

Test sample : CGSF, CGSF4	Implantation interval : 4 weeks															
	1		2		3		4		1		2		3		4	
Animal number :	CGSF	Gel	CGSF	Gel	CGSF	Gel	CGSF	Gel	CGSF4	Gel	CGSF4	Gel	CGSF4	Gel	CGSF4	Gel
Polymorphonuclear cell	0	X	0	0	0	X	0	X	0	X	0	X	0	X	0	X
Lymphocytes	1	X	0	0	0	X	0	X	0	X	0	X	0	X	0	X
Plasma cells	0	X	0	0	0	X	0	X	0	X	0	X	0	X	0	X
Macrophages	1	X	2	0	2	X	2	X	1	X	1	X	0	X	0	X
Giant cells	0	X	0	0	0	X	0	X	0	X	0	X	0	X	0	X
Necosis	0	X	0	0	0	X	0	X	0	X	0	X	0	X	0	X
Sub X2	4	X	4	0	4	X	4	X	2	X	2	X	0	X	0	X
Neovascularisation	1	X	0	0	1	X	1	X	1	X	0	X	0	X	0	X
Fibrosis	0	X	0	0	0	X	0	X	0	X	0	X	0	X	0	X
Fatty infiltrate	0	X	0	0	0	X	0	X	0	X	0	X	0	X	0	X
Sub-total	1	X	0	0	1	X	1	X	1	X	0	X	0	X	0	X
Total	5	X	4	0	5	X	5	X	3	X	2	X	0	X	0	X
Test-Control	-		4		-		-		-		-		-		-	
Ranking of irritation	Non-irritant		Slight-irritant		-		-		-		-		-		-	

Remarks

- SF - Thai silk fibroin scaffold
SF4 - Hydroxyapatite/Thai silk fibroin scaffold
CGSF - Conjugated gelatin/Thai silk fibroin scaffold
CGSF4 - Hydroxyapatite/Conjugated gelatin/Thai silk fibroin scaffold
Gel - Gelfoam®
X - No control available

Table F-7 Semi-quantitative evaluation of SF and SF4 scaffolds after 4 weeks of implantation (2nd evaluation)

Test sample : SF,SF4	Implantation interval : 4 weeks															
	N=1		N=2		N=3		N=4		N=1		N=2		N=3		N=4	
	SF	Gel	SF	Gel	SF	Gel	SF	Gel	SF4	Gel	SF4	Gel	SF4	Gel	SF4	Gel
Polymorphonuclear cell	0	0	0	X	0	X	0	X	0	X	0	X	0	0	0	X
Lymphocytes	0	0	0	X	0	X	0	X	0	X	0	X	0	0	0	X
Plasma cells	0	0	0	X	0	X	0	X	0	X	0	X	0	0	0	X
Macrophages	0	0	0	X	0	X	1	X	1	X	0	X	1	0	0	X
Giant cells	0	0	0	X	0	X	0	X	0	X	0	X	0	0	0	X
Necrosis	0	0	0	X	0	X	0	X	0	X	0	X	0	0	0	X
Sub X2	0	0	0	X	0	X	2	X	2	X	0	X	2	0	0	X
Neovascularisation	1	0	2	X	1	X	1	X	2	X	1	X	1	0	0	X
Fibrosis	0	0	0	X	0	X	0	X	0	X	0	X	0	0	0	X
Fatty infiltrate	0	0	0	X	0	X	0	X	0	X	0	X	0	0	0	X
Sub-total	1	0	2	X	1	X	1	X	2	X	1	X	1	0	0	X
Total	1	0	2	X	1	X	3	X	4	X	1	X	3	0	0	X
Test-Control	1		-		-		-		-		-		3		-	
Ranking of irritation	Non-irritant		-		-		-		-		-		Slight irritant		-	

Remarks

SF - Thai silk fibroin scaffold

SF4 - Hydroxyapatite/Thai silk fibroin scaffold

CGSF - Conjugated gelatin/Thai silk fibroin scaffold

CGSF4 - Hydroxyapatite/Conjugated gelatin/Thai silk fibroin scaffold

Gel - Gelfoam®

X - No control available

Table F-8 Semi-quantitative evaluation of CGSF and CGSF4 scaffolds after 4 weeks of implantation (2nd evaluation)

Test sample : CGSF, CGSF4	Implantation interval : 4 weeks															
	N=1		N=2		N=3		N=4		N=1		N=2		N=3		N=4	
	CGSF	Gel	CGSF	Gel	CGSF	Gel	CGSF	Gel	CGSF4	Gel	CGSF4	Gel	CGSF4	Gel	CGSF4	Gel
Polymorphonuclear cell	0	X	0	0	0	X	0	X	0	X	0	X	0	X	0	X
Lymphocytes	1	X	0	0	0	X	0	X	0	X	0	X	0	X	0	X
Plasma cells	0	X	0	0	0	X	0	X	0	X	0	X	0	X	0	X
Macrophages	1	X	2	0	2	X	1	X	1	X	1	X	1	X	1	X
Giant cells	0	X	0	0	0	X	0	X	0	X	0	X	0	X	0	X
Necrosis	0	X	0	0	0	X	0	X	0	X	0	X	0	X	0	X
Sub X2	4	X	4	0	4	X	2	X	2	X	2	X	2	X	2	X
Neovascularisation	2	X	1	2	1	X	1	X	1	X	1	X	1	X	1	X
Fibrosis	0	X	0	0	0	X	0	X	0	X	0	X	0	X	0	X
Fatty infiltrate	0	X	0	0	0	X	0	X	0	X	0	X	0	X	0	X
Sub-total	2	X	1	2	1	X	1	X	1	X	1	X	1	X	1	X
Total	6	X	5	2	5	X	3	X	3	X	3	X	3	X	3	X
Test-Control	-		3		-		-		-		-		-		-	
Ranking of irritation	-		Slight irritant		-		-		-		-		-		-	

Remarks

- SF - Thai silk fibroin scaffold
SF4 - Hydroxyapatite/Thai silk fibroin scaffold
CGSF - Conjugated gelatin/Thai silk fibroin scaffold
CGSF4 - Hydroxyapatite/Conjugated gelatin/Thai silk fibroin scaffold
Gel - Gelfoam®
X - No control available

BIOGRAPHY

Miss Hathairat Tungasana was born in Nakornsawan, Thailand on June 7, 1982. She finished the high school education in 2000 from Nakornsawan school. In 2004, she received her Bachelor Degree in Science with a minor in Chemical Engineering, Department of Chemical Technology, Chulalongkorn University. After the graduation, she worked at the Siam Ceramic Group Industries Co., Ltd for 2 years and then she continued her graduate study in Biomedical Program (MSc), Graduate School, Chulalongkorn University.

Some parts of this work were presented at the conferences.

Tungasana H., Bunaprasert T., Damrongsakkul S., “In vitro biodegradation behavior of composited scaffolds prepared from hydroxyapatite, gelatin and silk fibroin”. The 4th world congress on regenerative medicine (WCRM), Centara Grand Hotel, Bangkok, Thailand, 12-14 March 2009.